THE DESIGN AND VALIDATION OF A DISCRETE-EVENT SIMULATOR FOR CARBOHYDRATE METABOLISM IN HUMANS

by

Husam Ghazaleh

A Dissertation Submitted in
Partial Fulfillment of the
Requirements for the degree of

Doctor of Philosophy
in Engineering

at
The University of Wisconsin-Milwaukee
Fall 2020

ABSTRACT

THE DESIGN AND VALIDATION OF A DISCRETE-EVENT SIMULATOR FOR CARBOHYDRATE METABOLISM IN HUMANS

by

Husam Ghazaleh

The University of Wisconsin-Milwaukee, 2020

Under the Supervision of Professor Mukul Goyal, Ph.D.

CarbMetSim is a discrete event simulator that tracks the changes of blood glucose level of a human subject after a timed series of diet and exercises activities. *CarbMetSim* implements wider aspects of carbohydrate metabolism in individuals to capture the average effect of various diet/exercise routines on the blood glucose level of diabetic patients. The simulator is implemented in an object-oriented paradigm, where key organs are represented as classes in the *CarbMetSim*. Key organs (stomach, intestine, portal vein, liver, kidney, muscles, adipose tissue, brain and heart) are implemented to the extent necessary to simulate their impact on the production and consumption of glucose. Metabolic pathways (glucose oxidation, glycolysis and gluconeogenesis) have been taken in account in the operation of various organs. In accordance with published research, the impact of insulin and insulin resistance on the operation of various organs/pathways is captured. *CarbMetSim* offers broad versatility to configure the insulin production ability, the average flux along various metabolic pathways and the impact of insulin resistance on different aspects of carbohydrate metabolism. However, the *CarbMetSim* project has not yet been finished. There are many

aspects and metabolic pathways that have not been implemented or have been implemented in a simple manner. Also, additional validation is required before the simulator can be considered ready for use by people with Diabetes.

To

my parents,

my wife,

and my daughter and son.

TABLE OF CONTENTS

LIST OF FIGURES

LIST OF TABLES

ACKNOWLEDGMENTS

I would like to thank my advisor, Professor Mukul Goyal, for all his help and guidance over the years. You have set an example of excellence as a mentor, instructor, researcher, and role model. Also, I would like to express my gratitude to the members of my thesis committee, Professor Ethan Munson, Professor Hossein Hosseini, Professor Hamid Seifoddini, and Dr. Robert Blank. I would like to thank the Computer Science Faculty for supporting me during these years of graduate study.

Chapter 1

Introduction

Diabetes mellitus, also called diabetes, is a group of diseases that affect how the human body regulates the blood sugar (*glucose*) level and is mainly related to abnormally high glucose levels in the blood. Understanding the role of one of the key hormones (*insulin*) in the human body that regulates blood glucose will help us understand the underlying causes for developing the disease. In general, the human body uses food to produce the energy needed for daily activities and cells' chemical reactions. The energy is formed by breaking down the consumed food or drink into simple sugar forms called glucose. Glucose is transported through the bloodstream to the body's cells by the insulin hormone to be utilized as a fuel source for different cell's chemical reactions and metabolism processes. The insulin hormone is produced by the beta cells in the pancreas, and it is the primary transporter of glucose to the body's cells. It binds to the insulin receptors on the body's cells, signaling them to absorb glucose from the bloodstream. Usually low insulin levels circulate constantly throughout the body when the Blood Glucose Level (BGL) is low. However, when the BGL increases due to meal ingestion, for example, insulin levels spike to return BGL to the normal level and restore the body to the normoglycemia status (the presence of a normal concentration of BGL). Besides, insulin signals the liver to absorb glucose and store it as *glycogen* in the liver's cells. If the amount of glycogen exceeds the limit, glucose will be converted into *fatty acids*, transferred to other parts of the body, and stored as fat in tissues. On the other hand, the *Glucagon* hormone produced by the alpha cells in the pancreas regulates BGL when it is low by signaling the liver to convert the stored glycogen back to

glucose, which in turn will raise BGL and return the body status to the normoglycemia.

Knowing the basic relationship between the insulin hormone and BGL helps us to cite formal definitions of the disease here. In this literature, I am referencing two definitions of the disease that have been stated by two prestigious diabetes research institutes in the USA. The American Diabetes Association [6] defines Diabetes as " a group of metabolic diseases characterized by hyperglycemia (high BGL) resulting from defects in insulin secretion, insulin action or both ". Moreover, the Diabetes Research Institute foundation [36] states that it is a serious condition that occurs when the body cannot make or effectively use its own insulin.

Diabetic people are classified into two different types[36][34][6]: type I and type II. In the type I group, the pancreas cannot produce insulin at all, or it just produces very little of it. This occurs because the beta cells of the pancreas are attacked and damaged by the immune system. Type I diabetic patients are insulin dependent, and they must take insulin dosages as part of their treatment. Insulin dosages can be taken by injection with a needle or with an insulin pump. People with type I usually develop the disease at a young age. Therefore, it is less common than the other type (type II), and accounts for only 5–10%[34]of those who have diabetes. On the other hand, in the type II diabetes group, the body's cells resist insulin signals and do not absorb glucose from the bloodstream (can't effectively use it). Also, in some cases the pancreas cannot produce sufficient amounts of the insulin hormone. Usually type II diabetes is developed due to lifestyle issues, such as obesity and lack of exercises. Treatments require following healthy lifestyle changes, taking medications if needed, and others. Diabetes type II can be developed due to genetic issues as well. It is the most common type, and it accounts for 90–95% [34] of those who have diabetes.

The World Health Organization (WHO) published a global study [84] reporting that the number of diabetic patients worldwide has increased from 108 million in 1980 to 422 million in 2014. Also, [21] noted that the commonness of the disease among adults over

18 years old has risen from 4.7% in 1980 to 8.5% in 2014. Unfortunately, the data also shows that around two-thirds of all diabetes cases occur in middle and low-income countries [6]. On the other hand, in the U.S there are 30.3 million people who have diabetes (9.4% of the U.S. population)[82][33], this includes adults aged 18 years or older and people who were not aware of it or did not report having diabetes (7.2 million or 23.8% of people with diabetes)[33]. The global financial cost of diabetes is significant and will increase by 2030 [14]. The annual cost of diabetes (including the cost of treatment) was calculated in international dollars by [117], and it was estimated at 825 billion dollars per year, with the highest cost to individual countries being in China ($170 billion), the USA ($105 billion), and India ($73 billion). These calculations do not include workdays lost due to the disease, which would significantly increase the costs if incorporated, as the author claimed.

A diabetic patient may develop serious health complications if his\her BGL is not controlled appropriately. These health complications are specific and varied. The level of the complications and difficulties depends on the patient's lifestyle and his\her awareness of diabetes-associated health issues. In general, the following health problems may occur for a diabetic patient who does not follow a healthy lifestyle or control his\her BGL: neuropathy, nephropathy, retinopathy, cardiovascular disease, stroke, and Peripheral Artery Disease (PAD)[86]. Moreover, diabetic patients with uncontrolled BGL may develop hyperglycemia (high BGL) that causes chronic damage such as retinopathy and kidney failure [105]. Also, diabetic patients (specifically type I) may suffer hypoglycemia episodes. The hypoglycemia episode happens when BGL is much lower than the normal levels. It usually occurs as a side effect of the blood glucose lowering medications. Hypoglycemia may lead to brain damage, coma, and, eventually, death [105][104].

To avoid these health complications, the patient needs to regularly see his\her endocrinologist, take medicines (if required), and control non-clinical parameters that significantly

affect and help maintain healthy BGL (glycemic control). Firm glycemic control is widely proven in preventing or reducing many diabetes health complications.[80][41][42] [95][109][65]. For instance, muscles absorb glucose from the blood when the human body is engaged in physical exercises, even in the absence of insulin. These exercises may cause hypoglycemia if it is not carefully coordinated with food and medication intake. Following a healthy lifestyle that includes a healthy diet and exercising regularly must be coordinated with daily BGL monitoring to help maintain BGL as close as possible to the normal ranges over time.

To observe BGL daily, Continuous Glucose Monitoring (CGM) portable sensors [62] have been developed. These devices help the diabetic patient track his\her BGL continuously and automatically throughout the day. These devices can help control BGL. But either they are expensive or they are not easily available to a large population of diabetic patients worldwide. Diabetic patients will benefit from having an available and free tool that will help them decide how they should plan their food and exercise activities to keep their BGL under control. Indeed, they need help in realizing the impact of a particular sequence of food and exercise activities on their BGL. One solution is to build a simulation tool that reasonably predicts the impact of diet and exercise activities on patient's BGL using the vast knowledge of energy metabolism in human beings. A few similar simulators exist [64][72] but are designed toward predicting the impact of individual meals and are not available in a manner that can be freely used by individuals.

In this thesis, a *CarbMetSim* [48] (the **Carb**ohydrate **Met**abolism **Sim**ulator) is described. *CarbMetSim* is an open-source [47] simulation software that predicts minute by minute BGL in response to an arbitrary length sequence of food and exercise activities. The proposed simulator is freely available and it is based on discrete event model, in contrast to existing simulation tools that are classifed as continuous time models that use differential and algebraic equations to describe physiological detail. In *CarbMetSim*, the time increments

in ticks, where each tick is one minute long. At the start of each tick, *CarbMetSim* fires the food/exercise events that need to be fired at the time and involves various simulated body organs to perform the work that is supposed to be happening during this tick.

CarbMetSim implements wider aspects of carbohydrate metabolism in individuals to capture the average effect of various diet/exercise routines on the BGL of diabetic patients. The simulator implements the following key organs: stomach, intestine, portal vein, liver, kidney, muscles, adipose tissue, brain and heart. The organs have been implemented to the extent necessary to simulate their impact on the production and consumption of glucose. Moreover, the following metabolic pathways have been taken in account in *CarbMetSim*: glucose oxidation, glycolysis and gluconeogenesis. These pathways are simulated in the operation of various organs. In accordance with published research, the impact of insulin and insulin resistance on the operation of various organs/pathways is captured. *CarbMetSim* offers broad versatility to configure the insulin production ability, the average flux along various metabolic pathways and the impact of insulin resistance on different aspects of carbohydrate metabolism. Thus the simulator can be customized to a given individual by using appropriate values to various configurable parameters.

However, the *CarbMetSim* project has not yet been finished. There are many aspects and metabolic pathways that have not been implemented or have been implemented in a simple manner. For instance, the protein and lipid metabolism are implemented in a simplified manner. *CarbMetSim* doesn't take the monosaccharides (other than glucose) into consideration and assumes that after digestion all the dietary carbohydrates become glucose. Moreover, the impact of insulin is captured in a simplified manner and does not model other important hormones such as glucagon. The impact of short-term externally injected insulin is not yet modeled, and it is currently possible to simulate just aerobic exercise. Finally, the simulator cannot yet translate a user's diet/exercise/BGL data into the values of simulation

parameters governing the behavior of different organs.

Chapter 2

Modeling carbohydrate metabolism in humans—A literature review

Oviedo's paper [85] provides a dense review of most of the significant BGL prediction models and the models that predict hypo\hyperglycemia episodes for type I diabetic patients. The paper only covered the models that have been published between 2010 and spring 2016, due to the massive numbers of the published models in the glycemic control. BGL prediction models were classified into four different groups: physiological models group, data-driven models group, hybrid models group, and control-oriented prediction models group.

Physiological models are mathematical models that simulate all or some of the physiological processes of glucose consumptions (glucose metabolism) and the corresponding insulin actions that depend entirely on the current levels of glucose in the blood stream. Generally, these models consist of compartmental sub-models such as an insulin absorption sub-model and a carbohydrate digestion sub-model that simulate all the events that directly affect BGL. The common inputs for these sub-models are carbohydrate intake, insulin therapy, physical activities, and stress. Building these models requires a solid physiological knowledge of all the related processes of glucose metabolic process. This knowledge is needed to simulate these metabolic processes and to identify all the physiological parameters that are required to describe the model accurately. Consequently, physiological models are classified based on the complexity into two main subgroups: minimal and maximal models. The minimal models simulate the vital physiological processes of glucose metabolism and insulin action by using limited number of mathematical equations and parameters. On the other hand,

the maximal models or the comprehensive models use the available knowledge to simulate all the physiological processes of the glucose metabolism and insulin action by using a full and complex set of equations and parameters. The Dall Man Model [24] , The Hovirka [51], and Bergman minimal model [10] are the most popular used physiological models for BGL predictions.

Data-driven models are less complicated than physiological models. These do not simulate the physiological processes of glucose metabolism, but they employ different artificial techniques on the collected patient's daily activities to predict future BGL level. The main goal of these models is to simulate how food intake, exercises, and insulin therapy affect BGL. However, simple mathematical equations are used to identify a few parameters to simulate the glucose kinetics and insulin action. There is no single dominantly used artificial method in this group due to the massive number of existing machine learning techniques and the ability of mixing these techniques to achieve more accurate predictions.

Hybrid models combine the physiological models and the data-driven models in predicting BGL and hypo\hyperglycemic episodes. The physiological models used here usually are the meal models and insulin models. The Dalla Man meal model, the Lehmann model, and the Deutsch model [68] are the most popular models used to model meal and glucose absorption. However, Berger's model and the Dalla Man model are the most used models in considering insulin as an input. Data-driven models are used to draw the relationship between the user's activities and the outputs (future BGL). User activities are the carbohydrates intake and insulin dosage. All the surveyed models in this group used carbohydrate as a main input, while 78.5% of the surveyed papers use insulin as a secondary input [85].

The control oriented prediction models group includes all the models that are implemented in controllers such as Artificial Pancreases (AP) and belong to one of the previous groups. The majority of these models belong to the data-driven group, while the few others

belong to the physiological group and the hybrid group.

2.1 Knowledge-driven Models

The physiological models or the knowledge-driven models are mathematical models that are based on human physiology. Indeed, these models are a set of differential and algebraic equations, and they represent different factors as different compartmental models that affect each other [19]. For instance, the models in [13][2][40] are linear models that replicate the BGL and the insulin level in the blood, and they show that the rate of their presence and absence were linearly proportional to their corresponding levels in the blood. On the other hand, [18] proposed a non-linear model that considered additional hormones besides insulin hormone as glucagon. Moreover, [35] proposed a model that composed six compartment model, one each for BGL, liver glycogen, muscle glycogen, plasma insulin, plasma glucagon and free fatty acids in plasma. The addition or removal from each compartment occurred in a non-linear fashion. Other distinguished non-linear multi-compartment models were the models developed by [17], [55],[22], and [20]. The models are more complex and cover many physiological details. An overview of the several knowledge-based models are presented in [103]. This section covers some of the later models.

Bergman et al. introduced a model [10][11] that quantifies the sensitiviy of an individual's beta cells to the his\her BGL and the sensitivity of the individual's BGL to the insulin level in his\her bloodstream. The proposed model was a minimally complex mathematical model that is able to capture the individual differences in the two sensitivities mentioned above. However, the model has been modified by Furler et al [38]. Furler et al. allowed for the absence of insulin production by the pancreas and external insulin infusion. Moreover, Bergman et al.'s model has been extended by [98] to include the level of free fatty acids in plasma. Also it has been extended in [99][25] to include the impact of physical exercise.

Finally, Bergman et al.'s model was used to study the closed and semi-closed loop optimal control algorithms to define the insulin infusion profile for an individual [83][32].

In [107], multi-compartment model for glucose circulation was proposed and developed, where each related organ was modeled as a separate compartment. Another multi-compartment model was introduced by Guyton et al. [49]. The model consists of:

1. A glucose circulation subsystem. Separate compartments were developed for liver glucose, liver glycogen, kidney glucose, brain tissue glucose, brain blood glucose, peripheral blood glucose (muscles, adipose tissue), peripheral tissue glucose, central blood glucose (i.e. gastrointestinal tract), and central tissue glucose.

2. Insulin circulation subsystem. Separate compartments were developed for liver insulin, which represents insulin from pancreatic beta cells, kidney insulin, peripheral blood insulin, peripheral tissue insulin, central blood insulin and central tissue insulin.

There are 32 non-linear ordinary differential equations (ODEs) with 11 non-linear ODEs in the model just to simulate the insulin secretion from the pancreas[103]. Another physiologically complex multi-compartment model was proposed by Sorensen [103] that includes a simplified model for pancreatic insulin secretion. The multi-compartment model made up of 22 non-linear ODEs, of which 11 ODEs were associated with glucose circulation, 10 ODEs with insulin, and 1 ODE with glucagon. The Guyton/Sorensen models were updated by Parker et al. [87] [88]. The updated versions consider the uncertainty in parameter values and include a sub-model for gastric emptying of carbohydrates in a meal [68]. In [51], Hovorka et al. developed a multi compartment model of glucose and insulin kinetics. The model is part of another predictive controller model for sub-cutaneous insulin infusion for people with type I diabetes. The model consists of:

1. Two compartment glucose subsystems (modeling glucose absorption, distribution and disposal).

2. Two-compartment insulin subsystems (modeling insulin absorption, distribution and disposal).

3. Insulin action subsystem (modeling insulin action on glucose transport, disposal and endogeneous production).

Dalla Man et al., in their study [24], developed a model that binds the concentrations of glucose and insulin plasma to different glucose and insulin rates. These rates are:

1. The rate of arrival of glucose from the gastro-intestinal tract.

2. The rate at which the glucose is produced by liver and kidney organs.

3. The insulin dependent and independent rates of glucose usage.

4. The rate of renal extraction of glucose.

5. The rate of insulin secretion by beta cells.

6. The rate of insulin degradation.

The study collected the data from 204 normal and 14 type II diabetic subjects. These experiment data determined the values of the model parameters. The model was used to simulate patient behavior in UVA/PADOVA Type I Diabetes Simulator [64] in order to examine the closed control strategies for insulin pumps. [72] modified the Dalla Man's model by combining glucagon secretion/action/kinetics and non-linear increase in insulin-dependent glucose utilization as BGL declines below the normal range. The new modifications were implemented in a new version of the UVA/PADOVA simulator.

Our *CarbMetSim* simulator is a physiologically complex model like the models presented by Tiran et al. [107], Guyton et al. [49], Sorensen [103] and Dalla Man [24]. The main difference is that *CarbMetSim* uses software to implement the physiological details of various body organs, and these details are implemented as objects whereas the existing models used ODEs to model physiological details. Implementing physiological details in software allows for more complex behavior to be considered and implemented than what is possible using ODEs. Furthermore, it is easier to modify physiological behavior implemented in software than via ODEs. Therefore, the presented simulator is an improvement over existing ODE-based approaches. It is hoped that these benefits coupled with its open-source nature will allow *CarbMetSim* to emerge as a popular simulation model of human metabolism for both diabetes research and self-management tools for diabetic people.

2.2 Data-driven Models

In this section, several significant data-driven models for predicting BGL are covered. These models were proposed either for diabetic patients type I and\or type II. Data-driven models are black box models that aim to find the relationship between the inputs and the outputs of a certain system. In the art of predicting BGL in diabetes, they extract the information hidden in the patients' data in order to model the glucose response to various events, without explicit knowledge of the process behavior of the glucose-insulin regulatory system. The complexity of the data-driven models determines the desired observed inputs. Usually the inputs are the recently recorded BGL values, food intake components (such as carbohydrates, fats, and proteins), exercises, stress, insulin dosages and time of insulin injections. Moreover, the density of the collected BGL readings play a main role in determining the accuracy of the predictions. Data-driven models are easier to be designed and developed in comparison to the physiological models. However, the models cannot provide

any explanation of how the predicted values are obtained. In general, data-driven models are classified in two families: Machine Learning Models and Time-Series Models [41]. Machine learning methods are mathematical descriptions of real-world processes that include methods of data analysis to automate analytical model building. Different machine-learning approaches have been used to model the relationship between recent past BGL values and patient activities with the future BGL. These approaches include rule-based models, multi-model approaches, Gaussian mixture models (GMM), vector machines for regression (SVR), reinforcement learning, random support vector models, and artificial NN (ANN) models, among others. On the other hand, time series analysis predicts future events based on recent events that have been gathered and spotted at regular time intervals. It comprises methods to extract meaningful patterns of the collected data that aid in designing an accurate prediction model.

The Velletta et al. model [109] is an example of using a black box model to predict future BGL based only on the patient's activities. The research work used a Gaussian process and other existing models to model the relationship between the patient's activities and their BGL, minute by minute. Patients' exercises and BGL values were monitored continuously. Patients were instructed to wear the exercise monitoring device and the CGMS for approximately two weeks. The CGMS needs to be replaced every three days. Several existing models have been used to generate part of the required parameters for the Gaussian process. For instance, the generic insulin model [106] and the popular Lehmann's food model [68] have been used to generate the insulin and the carbohydrate parameters, respectively. The CGMS generated the related glucose parameters, and the exercise monitoring system extracted the following parameters from the collected physical activity data: the METs (Metabolic Equivalent) in (kcal/kg/hr),which is the amount of calories that the body burns to keep itself functioning, Heat flux in (W/m2), and skin temperature in Celsius. Then,

a Gaussian process [92] was used to return a non-parametric probabilistic model, where the mean and covariance functions report all knowledge about the modeling process. The inputs of the model are: glucose, carbohydrate intake, insulin, METs, Heat flux, and skin temperature. The results indicated that the model can predict BGL in the long term, but the predicted values were higher than the measured ones. However, it was able to track the decreases and increases in BGL in the observed period. There are two limitations of the proposed model: the model considers the carbohydrate as the only source of glucose for the human body. However, fat and protein also are sources of glucose as well, which the model does not consider in the modeling process. The model does not consider other parameters that may affect the insulin absorption, such as the amount of the dose, the site of application, and exercises.

Similar to Rollins et al.'s model [95] and Velletta et al.'s model [109], Georga et al. prposed a model [41] that uses a multi-parametric set of free-living data to predict BGL for type I diabetic patients. The model comprised three white box compartmental models that mimic the glucose–insulin regulatory system and a fourth black box model that predicts BGL. The compartmental sub-models are the meal model, the insulin model, and the physical exercise model. They measure the effects of food intake, exercises, and medications on BGL, respectively. Indeed, they are used to simulate the related physiological processes to produce the needed parameters, which will be used later as inputs for the prediction model. Modeling the effects of the physical exercises on BGL was developed using two different approaches. The first approach represents the physical exercise input to the prediction model as a set of the collected data (Metabolic Equivalent of Task (MET), the heat flux (hf), and the skin temperature (st) variables) that was gathered from the exercise sensor armband. The second approach represents the physical exercise input as a set of the generated outputs (glucose concentration and insulin concentration) of the exercise sub-model.

The compartmental models are represented and influenced by other existing sub-models. Specifically, the insulin sub-model is a combination of Tarin et al.'s model [106] and Cobelli et al.'s model [20], with some assumptions and modifications that were made by the authors. The insulin sub-model simulates the absorption and the pharmacokinetics\pharmacodynamics of subcutaneously injected insulin as it is described in [106]. It uses [20] model to estimate plasma insulin concentration as well. Similarly, the meal sub-model uses [68] model to mimic the processes of ingestion and the absorption of carbohydrates. Two assumptions have been made about representing the percentage of glucose in the blood: the rate of gastric emptying is a trapezoidal function and the intestinal glucose absorption follows the first order linear kinetics. The parameters in the meal sub-model are obtained from [68] and they are patient-independent. Finally, the exercise sub-model uses [99] model to simulate the physiological processes that occur during an exercise event and in the recovery period. Indeed, the authors developed an algorithm that determines the most significant physical activities performed by the patient by analyzing the measurements provided by the exercises sensor armband. Then, the corresponding data of these exercises are fed into the [99] model to simulate the effects of exercises on BGL. The proposed algorithm in the exercise sub-model provides the patient an option not to wear the activity monitor continuously throughout the day, but only during an exercise.

The prediction sub-model uses support vector machines for regression (SVR) [101] and [12] to predict BGL, due its effectiveness on large and dimensional datasets, which is the case in glucose prediction problems. The prediction sub-model receives the following inputs from the mentioned compartmental models: the rate of glucose appearance in plasma after a meal, the plasma insulin concentration, the physical activity related variables, and the s.c glucose measurements obtained from CGMS. The predictions are carried out for four different Prediction Horizons (PH): 15 ,30 ,60 and 120 minutes. The study uses root mean

squared error (RMSE) and the correlation coefficient r to evaluate the prediction accuracy. The Clarke's Error Grid Analysis is also used to evaluate the clinical significance of the errors between the predictive and measured BGL. The published results demonstrate that the short-term prediction (15 or 30 minutes) is more accurate and highly correlated with the measured glucose values (0.95 for 15-minutes PH, and 0.88 for 30-minutes PH). However, the model performance decreases when the PH increases to 60 or 120 minutes. The two approaches used to describe the exercise activity produced approximately equal results. Moreover, most of the predicted glucose points were on zones A and B on Clarke Error Grid Analysis, and there are no points belonging to the erroneous E zone, which represents clinically acceptable results. The model has some limitations; it does not consider the effects of fat, protein, and the glycemic index on the digestive and absorptive processes. Additionally, it does not consider other factors that affect the insulin absorption and insulin kinetics processes, such as body temperature. It is worth pointing out that Georga et al.'s model [41] is the first study that considers the impact of physical exercises on the future predicted BGL, and it is the first study that fed the exercise model with real sensor data to measure the exercise intensity.

[108] designed and developed a number of different linear, compartmental neural networks models for predicting the BGL of diabetic patients. The goal of the paper was to evaluate the neural network's technique performance by comparing it with standard models such as the linear model, and with complex models such as the compartmental model, each of which simulates all the physiological processes related to diabetes. The following is a brief description of the proposed compartmental model and the two neural networks models. The compartmental model (non-linear model) consists of the following sub-models that mimic human organs' operations to regulate the BGL in the human body: kidney, blood, liver, digestive tract, insulin dependent utilization (muscles), and insulin independent utilization

(red blood cells). Food, insulin, and exercises were the gathered inputs for the model. The effects of these inputs on BGL were approximated and delayed by linear response functions. These inputs were mapped to corresponding response functions by a functional block called *Md*. Then, the response functions were fed in a second compartment model called *Mn* function to simulate the dynamics of the BGL, using a non-linear difference equation. The non-linear equation models the following interactions of the glucose dynamics: the increase of the BGL due to consuming carbohydrates, the insulin-dependent glucose production of the liver, the insulin-dependent usage of BGL, the insulin-independent usage of BGL, the renal clearance, and the effects of exercises on lowering BGL. The parameters of the model were not adapted from the training data, but derived from other literature mentioned in [108].

The used non-linear equation in the *Mn* functional block is derived from unreliable physiological assumptions that do not simulate all the physiological interactions correctly. Therefore, the authors replaced the *Mn* functional block with a Recurrent Neural Networks (RNN) model to simulate the physiological interactions appropriately. The inputs for the model are insulin, food, exercise, and the current and previous estimation of the BGL. It has been chosen due its ability to accept previous predictions as an input and use these measurements to improve the prediction process. Two different modes were used to run the RNN: free running (FR) mode and the teacher forced (TF) mode. In the free running mode, the network predictions were iterated for training and prediction. While in the teacher forced mode, the measurements of the BGL were substituted for the predicted values whenever available in the training and prediction phases. Real time recurrent learning rules were used to adapt the weights in the RNN.

On the other hand, Time Series Convolution Neural-Network Models (TSCNN) has been proposed to predict BGL. TSCNN is an appropriate solution for applications where past

measurements are not always available. TSCNN is exploited when there is a desire to avoid recurrent learning rules and to predict new values without receiving all the past measurements. However, TSCNN may need to receive relevant input that might have occurred a long time period in the past (in this application, up to 24 hours). Therefore, to limit the input space, and not end up with a large input space that leads to overfitting, the authors have added several approaches to determine the appropriate size of the time window to receive related inputs. These approaches handle the problem either by determining the size of the window precisely (Hard Limited Time Windows TSCNN-HL) or softly (Soft Competitive Fixed-Time Windows TSCNN-SC).

Based on the authors' opinion, predicting BGL applications encounter two essential problems. The first problem is related to the number of times that BGL is measured each day. Unfortunately, BGL were measured a few times every day, and therefore the model missed many BGL measurements (assuming no CGMS has been used in this application). Secondly, the BGL dynamic system is highly stochastic: such that the standard deviation of the residual error was around 54 mg/dl in the proposed application. This value is considered highly significant, especially if we consider that the mean BGL for a healthy person is around 100mg/dl. Therefore, the authors applied Linear Error Modeling rules (LEM) on all the proposed models to simulate all the non-linear interactions deterministically, to obtain better prediction results, and to avoid solving complex integrals that are required for most stochastic non-linear dynamic models.

As can be seen, Tresp et al. [108] have introduced several different models with different variations and complexities. These models are the RNN, RNN-FR, RNN-TF, RNN-LEM,TSCNN, TSCNN-LEM, TSCNN-HL, TSCNN-SC, compartmental model, compartment model-LEM, and linear model. To evaluate these different predictive models, the explained variance is used. It was defined as $(1 - MSPE(model)/MSPE(mean)))$, where

MSPE (model) is the mean squared prediction error on the test set of a certain model, and MSPE (mean) is the mean squared prediction error of predicting the mean. The results showed that RNN-LEM gave the best results and outperformed both of the compartment models and TSCNN approach. The reasons that RNN has better results than the compartmental model might be attributed to the greater flexibility obtained using the RNN model, which does not depend heavily on prior physiological assumptions. Similarly, RNN outperformed the TSCNN approach due to the fact that RNN better represents dynamical systems than models whose predictions only depend on past inputs.

[91] compared the performance of the Multilayer Perception (MLP) neural network and Elman-RNN in predicting BGL for type I diabetic patients. MLP NN consisted of three layers of neural networks with a hidden layer that contains five neurons, and one output layer with one neuron. Neuron active functions of each layer were used to compute the threshold of the output layer. The *logsig* activation function was used for the output layer, and the *tansig* activation function was used for the hidden layer. The network was trained by a back propagation method. On the other hand, the Elman RNN has been modified by adding an additional feedback layer to include past activities in the prediction process. Both models have the same number of neurons, layers, type of activation functions, and training algorithm. Moreover, the input set for the two models were the same, and it included the type of insulin (short acting or long acting), the time between two consecutive glucose measurements, carbohydrate intakes, exercises intensity, stress levels, and BGL measurement at the start of the given period of time. The only difference between the two models is the feedback loops that were added in Elman RNN, as mentioned earlier. The feedback loops provide the Elman model with an internal memory that remembers the dynamic characteristics of the inputs.

The mean absolute error between the observed and predicted BGL was used to evaluate

the two models. The Elman RNN model outperformed the MLP NN model in the prediction accuracy. The mean absolute of prediction errors for the testing step of Elman RNN was equal to 1.04 mg\dl, whereas the mean absolute prediction errors for the testing step of MLP NN was equal to 2.41 mg\dl. The authors attributed the results with the fact that the current state of BGL in the glucose metabolism depends heavily on the activities that took place in the past, and the new modification of the Elman RNN satisfies this factor by its internal memory property.

The Elman neural network has been used with a neuro-fuzzy expert system in [100] to predict BGL, and it suggests a short term therapy for type I diabetic patients. The system predicts the next BGL value at time *t+1* from the previous measured BGL, anticipated diet, exercises, and insulin regimen events. It all happened at time *t*. These inputs and variables were used to generate the best set of suggested exercises, diet regimen, and insulin regimen to help the patient reach the targeted BGL. The training of the neural network was performed by using a back-propagation method, incorporating momentum, and an adaptive learning rate. The *tan-sigmoidal* activation function was used in the recurrent layer, whereas the *linear function* was used in the output layer. Ninety-five recurrent layer neurons were used to give the best results. To train the neural network, the following vector inputs were collected from the patient; the insulin vector that includes the time, the site of the injection, and the type of the insulin; the diet vector that includes the consumed carbohydrates portion and the time of meals; the exercise vector that includes the duration, the strength, the endurance, and the time of exercise; the BGL vector that includes the measurement value, the time of the measurement, and the prediction time; and finally a vector that contains the stress, illness, and other parameters.

The network was trained by allowing the patient to enter his\her BGL at time t and at time *t+1*. They had to supply the neural network with all of the events (inputs) that

occurred between these two times. Then the neural network was trained using the value of BGL at time *t+1*. After this, the neural network was presented with the events that occurred between *t+1* and *t+2*. The neural network was then trained with the BGL value at time *t+2*. In other words, the output of the trained network is the BGL of the following event step.

To evaluate the model, the difference between the prediction value and the actual value of BGL was computed. A certain value was specified to classify the performance of the proposed system. It was determined that if the difference value is less than 27mg\dl, then the performance of the model is classified as satisfactory; otherwise it will be considered as poor performance. The paper showed that the prediction values and the measured values were very close for the two cases that the model was tested on, with a difference equal to 27mg\dl or less.

A different and an interesting approach has been discussed in Kok's thesis [63] to predict BGL. The proposed system does not use a single neural network model to predict BGL for all time periods of a typical day. It has been assumed that the accuracy of the prediction depends mainly on the time of the day predicted and the factors that affect the BGL practically during that period (factors that influence BGL vary during the day). Moreover, it has been shown that there is no a particular neural network structure that performs perfectly on all of the different time periods of a typical day. Therefore, the day has been divided into four different time periods: morning, afternoon, evening, and night. A different neural network structure has been applied to each time period. For instance, a small architecture neural network with a single hidden layer with 2 nodes and a double hidden layer with 1 or 2 nodes in the first layer was used in the morning period. Moreover, the proposed approach uses a different set of input variables for each time period. The input variables of the morning period are different from the input variables of the afternoon, evening, and night periods. The input

variables of the afternoon period are also different from the input variables of the morning, afternoon, and evening periods, etc. For example, the inputs for the afternoon period are BGL, the amount of short acting insulin, food intake, and exercise and stress, while the input for the morning period are BGL, the amount of short acting insulin, food intake, and exercise and stress during the interval, long acting insulin over the past 24 hours, exercise added up squared values during past 24 hours, and the interval length. The Trial and Error method was used to determine the best input set for each time period. The total number of the input variables for the whole day was equal to 19 different inputs.

RMSE was used to evaluate the proposed neural network models and the associated inputs and parameters. Moreover, the performance of the models had been compared in different aspects, such as the structure of the neural network, the learning rate, and the model performance. The obtained results showed that the average RMSE for the morning, afternoon, evening, and night periods were 41.4 mg\dl, 37.8 mg\dl, 43.2 mg\dl, and 41.4 mg\dl, respectively. Furthermore, the best RMSE for the four mentioned time periods were 32.4 mg\dl, 32.4 mg\dl , 37.8 mg\dl, and 39.6 mg\dl, respectively. In other words, the best achieved prediction accuracies were in the range of 30-40 mg\dl, which is considered a promising result, specifically when compared to the AIDA's results [69], which has an RMSE value equal to 35mg\dl.

Baghdadi's et al.'s model [8] followed the same methodology applied in Kok's model [63] to predict BGL. It divides the typical day into four different time periods and predicts BGL for each time period separately. The typical day was represented by eight BGL measurement points that were collected at breakfast, after breakfast, lunch, after lunch, dinner, after dinner, at night, and before sleeping. Each time period contains three of these measurement points; the first one was collected at the beginning of the time period, the second one during the time period, and the last one at the end of the time period. Indeed, the authors used the

same 19 inputs that were used in Kok's research work. However, the pruning method was used to eliminate unimportant inputs for each time period and select the best input set for each time period. The input variables that have the lowest weight vector were eliminated for each time period, and those that do not affect the performance factor negatively were considered as input variables.

The Radial Basis Function (RBF) neural network has been used to predict BGL for each interval. It consisted of an input layer of source nodes, a hidden layer of high enough dimension, and an output layer that provided the response of the network to the activation patterns applied to the input layer. The average RSME was computed to evaluate the application, and the following are the corresponding values for the morning, afternoon, evening, and night periods: 1.4868 mg\dl, 0.9234 mg\dl, 0.6714 mg\dl, and 0.2124 mg\dl. In addition, the model outperformed Kok's model [63] and the AIDA system [69] with an RSME equal to 0.216 mg\dl. The obtained results, however, need to be verified more by testing the model on different data sets, and by comparing it with different models.

Following the same methodology in [63] and [8], Zainuddin et al.[116] proposed an expert system that uses the principal component analysis (PCA) technique, and Wavelet Neural Network (WNN) to predict BGL for different time periods in a typical day. The same collected 19 input variables in [63] and [8] were used, and the same methodology of modeling the day time periods was followed as well. Moreover, Zainuddin et al. proved that inputs that influence BGL vary during a day (stated in Kok's thesis too) by calculating the correlation coefficients R between the BGL of morning, afternoon, evening and night periods. It was shown that BGL for the morning, afternoon, evening, and night periods were not highly correlated to each other. For instance, the correlation factor between the morning and afternoon time periods was 0.1168, which indicated a weak correlation between the two time periods. These results might be explained by the fact that inputs that influence BGL

dominate at different time periods. In other words, inputs affect BGL concentrations for a few hours only, but are not continuous for the rest of the day.

The PCA technique used to extract the set of inputs that significantly affect BGL concentrations from the whole collected input sets make all of these correlated extracted inputs independent of each other. In the proposed application, PCA reduced the number of input variables from 19 different input variables to four input set for each time period. Three WNN models were applied to each time period. Each of these models implements a different embedded wavelet family in the hidden layer. The following wavelet families acted as activation functions in the hidden layers have been used: Mexican Hat, Gaussian wavelet, and Morlet. Moreover, the learning method of the neural network was determined by solving the pseudo-inverse with fixed parameter initialization. To avoid the overfitting problem, the multifold cross validation technique was used. It is worth pointing out that Zainuddin et al. model [116] was the first application that uses WNN in modeling BGL variations.

Several wavelet families have been used to predict BGL for each time period. RMSE was used to compare the performance of these families and to compare the performance of the application with the performance of [63] and[8]. The experiments showed that the WNN with Gaussian Wavelet (as activation function) had the best performance with the lowest RMSE for all the time periods. Therefore, it my be compared with kok's model and Baghdadi's et al.'s model. Zainuddin et al.'s model had better performance than kok's model, because the latter used a random selection method to collect the inputs, while Zainuddin et al.'s model used PCA to extract only the inputs that affect BGL significantly. On the other hand, the proposed application outperformed Baghdadi et al.'s model in the morning, afternoon, and evening periods. Combining the Gaussian function with the WNN helped the proposed application perform better than Baghdadi's et al.'s model, which uses the Gaussian function alone in the hidden nodes. However, Baghdadi's et al.'s model had a better performance in

the night interval due to the used input selection method that eliminated the past inputs from previous time periods. PCA considers all the related and valuable inputs that may influence BGL from past and present user activities, which may span more than 36 hours from the present glucose measurement, and consequently affect the prediction process negatively.(For the night interval, the RMSE of Baghdadi's et al model was 0.2124 mg\dl, whereas for the Zainuddin et al. model it was 0.306 mg\dl.)

[78][79] proposed an application that combines compartmental models and neural network models to make short-term BGL predictions. The compartmental model consists of five physiological models that simulate the effects of different types of injected insulin on plasma insulin concentration and the effects of consuming carbohydrates on the BGL. Those models are: Quick Acting (QA) Insulin Kinetics model, Short Acting (SA) Insulin Kinetics model, Intermediate Acting (IA) Insulin Kinetics model, Long Acting (LA) Insulin Kinetics model, and a model for glucose absorption from the gut. The outputs of these models, along with the recent BGL measurements, were used as inputs for the proposed neural network models to predict BGL. The two proposed neural network models are the Feed-Forward Neural Network (FFNN) and the RNN. The FFNN was trained by the batched back propagation algorithm and receives the following inputs: the most recent BGL measurement, the four vectors that describe the effects of the four types of insulin, and a vector that describes the effect of food intake. On the other hand, the RNN was trained by the online Real Time Recurrent Learning algorithm (RTRL), and it receives the following inputs: the current and previous BGL predictions, glucose concentration into the blood from the gut, and the concentration of insulin plasma after the injection of any type of insulin. The RTRL algorithm simulates the dynamic system in real time by updating the weights of the model according to the received inputs. Two different methods have been used to train the RNN: the Free-Run (FR) method and the Teacher-Forcing (TF) method. In the RTRL–FR method, the RNN ignores the

available glucose measurement, while in the RTRL–TF method, the RNN substitutes the actual output for the corresponding available glucose measurement.

The RMSE, and the correlation coefficient (cc) have been computed for all the proposed models. The results obtained from the performance assessment showed that the FFNN and RTRL-TF models performed better than the RTRL-FR model in all the patients' cases (data from children with type I diabetes have been used). Although the performance of FFNN was slightly better than the on-line RTRL-TF model, the authors preferred the on-line RTRL-TF model due to its ability to adapt the weights when a new input is received.

As we have seen, neural networks have been used intensively to predict BGL and help diabetic patients to know their future BGL concentrations ahead of time to achieve a better life style. Indeed, different structures with different input sets have been investigated to estimate BGL accurately. Some of the proposed methods used the food, exercises and insulin as input sets for their models ,as we have seen, while other models used unordinary input sets to estimate BGL for diabetic patients. For instance, [44] used blood glucose concentration, skin impedance, and heart rate as inputs to the proposed model to simulate BGL variations for type I diabetic patients. The application used a multilayer feed forward neural network to make the prediction and back propagation training method to adapt the weights. The estimated BGL was found to be correlated to the actual BGL with an accuracy within 10%. On the other hand, other published literature focused only on comparing the performance of different neural network structures in simulating the glucose dynamic system without estimating the future BGL. For example, [120] [119] compared the performance of RNN-Levenberg-Marquardt (LM) and Polynomial Neural Networks (PNN) in simulating BGL. The two models were fed by the same set of inputs (insulin, exercises, meals, BGL, and the time period between two consecutive glucose measurements) and were applied under the same conditions. The results showed that the LM-NN model outperformed the PN model

due to the type of the gathered data (not a PN type of data), and that the PN model could not successfully use the patients' activities to predict BGL.

On the other hand, time series models are used to predict future events based on recent events that have been gathered at regular time intervals. To utilize time series models in predicting BGL, the models were recursively defined at each sampling step and incorporated with a change detection method that enabled dynamic adaptation of the model to inter- and intra- subject changes and glycemic unsuitability. [15] is one of the first papers that used time series analysis methods to test whether BGL can be predicted or estimated from past BGL values. To determine if the BGL values are predictable, it was required to analyze the BGL data and test if there is a stable or evident structure in the observed data, and if the data are stationary. The paper used the autocorrelation function (ACF) to study the correlation between individual data points and measure the dependency between individual measurements that change over time. The sequence of ACF coefficients depicts the statistical dependence between the pairs of data separated by fixed-time intervals throughout the sampling process. If the data were found statistically dependent, this implied that some predictable structure exists. Moreover, if the process readings had been and remain stationary, this means that the process can be used to predict future values. The paper ,through a series of steps, proved that BGL has a structured pattern and it is stationary and predictable. A linear auto regressive model was used to predict future BGL in general, and to evaluate the linear predictability of the glycemic dynamics during glycemic disturbances. It was evaluated on different PH values, such as 10, 20, and 30 minutes. The results demonstrate that the 10- and 30- minute predictions followed the general path of BGL data. However, the 10-minutes prediction was better than the other one. The average root mean squared error value of predicting BGL with PH equals 10 minutes (under stationary disturbances) was equal to 3.60 mg\dL, which is considered an acceptable error range. Since this study, most

of the published works in this art use the auto-regressive(AR) prediction technique to predict BGL in utilizing recent BGL values. However, other studies include different inputs such as exercises and foods to increase prediction accuracy.

[104] built on Bremer and Gough's model [15] to answer a question regarding the ability of predicting BGL ahead of time to prevent or avoid hypo\hyperglycemic conditions that diabetic patients may experience. The study utilized patients' history BGL data to answer the question. These data were collected from 28 diabetic patients and monitored every three minutes for an 48-hour period. A linear model and a first-order AR model have been used with time-varying parameters. These parameters were calculated using weighted least squares on every new collected BGL sampling. Moreover, all the sample data were assigned different weights using the *forgetting factor* that improves the fit of the most recent data. Without using the forgetting factor (assigned a small value), it might take hours or days before the actual sampling time would influence the prediction.

The results proved that BGL can be predicted ahead of time, with a PH equaling to 30 minutes. This time horizon is considered a sufficient margin to take all the needed actions or treatment steps to recover a diabetic patient from hypo\hyperglycemic symptoms. Two quantitative assessments were used to compare the two models; the mean square prediction error (MSPE), and the energy of the second-order difference of the predicted profile (ESOD). MSPE determines the closeness of the predicted BGL to the measured ones, while ESOD evaluates the oscillation in the predicted BGL values. Comparing the two models using MSPE shows that they were close and similar in performance. However, evaluating the models using the EDOS technique show that the polynomial model was slightly smoother than the AR model. Another evaluation has been taken to evaluate the effects of increasing the length of PH on the precision of the prediction. As expected, increasing PH causes a larger prediction error and q wider oscillation in the predicted BGL. In general, the paper

preferred Average Glucose (AG) rather than the linear models in many aspects, especially when the forgetting factor value is considered.

[30] [28] [29] used time-series analysis to design the subject-specific glucose prediction model. The model is a low-order linear model that predicts BGL with a PH equal to 30 minutes, and it addresses the variabilities and fluctuations of BGL. It was incorporated with recursive identification and change detection methods to provide a quick adaptive response. These methods adapted the model dynamically to any changes in BGL and for any glycemic disturbances. At every BGL sampling, the system updates the parameters dynamically to reflect new information about the BGL readings. The weighted recursive least square algorithm is used to implement the recursive identification feature. The algorithm captures the BGL fluctuations or glycemic disturbances by decreasing the value of the forgetting factor when a constant change in the models' parameters is found. This way, past readings are precluded and faster convergence to new parameters is included. The parameters are not updated if the changes were not persistent. Moreover, future BGL values are predicted from the recent readings without requiring any prior information about the glycemic disturbances, such as meal consumption or insulin administration.

The proposed model in [95] [96] is a multivariate time series model that incorporated external information regarding insulin, food and physical exercises. It estimates future BGL by simulating the effects of measured inputs on BGL over a long period of time. The suggested solution proposed was a causation model that correlates the changes of BGL to the recent patients' activities (measured inputs). The measured inputs consist of 24 disturbances and are grouped into three main sets: food, activity, and stress. However, they have been reduced to 11 variables that include three food variables, seven activity variables and a time of day (TOD) variable, which is measured in minutes and represents the number of minutes in a single day. The effects of each input on BGL was determined independently and in isolation

of other inputs. However, the data were collected under free-living conditions and these data in general are highly correlated data. For instance, the carbohydrates and fats variables in the food set are highly correlated variables; they are usually increased and decreased together. Moreover, the input data can have non-linear dynamic and interactive impacts on BGL. The dynamic behavior defined as the delay between the occurrence of the input (food intake, physical exercises,etc) and the output response (future BGL).The interactive behavior is described as the modeling process of the effects of two or more variables concurrently on the desired output. For instance, the exercise event can increase or decrease BGL based on the food consumption history. Therefore, to model the effects of each input separately and address the dynamic behavior of the inputs on BGL, the block-oriented Wiener model [94] was used. In the Wiener model, each input (disturbance) is connected to a dynamic linear, block which is a set of differential equations. The intermediate output of the dynamic block is a variable that represents the dynamic response (behavior) of the corresponding input. These intermediate outputs are then passed into a static non-linear block that computes the final output, which is the glucose concentration in this context. In other words, the highly correlated inputs that enter the Wiener model will be broken down to weakly correlated variables represented by the intermediate dynamic variables. Then the effects of these weak variables are used to compute the future BGL. For instance, the intermediate variables that represent the carbohydrates and fats inputs will be weakly correlated, because their inputs have different dynamic behaviors; carbohydrates have a shorter residence time than the fats. The model was evaluated by the average absolute error (AAE) performance method. It computes the absolute difference between the measured glucose concentration and the modeled glucose concentration. The model was performing well with an AEE of 13.3 mg/dL and a fitted correlation coefficient of 0.70 for 5 min predictions. The suggested model helps type I and type II diabetic patients to manage their BGL by modeling the effects of the

food, physical exercises disturbances, and other various daily activities on the BGL. The model estimates BGL from 11 measured variables, only without utilizing previous measured glucose measurements. It is worth mentioning that this study also proposed a sub-model that predicts BGL by utilizing only the recent glucose measurements. The sub-model predicts BGL in k-steps-ahead (KSA). The results showed that BGL can be predict accurately when the number of k-steps is small, or when the PH value is short (less than 60 minutes). However, its performance degraded when the number of k-steps increased, or when the PH get longer (more than 60 minutes).

To validate the model, two continuous glucose data sets obtained under hospitalized and normal daily life conditions were used. The BGL was measured every 5 minutes for an 48 hour period in the two sets. The Sum of Squares of the Glucose Prediction Error (SSGPE) and Clarke Error Grid analysis (CG-EGA) were applied to validate the model on the two used sets. It was proved that the model was able to track and predict BGL accurately with a PH equal to 30 minutes. Since the proposed system has a small number of parameters and its computations are considered light, it can be integrated in portable devices for early hypo\hyperglycemic alarms, and for closing the glucose regulation loop with an insulin pump. The prediction model was used also in [28] to measure the required insulin infusion rate, and in [29] to predict hypo\hyperglycemic episodes and provide early notifications.

In conclusion, this section covered the significant published literature of predicting BGL on different aspects and facets. Several shared notes and findings can be summarized in the following points. A shared common finding between all the studied models is the negative correlation between the accuracy of the BGL prediction and the PH, where the accuracy of the prediction decreases when the PH increases. In fact, the most examined range for PH in the covered models is between 15 minutes to 120 minutes, with 30 minutes as the most examined value. Moreover, PH is affected directly by the type and kind of the gathered

inputs, such as exercises, insulin therapy, and\or food components. Nonetheless, few studies included other inputs that are associated with exercise activity such, as heat flux, galvanic skin response, energy expenditure (EE), heart rate, rate of perceived exertion, and sleep. Even though the main goal of most of the investigated models was predicting BGL and\or hypo\hyperglycemia risks, there are other studies that use a classifier to identify related life-threatening situations by mapping inputs to pre-established classes of recommendations [85]. Finally, the examined models have a general trend to individualize the prediction process by considering the personal lifestyle and patients' physiology to produce more accurate results.

2.3 The preliminary version of *CarbMetSim*

This section summarizes the preliminary version of *CarbMetSim* described in Aydas' dissertation [7]. However, all the aspects of the simulator were redesigned after this preliminary version as it is described in chapter 3 and chapter 4 [48].

2.3.1 Food and Exercise Description

CarbMetSim represents meals (in the preliminary and recent version) in terms of their serving size and the quantity of *rapidly available glucose* (RAG), *slowly available glucose* (SAG), protein, and fats per serving. The RAG component consists of sugars and the rapidly digestible starch (i.e. starch that was digested in vitro within 20 minutes [27],[56]), whereas the SAG encompass the slowly digestible starch (i.e. starch that was digested in vitro between 20 and 120 minutes [27],[56]). The preliminary and the current implementation of *CarbMetSim* considers the impact of protein and fat in food on gastric emptying, and this illustrates why the protein and fat components per serving are included in the food description. However, *CarbMetSim* in both implementations does not have a detailed

implementation of protein and lipid metabolism. Also, the simulator does not take into account the effect of dietary fiber (non-starch polysaccharide part of the carbohydrates) on gastric emptying, even though fibers in food are known to have an impact on gastric emptying. *CarbMetSim* does not represent protein in terms of its amino acid contents. Aerobic exercises are the only exercises that were supported by *CarbMetSim*. An exercise activity was described in terms of its intensity in units of METs, where 1 MET is 1 kcal of energy expenditure per kg of body weight per hour.

2.3.1.1 Modeling Insulin Production

The current insulin level in the preliminary and current implementation of *CarbMetSim* is represented by a variable called *insulinLevel*. In the preliminary implementation of *CarbMetSim*, the value of the *insulinLevel* was determined using the following four configurable parameters :

1. *baseGlucoseLevel_* : represents the typical fasting BGL of the individual (default value equals 100 mg/dl).

2. *highGlucoseLevel_*: represents the typical peak BGL the individual experiences (default value equals 200 mg/dl).

3. *baseInsulinLevel_*: represents the insulin level in the blood when the BGL is less than or equal to *baseGlucoseLevel_* (assigned a value between 0 and 1); The *baseInsulinLevel_* must be less than or equal *peakInsulinLevel_*.

4. *peakInsulinLevel_*: represents the ability to produce insulin (assigned a value between 0 and 1).

This implementation of *CarbMetSim* assumed a value between *baseInsulinLevel_* and *peakInsulinLevel_* for the *insulinLevel* variable. The *peakInsulinLevel_* parameter reflects

the ability of producing insulin. A value 1 implies a normal insulin production, where a value 0 denotes there is no insulin production (from pancreas) at all. Assigning a value x (between 0 and 1) for the *peakInsulinLevel_* variable indicates that the peak insulin production is just x times the normal peak. The value of the *insulinLevel* is set according the following rules. If the BGL is less than or equal to the *baseGlucoseLevel_*, the *insulinLevel* stays at *baseInsulinLevel_* . However, the variable increases linearly from *baseInsulinLevel_* to *peakInsulinLevel_* as the BGL increases from *baseGlucoseLevel_* to *highGlucoseLevel_*. If the BGL becomes greater than or equal to *highGlucoseLevel_*, the *insulinLevel* stays at *peakInsulinLevel_*. This module in the current implementation of *CarbMetSim* has been changed and updated dramatically.

2.3.1.2 Modeling Glucose Transport

CarbMetSim models the active and passive glucose transporters. The active transporters move glucose from a low concentration to a high concentration, while the passive transporters such as Glucose Transporters (GLUTs) move glucose from a high concentration to a low concentration. The acutal average amount of glucose that is transfered per minute via active transporters is computed as a poisson distributed random variable. However, *CarbMetSim* uses Michaelis Menten kinetics (described later in Section 3.3) to determine the amount of glucose transferred in a minute via passive transport. GLUT4 is the passive transporter that helps the muscles to absorb glucose from the bloodstream. The number of active GLUT4 depends on the insulin level in the bloodstream. This implementation of *CarbMetSim* models GLUT4 transporters in the resting state and uses a paramter called *glut4Impact* to model the insulin resistance and the reduced activation of GLUT4 transporters in diabetic patients. The simulator also models the impact of insulin on GLUT4.

2.3.1.3 Modeling Glucose Consumption (Modeling Glycolysis)

Glycolysis is a process that breaks down glucose to extract energy for cellular metabolism. In *CarbMetSim* the following organs uses anaerobic glycolysis to extract energy: Muscles, Liver, Kidneys, Intestine and Blood. Each of the mentioned organs has two configurable parameters: *glycolysisMin_* and *glycolysisMax_*. The organ generates at each tick a poisson distributed random number (x), with *glycolysisMin_* as the mean value and *glycolysisMax_* as the maximum value. Then based on the glucose availability in the organ, the glycolysis process consumes glucose in a tick according to this formula: $x + insulinImpact * (glycolysisMax\_ - x)$. The *insulinImpact* variable is a factor that increases in value with an increase in the *insulinLevel*. The simulator also used a configurable multiplicative parameter called *glycolysisImpact_* to modify the *glycolysisMax_* parameter associated with each organ. *glycolysisImpact_* is utilized to model the impact of diabetes on glycolysis flux. Part of the glucose consumed for glycolysis is converted to lactate, which is then added to the Blood object. The recent implementation of the simulator uses different parameters and rules to model the glycolysis process.

2.3.1.4 Modeling Gluconeogenesis

gluconeogenesis is a process that takes place in the liver and the kidney. It produces glucose by consuming lactate, glycerol, glutamine and alanine[56],[74]. Gluconeogenesis normally happens when the insulin level is low; however, high gluconeogenesis flux may occur with diabetic patients when their insulin level is high [71],[56]. The preliminary implementation of the simulator modeled the impact of insulin on gluconeogenesis flux by multiplying it with a factor that decreases in value with an increase in the *insulinLevel*. Also, it used a configurable multiplicative parameter *gngImpact_* to model the impact of diabetes on

gluconeogenesis flux by modifying the configured gluconeogenesis flux. Only the lactate concentration in the blood is being tracked in the simulator. Other substrates are assumed to be always available in sufficient quantity to allow gluconeogensis to occur.

2.3.1.5 Modeling Liver Glycogen Synthesis and Breakdown

Liver stores excess glucose in the blood during the post-prandial state as glycogen and it breaks down the stored glycogen. It releases the generated glucose to the blood during the post-absorptive state. The two mentioned processes help the human body to maintain glucose homeostasis. The preliminary implementation of *CarbMetSim* modeled the synthesis and breakdown processes simultaneously at configured rates modified by two factors each: the impact of insulin on these two processes, and the affecting of the *liverGlycogenSynthesisImpact_* and *liverGlycogenBreakdownImpact_* parameters on the glycogen synthesis and glycogen breakdown processes, respectively. For the glycogen synthesis process, the insulin factor increases in value with an increase in the *insulinLevel*. However, for the glycogen breakdown, the factor decreases in value with an increase in the *insulinLevel*. The second factor is used to model the impact of diabetes on glycogen synthesis and breakdown in the liver by modifying the configured rates multiplicatively.

2.3.2 CarbMetSim Design and Implementation

CarbMetSim is a discrete event simulator that traces how BGL in the human body is changed after a timed series of diet and exercises activities. The simulator is implemented in an object-oriented paradigm, where the key organs are represented as classes. This section covers the design and preliminary implementation of *CarbMetSim*.

2.3.2.1 HumanBody

The HumanBody class contains the following organ objects: *Stomach, Intestine, PortalVein, Liver, Kidneys, Muscles, AdiposeTissue, Brain, Heart, and Blood.* At the beginning of a simulation, the *HumanBody* uses *priority queue* to read the food events and its description. Also, it reads the intensity of different exercise activities in units of METs (into the same priority queue) and other simulation parameters that impact the operation of the human body organs. After firing a food event, the simulator adds the consumed food to the Stomach. Also, the simulator recognizes when there is no food left in the Stomach. The simulator updates\rest the energy needs of the simulated subject when there is an exercise event fired and when the simulated subject is in the reseting state, respectively. In other words, the simulated subject in *CarbMetSim* can be in any of the following body states: *Fed_Resting, Fed_Exercising, PostAbsorptive_Resting, and PostAbsorptive_Exercising.*

2.3.2.2 Blood

CarbMetSim represents the bloodstream via the *Blood* object. The *Blood* object exchanges glucose and other substrates with various organs. It maintains the following variables: glucose, lactate, branched AminoAcids, unbranched AminoAcids, *insulinLevel* variable, and *fluidVolume_* (the blood volume in the simulator). *CarbMetSim* does not maintain any other hormones in the Blood object other than *insulinLevel.*

2.3.2.3 Stomach

In *CarbMetSim*, the gastric emptying process is motivated by [54]. It is a simple mode that takes into consideration the role of fat\protein in slowing down the gastric emptying process. When a food event is fired, the consumed food enters the Stomach instantaneously, and its contents are added to any existing stores of RAG, SAG, protein and fat. *CarbMetSim*

assumes that all the food in the Stomach is in the chyme form and this amount of chyme that leaks to the Intestine (each minute) consists of one part determined using a poisson distribution (with a default mean 100 mg) and another part proportional to the total amount of chyme currently present in the Stomach. The proportional part increases linearly with a decrease in the energy density of the chyme. When the chyme consists entirely of fat (with energy density 9.0 kcal/g), the minimum value of this proportionality constant is 0.01 (the default value), and it represents the fraction leaking out of the *Stomach* object each minute (where chyme consists entirely of fat). On the other hand, when the chyme consists entirely of carbohydrate (with energy density 4.0 kcal/g), the maximum value is 9.0/4.0 times the minimum value, and it represents the fraction leaking out of the *Stomach* each minute. *CarbMetSim* does not take into account other factors that impact the gastric emptying process, such as the solid/liquid nature of food and the fiber content. Therefore, a bolus of chyme leaks from the Stomach into the Intestine every tick until the Stomach is empty.

2.3.2.4 Intestine

Carbohydrates are converted to one monosaccharide-glucose in the Intestine object. Once the Intestine receives bolus of chyme object from the Stomach, it digests some amount of its RAG/SAG component (the amount digested is calculated using normal distributions), such that most of the RAG/SAG components of a bolus are digested within 20 and 120 minutes respectively. The generated glucose of the digested RAG/SAG is added to the *glucoseInLumen* variable, where this variable represents the total glucose in the intestinal lumen. The fat components of the chyme object are simply added to the AdiposeTissue, and the protein components are added to a common protein pool in Intestine. The Intestine digests a small amount of the protein and transfers the generated amino acids to the PortalVein. On the

other hand, the glucose is moved from the intestinal lumen to the enterocytes, and then from the enterocytes to the portal vein. The Intestine object maintains two variables: *glucoseInLumen* and *glucoseInEnterocytes*, where these variables represent total glucose in the intestinal lumen and in enterocytes, respectively. In details, the Intestine moves some glucose from glucoseInLumen variable to glucoseInEnterocytes variable, so the amount moved has an active transport component (determined by poisson distribution) and a passive transport component (determined by Michaelis Menten kinetics). Also, glucose is moved from the enterocytes (glucoseInEnterocytes) to the portal vein at each tick using Michaelis Menten kinetics. Finally, the intestinal cells receives some of their energy via glycolysis process. If the glucose in enterocytes is not sufficient, the extra glucose needed for glycolysis comes from the Blood object.

2.3.2.5 PortalVein

The portal vein carries blood that moves through the intestinal tract to the liver. *CarbMetSim* represents the portal vein as a separate class from the rest of the circulatory system (represented by the Blood object) due its special role as a conduit from the intestine to the liver. PortalVein object carries the glucose and amino acids generated from the food digestion in the Intestine to the Liver. Also,the PortalVein moves all the amino acids received from the Intestine to the Liver during each tick. Because the portal vein is a part of the circulatory system, *CarbMetSim* maintains the glucose concentration of the PortalVein as rest of the circulatory system, when no new glucose is being received from the intestine.

2.3.2.6 Liver

The Liver's operations are implemented in the *CarbMetSim* as following. Liver absorbs via GLUT2s some glucose from the PortalVein when the glucose level in the PortalVein is

higher than what is in the Liver. On the other hand, if the glucose concentration in the Liver is higher than what is in the Blood, some glucose will be released to the Blood via GLUT2s. The amount of the glucose absorbed/released is determined using Michaelis Menten kinetics. Liver converts some of the glucose to glycogen and breaks down some glycogen to glucose in the manner described previously. Moreover, Liver converts excess glycogen to fat, and stores it in AdiposeTissue when the glycogen level exceeds its maximum configured value (equivalent to 120 grams of glucose by default). The Liver consumes some glucose for glycolysis and produces glucose via the gluconeogenesis process. 93% of unbranched amino acids received from the PortalVein is consumed by the Liver, and the rest (along with all the branched amino acids) is released to the Blood.

2.3.2.7 Kidneys

One of the significant tasks for the kidneys is filtering the blood from waste and extra fluid. The kidneys obtain the needed energy for this task from the oxidation and glycolysis processes. *CarbMetSim* represents the kidney operations in the Kidneys object. At each tick, the Kidneys do the following: Glycolysis, Gluconeogenesis, and Glucose Excretion in Urine. In the later operation, when the glucose concentration in the Blood object increases from 11 mmol/l (by default [43]) to 22 mmol/l , the glucose excretion in urine increases linearly from zero to a certain peak level (100 mg/min by default).

2.3.2.8 Muscles

CarbMetSim represents the skeletal muscles in the Muscles class. The preliminary implementation of *CarbMetSim* simulates the response to aerobic exercise only. The summary of the simulator's operations when the HumanBody is in Fed Resting, PostAbsorptive Resting, Fed Exercising, or PostAbsorptive Exercising states is as follows.

The Muscles perform the following operations when the HumanBody is in the Fed Resting or PostAbsorptive Resting state (during a tick):

1. Glucose Absorption: Where the glucose is absorbed by GLUT4 as stated previously. Moreover, a basal absorption via GLUT1s happens at a certain configured rate.

2. Glycolysis: A portion of absorbed glucose is consumed via glycolysis and the resulting lactate is added to the Blood.

3. Glycogen Synthesis: Some of the absorbed glucose is converted to glycogen when the glycogen store of the Muscles is less than a configurable maximum value.

4. Oxidation: Remainder of the absorbed glucose is consumed via oxidation.

5. Fatty Acid Consumption: Muscles consume fat from the AdiposeTissue to meet the remaining energy needs when the glycolysis and glucose oxidation processes do not meet the energy needs during the resting state.

The Muscles perform the following operations when the HumanBody is in the Fed Exercising or PostAbsorptive Exercising state (during a tick):

1. Oxidation: Glucose absorbed from Blood or derived from locally stored glycogen is oxidized to meet portion of the energy needs of the human body during exercise.

2. Glycolysis: The glycolysis flux increases from the average value (glycolysisMin_) linearly with exercise intensity. The peak level (glycolysisMax_) is achieved when the intensity of the exercise is 18 METs. The glucose 6-phosphate consumed for glycolysis comes from locally stored glycogen.

3. Fatty Acid Consumption: Muscles consume fat from the AdiposeTissue to meet the remaining energy needs when the glucose oxidation and glycolysis described above do not meet the energy needs.

2.3.2.9 Adipose Tissue

The AdiposeTissue in *CarbMetSim* serves as the storage for fat. The Liver converts excess glycogen to fat and then stores it in the AdiposeTissue. Also, the Intestine object adds the fat contents in chyme to the AdiposeTissue object. The Muscles object removes fat from the AdiposeTissue to meet the energy needs. *CarbMetSim* does not have detailed implementation of the lipid metabolism.

2.3.2.10 Brain

The brain uses GLUT3 transporters to absorb glucose from the bloodstream and oxidizes glucose to meet the energy needs. The brain oxidizes about 120 g of glucose per day, which is equivalent to absorbing 83.33 mg of glucose per minute [57]. *CarbMetSim* models the brain operation in the Brain class, where the Brain object consumes on average 83.33 mg of glucose every minute from the Blood object.

2.3.2.11 Heart

The heart meets most of its energy needs by oxidizing fatty acids. Also, it utilizes glucose and lactate to meet up to 30% of the its energy needs[57]. The Heart object in *CarbMetSim* models the heart operation. It absorbs glucose to meet its energy needs during the fed state.

As mentioned previously, all the aspects of the simulator were redesigned after this preliminary version as it is described in subsequent chapters.

Chapter 3

Key Aspects in CarbMetSim design

This chapter describes the key aspects of *CarbMetSim's* design.

3.1 Food, Exercise and Human Subject Description

CarbMetSim represents meals in terms of their serving size and the quantity of *rapidly available glucose* (RAG), *slowly available glucose* (SAG), protein and fats per serving. The RAG component consists of sugars and the rapidly digestible starch (i.e. starch that was digested in vitro within 20 minutes [27],[56]), whereas the SAG encompass the slowly digestible starch (i.e. starch that was digested in vitro between 20 and 120 minutes [27],[56]). The dietary fiber (non-starch polysaccharide part of the carbohydrates) is currently not considered or represented in the simulator, even though fibers in food are known to have an impact on gastric emptying. Also, the simulator does not have a detailed implementation of protein and lipid metabolism. It provides a model of the impact of protein and fat contents of food on gastric emptying. Therefore, the total amount of protein and total amount of fat per serving is listed in the food description, which is one of the input files to the simulator. *CarbMetSim* presently does not represent protein in terms of its amino acid contents. Gleeson [45] stated that 3 of the 20 amino acids have branched chains; therefore a general assumption is made that 85% of amino acids that come from protein digestion have unbranched chains and the remainder have branched chains.

Aerobic exercises are the only exercises that can be simulated by *CarbMetSim*. An exercise activity is described in terms of its intensity in units of METs, where 1 MET is

1 kcal of energy expenditure per kg of body weight per hour. By convention, 1 MET is considered equivalent to 3.5ml of oxygen consumption per kg of body weight per minute. In general, each person consumes oxygen up to a certain rate. This personalized maximal rate, called ($\%VO_2max$), depends on the following factors or attributes of the individual being simulated: gender, age and fitness level of the individual [58].

Representing the intensity of a physical activity in terms of the associated oxygen consumption rate determines the relative fraction of the glucose and fatty acids oxidized to meet the energy needs of the exercising muscles. Note that the intensity reported as the % age of the individuals ($\%VO_2max$), and it represents the specific oxygen consumption rate associated with each individual. Therefore, *CarbMetSim* needs to know the gender, age and fitness level within the age group of the individual being simulated to estimate the ($\%VO_2max$) for the individual using the tables in Kaminsky, et al. [58].

3.2 Modeling Insulin production

BGL is one of the main factors that determines the insulin level in the blood. If the BGL is high, the insulin level will increase in order to simulate the liver and the muscle tissues to absorb glucose from the blood, and also to signal both the liver and the kidneys to minimize or halt the endogeneous glucose production through glycogen breakdown and gluconeogenesis processes. On the other hand, the insulin level in the blood decreases when an individual physically exercises, [110],[102],[111], [39],[115], and therefore the liver and the kidneys in response increase the production of glucose.

CarbMetSim uses a variable called *insulinLevel* (inside the *Blood* object) to represent the current insulin level in the blood, and it assigns values between 0 and 1 to the variable. The value of *insulinLevel* depends on the following variables:

1. current BGL,

2. the current exercise intensity (in $\%VO_2max$),

3. and other configurable parameters:

   (a) *minGlucoseLevel_*: represents typical hypoglycemic BGL.

   (b) *baseGlucoseLevel_*: represents typical fasting BGL.

   (c) *highGlucoseLevel_*: represents typical peak BGL, where (minGlucoseLevel_ < baseGlucoseLevel_ < highGlucoseLevel_).

   (d) *baseInsulinLevel_*: represents the typical fasting insulin level.

   (e) *peakInsulinLevel_*: represents typical insulin level when BGL is at peak, where where $0 \leq$ baseInsulinLevel_$\leq$ peakInsulinLevel_≤ 1.

   (f) *restIntensity_*: represents the oxygen consumption rate in $\%VO_2max$ when the individual is in rest state (not exercising), by default 2 METs converted to $\%VO_2max$.

   (g) *intensityPeakGlucoseProd_*: represents the exercise intensity in $\%VO_2max$ at which the liver and kidney produce glucose at the maximum rate (by default 20%).

CarbMetSim uses the following rules to determine the value of *insulinLevel*:

1. if the current BGL is less than or equal to the minGlucoseLevel_, the *insulinLevel* stays at value zero.

2. if the current BGL is between the minGlucoseLevel_ and the baseGlucoseLevel_, the *insulinLevel* depends on if the human subject being simulated is currently engaged in physical activity or not. If the human subject is practicing and the exercise intensity is greater than or equal to intensityPeakGlucoseProd_, the *insulinLevel* stays at zero.

On the other hand, the *insulinLevel* depends on the exercise intensity. As the exercise intensity decreases from intensityPeakGlucoseProd_ to the the restIntensity_, the *insulinLevel* increases linearly from zero to the baseInsulinLevel_ However, If the individual is in the rest state (not exercising), and the BGL increases from minGlucoseLevel_ to baseGlucoseLevel_, the *insulinLevel* increases linearly from zero to the baseInsulinLevel_.

3. In the time the BGL increases from the baseGlucoseLevel_ to the highGlucoseLevel_, the *insulinLevel* increases linearly from the baseInsulinLevel_ to the peakInsulinLevel_.

4. If the BGL is greater than or equal to the highGlucoseLevel_, the *insulinLevel* stays at the peakInsulinLevel_ value.

As discussed earlier, the peakInsulinLevel_ variable represents the peak ability to produce insulin. When peakInsulinLevel_ equals 1, this means that the pancreas produces a normal (or excessive, as in the case of initial stages of type II diabetes) production of insulin. However, assigning a value 0 to peakInsulinLevel_ means that the pancreas does not produce any insulin at all (type I diabetes). Assigning a value x (between 0 and 1) to the variable means that peak insulin production is just x times the normal peak.

The value of *insulinLevel* should be understood as the impact it has on various organ objects, rather than the absolute insulin concentration associated with a particular human subject. Indeed, the variable has a deep impact on the operation of different organ objects in *CarbMetSim*. In other words, it is not unexpected to have two different insulin concentrations for two individuals, in which both of them have the same value for the *insulinLevel*, because they have the same impact on carbohydrate metabolism related functions of the organs.

3.3 Modeling glucose transport

Two types of glucose transporters help in moving glucose into human body cells. The first type is the active transporters that move glucose from a low concentration to a high concentration, such as *Sodium GLucose coTransporters (SGLTs)* . The second type, are the passive transporters, such as *Glucose Transporters* (GLUTs) that move glucose from a high concentration to a low concentration.

The operation of active transporters in an organ is modeled by specifying the average amount of glucose transferred per minute via active transport. The actual amount transferred is a poisson distributed random variable. On the other hand, the simulator employ *Michaelis Menten* kinetics to set the amount of glucose transferred in a minute via passive transport. According to Michaelis Menten kinetics, the rate of transport (V) across a membrane depends on the difference in the substrate concentration (Y) across the membrane in the following manner: $V = V_{max}\frac{Y}{Y+k_m}$, where V_{max} is the maximum rate of transport and k_m is the substrate concentration difference at which the transport rate is half the maximum. The simulator uses the V_{max} value associated with a GLUT transporter in an organ to determine the number of transporters involved, and it treats the V_{max} (associated with a particular GLUT in a particular organ) as a poisson distributed random variable with a configurable mean.

There are many types of GLUT transporters in the human body, and one of them is the GLUT4 transporters. These transporters allow muscles to absorb glucose from the bloodstream, and therefore they play a main role in moving glucose into cells. GLUT4 transporters are activated by two different ways, depending on the status of the individual. If the individual is in the rest state (not exercising), the number of active GLUT4 transporters depends on the insulin level in the bloodstream. When the insulin level is low, GLUT4

transporters are inactive and the muscles do not absorb enough glucose from the bloodstream. GLUT4 transporters get active when the insulin level rises in the blood, and which makes the muscles to absorb excess glucose from the blood. On the other hand, GLUT4 transporters are activated when the human subject is engaged in physical activity. The exercise itself activates a sufficient number of GLUT4 transporters [93],[46],[112] to simulates muscles to absorb the needed amount of glucose from the bloodstream. The simulator replicates both behaviors. Indeed, *CarbMetSim* models the GLUT4 activation during the resting states by configuring the V_{max} value associated with GLUT4 transporters in the following manner:

1. Since muscles convert and store a large fraction of the absorbed glucose to glycogen and there is a limit on the amount of stored glycogen inside muscles, the current amount of muscle glycogen impacts the V_{max} value. In particular, when the muscle glycogen storage increases from zero to a configurable maximum value, the V_{max} value reduces linearly from a configurable maximum (7 mg/kg/min by default) to a configurable minimum (3.5 mg/kg/ min by default).

2. The impact of the insulin level is modeled by multiplying the V_{max} value with a factor that increases in value with an increase in the *insulinLevel*. The *insulinLevel* itself is used as the value of this factor, and it is assigned values between between 0 and 1. Intense physical exercise causes a temporary increase in glucose absorption by muscles [3] to make up for the glycogen lost during exercise, therefore the *insulinLevel* does not impact the V_{max} value in the first hour after a robust physical exercise activity (except if the current BGL is below the baseGlucoseLevel_).

3. The impact of insulin resistance in reducing the activation of GLUT4 transporters is modeled by multiplying the V_{max} value with a configurable parameter (glut4Impact_) that assumes values between 0 and 1 (by default 1.0).

3.4 Modeling glycolysis

Human tissues depend on glucose as one of the main sources of energy to maintain their metabolisms. Human cells either oxidize glucose completely or consume it anaerobically via the process of *glycolysis*. Aerobic metabolism (complete oxidation of glucose) generates 15 times more energy than anaerobic glycolysis, but it can only happen if oxygen is available. Tissues with access to sufficient amounts of oxygen oxidize glucose for their energy needs, whereas others use glycolysis. The following are the organs that use anaerobic *glycolysis* as an energy source in *CarbMetSim*: *Muscles, Liver, Kidneys, Intestine and Blood.* The insulin level in the bloodstream determines the amount of glucose consumed for glycolysis process. In other words, the consumed amount of glucose increases with the glucose availability (high insulin levels). The simulator models this process in the following manner:

1. There are two configurable parameters for each organ using glycolysis as an energy source: *glycolysisMin_* and *glycolysisMax_*. These parameters are in units of mg of glucose consumed per kg of body weight per minute.

2. At each tick, the organ generates a poisson distributed random number (min) with *glycolysisMin_* as the mean value and *glycolysisMax_* as the maximum value. Then, based on the glucose availability in the organ, the amount of glucose consumed in a tick for glycolysis is given by: $min + insulinImpact * (glycolysisMax\_ - min)$. The *insulinImpact* is a factor that is assigned a value between 0 and 1. It increases in value with an increase in the *insulinLevel*, and it is calculated using a sigmoid function, which is currently the CDF of a normal distribution with a configurable mean and standard deviation.

3. To model the impact of diabetes on glycolysis flux, *CarbMetSim* uses configurable

multiplicative parameters *glycolysisMinImpact_* and *glycolysisMaxImpact_* (with default values 1.0) to modify the values of *glycolysisMin_* and *glycolysisMax_* parameters associated with each organ.

The *glycolysis* process generates lactate, which serves as a key substrate for endogenous glucose production via *gluconeogenesis* (discussed later). Indeed, a fraction (by default 1) of the glucose consumed for glycolysis is converted to lactate, and added to the *Blood* object. Table 3.1 shows the default values for glycolysis related parameters for different organs. The relative contributions of different organs towards overall glycolysis flux were set as suggested in [43][113]. The default values of various configurable parameters in *CarbMetSim* were determined experimentally to provide a close match with published measurements performed on non-diabetic human subjects before and after a meal event [114].

Organ	glycolysisMin_ (mg/kg/minute)	glycolysisMax_ (mg/kg/minute)
Blood	0.0315	0.1135
Kidneys	0.0315	0.1135
Liver	0.0630	0.5675
Muscles	0.0630	0.8512
Intestine	0.0315	0.1135

Table 3.1: The default values for glycolysis related parameters in various organs.

3.5 Modeling gluconeogenesis

When the human body is not receiving new glucose via food and the glycogen store in the liver has been exhausted, the glucose is produced through a different metabolic pathway called *gluconeogenesis*. This metabolic pathway motivates the liver and kidneys to produce glucose from lactate, glycerol, glutamine and alanine [37],[75]. Typically, gluconeogenesis

occurs when the insulin level is low. However, diabetic people may experience high gluconeogenesis flux even when the insulin level is high[71][90].

The Liver and the Kidneys (in *CarbMetSim*) produce glucose via gluconeogenesis using the substrates mentioned above. *CarbMetSim* assumes that the substrates are always available in sufficient amounts to allow gluconeogenesis to take place. The simulator uses two configurable average rates to produce glucose; *gngLiver_* and *gngKidneys_* with a default value equal to 0.16 mg/kg/minute for each parameter.

CarbMetSim models the process of producing glucose via the gluconeogenesis pathway. If the *insulinLevel* is above the *baseInsulinLevel_*, the average gluconeogenesis flux is multiplied by a factor that has a value between 0 and 1. This factor decreases in value with an increase in the *insulinLevel* as per an inverse sigmoid function (currently, the complementary CDF of a normal distribution with a configurable mean and standard deviation). This simulates the process of the decrease in gluconeogenesis flux with an increase in the insulin level. On the other hand, the simulator models the increased gluconeogenesis flux when BGL is low and gluconeogenesis is probably the only source of glucose for the body. If the *insulinLevel* is below the *baseInsulinLevel_*, the average gluconeogenesis flux is multiplied by a factor that decreases in value from a configurable maximum ($gngImpact\_ \geq 1$, by default 6.0) to the minimum value 1 as the *insulinLevel* increases from zero to the *baseInsulinLevel_*.

3.6 Modeling Liver glycogen synthesis & breakdown

The liver plays an important role in monitoring and maintaining normal blood glucose concentrations. The liver stores and converts excess glucose in blood as glycogen when the insulin levels are high (during the post-prandial state). Also, the liver breaks down the stored glycogen and releases glucose to the blood when the insulin level is low (during the post-absorptive and exercising state). Diabetes may effect both glycogen synthesis and

breakdown in the liver.

The exact amount of glycogen synthesized by the *Liver* object during each tick is a poisson distributed random variable with a configurable average (*glucoseToGlycogenInLiver_*, 4.5 mg/kg/min by default). The amount of synthesized glycogen depends on the availability of glucose; also the poisson variable is modified multiplicatively by two factors. The first one models the effect of insulin on glycogen synthesis. The factor is assigned values between 0 and 1, and it increases in value with increases in the *insulinLevel*. It is calculated using a sigmoid function, which is currently the CDF of a normal distribution with a configurable mean and standard deviation. The second factor called *liverGlycogenSynthesisImpact_* modifies the configured average multiplicatively to model the impact of diabetes on glycogen synthesis in the Liver. It has value 1.0 as a default. The *Liver* object has a limited capacity to store glycogen, and hence any excess glycogen is converted to fat and stored in the *AdiposeTissue*.

As mentioned above, the glycogen breakdown in the liver serves as the key source of glucose, so the body does not run out of glucose, especially when no new glucose via food is entering the body or when the body is experiencing an intensive physical exercise, and the glucose needs of the body is high. Therefore, the amount of glycogen stored in the Liver that is broken down to glucose during a tick closely depends on the *insulinLevel*. In *CarbMetSim*, the average glycogen breakdown flux in the Liver is represented by *glycogenToGlucoseInLiver_* variable (0.9 mg/kg/min by default). When the *insulinLevel* is above the *baseInsulinLevel_*, the average glycogen breakdown flux in Liver is multiplied by a factor (between 0 and 1) that decreases in value with increases in the *insulinLevel* as per an inverse sigmoid function, which is currently the CDF of a normal distribution with a configurable mean and standard deviation. Typically, this occurs when the BGL is more than the *baseGlucoseLevel_*, to model the decrease in Liver glycogen breakdown when there is an increase in the insulin level. On the other hand, the simulator models the increased Liver

glycogen breakdown when BGL is below the *baseGlucoseLevel_*. If the *insulinLevel* is below the *baseInsulinLevel_*, the average Liver glycogen breakdown flux is multiplied by a factor that decreases in value from a configurable maximum (*liverGlycogenBreakdownImpact_* ≥ 1, by default 6.0) to the minimum value 1 as the *insulinLevel* increases from zero to the *baseInsulinLevel_*.

Chapter 4

CarbMetSim design and implementation

CarbMetSim is a discrete event simulator that tracks the changes of BGL of a human subject after a timed series of diet and exercises activities. The simulator is implemented in an object-oriented paradigm, where the Key organs are represented as classes in the *CarbMetSim*. On top of these classes, the simulator has a *SimCtl* (SIMulation ConTroLler) class and a *HumanBody* class. The SimCtl contains a data structure of type a *priority queue* that stores the food/exercise events sorted in order of their firing times. Also, the class maintains the simulation time in ticks, where each tick is a minute. At the beginning of the simulation, the *SimCtl* object reads all the food/exercise events into the priority queue. At each tick, the *SimCtl* object fires the events whose firing time has arrived. Once the event has fired, the simulator invokes the appropriate methods of the HumanBody class, and then makes each organ to do its work during the tick time.

In this chapter, the implementation and the operation of the different classes (the roles of organs) of the simulator are discussed and described. The default values of different parameters mentioned in this chapter were determined experimentally to provide a close match with published measurements performed on non-diabetic human subjects before and after a meal event [114]. Table 4.1 shows the default values of configurable parameters that determine the effect of *insulinLevel* on various metabolic processes.

4.1 HumanBody

The HumanBody class contains the following organ objects: *Stomach, Intestine, PortalVein, Liver, Kidneys, Muscles, AdiposeTissue, Brain, Heart and Blood.* At the beginning of a simulation, the *HumanBody* object does the following:

1. It reads the constituents of the consumed foods in terms of *rapidly/slowly available glucose (RAG/SAG)*, protein and fat.

2. It reads the intensity of different exercise activities in units of METs.

3. It calculates the maximal rate of glucose consumption ($\%VO_2max$), associated with the human subject being simulated using the tables in [58]. The simulator is supplied with the parameters of the individual's (being simulated) gender, age and self-assessed fitness level within his\her age group.

4. It reads other simulation parameters that impact the operation of different organs.

Parameter	Default Value
insulinImpactOnGlycolysis_Mean	0.5
insulinImpactOnGlycolysis_StdDev	0.2
insulinImpactOnGNG_Mean	0.5
insulinImpactOnGNG_StdDev	0.2
insulinImpactGlycogenBreakdownInLiver_Mean	0.1
insulinImpactGlycogenBreakdownInLiver_StdDev	0.02
insulinImpactGlycogenSynthesisInLiver_Mean	0.5
insulinImpactGlycogenSynthesisInLiver_StdDev	0.2

Table 4.1: Configurable parameters (and their default values) for the mean and standard deviation of normal distributions to determine the impact of *insulinLevel* on various metabolic processes.

The *SimCtl* object calls a HumanBody's method at each tick. This method causes other methods to engage with individual organ objects that allow the organs to do their work

during that tick. The HumanBody (through methods) adds the consumed food to the Stomach when *SimCtl* fires a food event; also, it get notified by the Stomach when there is no food left. On the other hand, the HumanBody updates the energy needs of the body when *SimCtl* fires an exercise event. When the exercise event ends, the HumanBody resets the energy needs to the resting state. Therefore, the HumanBody remembers whether the Stomach has some undigested food (Fed) or not (PostAbsorptive) and whether the body is currently engaged in exercise (Exercising) or not (Resting). The simulated human subject in *CarbMetSim* can be in any of the following body states: *Fed_Resting, Fed_Exercising, PostAbsorptive_Resting and PostAbsorptive_Exercising*. The simulator is configurable to allow different values for the configurable parameters that control the operation of the organs based on the current body state (Fed_Resting, Fed_Exercising, PostAbsorptive_Resting and PostAbsorptive_Exercising).

4.2 Blood

CarbMetSim represents the bloodstream via the *Blood* object, where the object collaborates with various organs to exchange glucose, amino acids and other substrates. The *Blood* object maintains the following substrate variables: glucose, lactate, branched AminoAcids (consumed by muscles, adipose tissue and brain) and unbranched AminoAcids. The *Blood* object also maintains the *insulinLevel* variable and a variable representing the blood volume (5 liters by default) called *fluidVolume_* . *CarbMetSim* maintains the insulin hormone only. At each tick, the *Blood* object updates the *insulinLevel* as described in Section 4.2. Also, some glucose is consumed for glycolysis in the manner described in Section 4.4.

4.3 Stomach

The process of emptying food from the stomach into the intestine is known as the *gastric emptying* process. Gastric emptying is a complicated process and it is affected by several factors such as the volume, particle size, viscosity, osmolarity, acidity and nutritional contents of the meal [70], [76] [52]. Several mathematical models have been proposed simulating the gastric emptying process. For instance, [73], [53] proposed exponential models, where [26] suggested power exponential functions. Other complicated models were proposed too. For example, [23] suggested a three-compartment model of the gastrointestinal tract where the gastric emptying rate follows a trough-shaped pattern (initially high followed by a non-linear decrease to a minimum value followed by a non-linear increase back to the initial maximum value). Moreover, [68] proposed a simple model for gastric emptying of carbohydrates in a meal, where the rate of gastric emptying has three phases—a linear increase phase, a constant maximum rate phase and a linear decrease phase.

In *CarbMetSim*, the gastric emptying process is motivated by [54]. It is a simple mode that takes into consideration the role of fat\protein in slowing down the gastric emptying process. When a food event is fired, the consumed food enters the Stomach instantaneously, and its contents are added to any existing stores of RAG, SAG, protein and fat. *CarbMetSim* assumes that all the food in the Stomach are in the chyme form and that the amount of chyme leaking to the Intestine each minute consists of one part determined using a poisson distribution (with a default mean 500 mg) and another part proportional to the total amount of chyme currently present in the Stomach. The proportional part increases linearly with a decrease in the energy density of the chyme. When the chyme consists entirely of fat (with energy density 9.0 kcal/g) the minimum value of this proportionality constant is 0.03 (the default value) and it represents the fraction leaking out of the *Stomach* object each minute.

On the other hand, when the chyme consists entirely of carbohydrate (with energy density 4.0 kcal/g), the maximum value is 9.0/4.0 times the minimum value, and it represents the fraction leaking out of the *Stomach* each minute. *CarbMetSim* does not take into account other factors that impact the gastric emptying process, such as solid/liquid nature of food, and the fiber content. Therefore, a bolus of chyme leaks from the Stomach into the Intestine every tick until the Stomach is empty. The nutritional composition of leaked chyme is the same as that of chyme present in the stomach.

4.4 Intestine

The following are the main four operations that occur in the *Intestine* object in *CarbMetSim*:

Carbohydrate Digestion:

The intestine uses different enzymes to digest the carbohydrates in the chyme (received from stomach) to produce *monosaccharides* such as glucose, fructose and galactose [57]. *CarbMetSim* converts all the carbohydrates in the chyme to just one monosaccharide—glucose. With every tick, the Intestine receives a bolus of chyme from the Stomach as long as there is some food in it. The Intestine class maintains a list of *Chyme* objects where each object includes the undigested RAG / SAG contents of each bolus obtained from the Stomach and the moment it acquired the bolus. Moreover, the Intestine digests a certain amount of RAG / SAG from a Chyme entity at each tick. The amount digested from a specific *Chyme* object is determined using normal distributions with default mean and standard-deviation, as follows: 2 minutes & 0.5 minutes for RAG and 30 minutes & 10 minutes for SAG. Most of the RAG and SAG contents of the bolus are digested within 20 and 120 minutes, respectively, after the bolus has entered the Intestine. The produced glucose from the Carbohydrate digestion is added to a variable (in *Intestine* object) called

glucoseInLumen. The variable represents the total glucose present in the intestinal lumen.

Fat and Protein Digestion: When the *Intestine* receives a chyme bolus, it adds its fat contents to the *AdiposeTissue*. Also, it adds the protein contents to a common protein pool in the *Intestine*. The *Intestine* object, at each tick, digests an amount of this protein and transfers the resulting amino acids to the *PortalVein*. This digested amount is determined as per a poisson distribution with a default mean 1 mg. The simulator does not keep track of the dietary protein's amino acid composition and makes a simple assumption that 85% of these amino acids are unbranched and the remaining 15% are branched.

Glucose Absorption from Intestine to PortalVein: Glucose moves from the intestinal lumen to the enterocytes through the border membrane of the brush and from the enterocytes to the portal vein through the basolateral membrane. The transmission from the intestinal lumen is carried out by the combination of active (SGLT-1) and passive (GLUT2) transporters in which the amount of GLUT2 transporters is dependent on the level of the glucose on the lumbar side. However, the transfer from the enterocytes to the portal vein takes place solely via passive GLUT2 transporters [57]. *CarbMetSim* uses two variables, *glucoseInLumen* and *glucoseInEnterocytes*, inside the the *Intestine* object, to represent the total glucose present in the intestinal lumen and in enterocytes, respectively. At each tick, the Intestine moves some glucose from the *glucoseInLumen* variable to *glucoseInEnterocytes* variable. The amount moved has an active transport component and a passive transport component. The active component is determined via poisson distribution, where the default mean equals 30 mg/minute. The passive transport component is determined using Michaelis Menten kinetics (assuming configurable volumes for the lumen and the enterocytes). The V_{max} value used for Michaelis Menten kinetics increases with glucose levels in the lumen with a default maximum value of 800 mg/minute. The K_m value used is 20 mmol/l by default

[57]. The transfer of glucose from the enterocytes to the portal vein is determined by transferring some glucose from *glucoseInEnterocytes*, at each tick, to the *PortalVein*. The amount moved is determined using Michaelis Menten kinetics (average V_{max}= 800 mg/ minute, K_m = 20 mmol/l by default [57]).

Glycolysis: In the way mentioned in Section 4.4, the intestinal cells get some of their energy via glycolysis of glucose. If the glucose in enterocytes (*glucoseInEnterocytes*) is not enough, the extra glucose needed for glycolysis comes from the bloodstream (the *Blood* object).

4.5 PortalVein

The portal vein carries blood that passes through the intestinal to the liver. *CarbMetSim* treats the portal vein as a separate class from the rest of the circulatory system (represented by the Blood class), due to its particular role as a conduit from the intestine to the liver. *CarbMetSim* passes the glucose and amino acids, resulting from food digestion in the Intestine, to the Liver through the PortalVein. Because the portal vein is part of the circulatory system, where no new glucose is obtained from the Intestine, the portal vein must have the same glucose concentration as the rest of the circulatory system. It is implemented in the following way with *CarbMetSim*. At the beginning of a tick, there is no glucose in the PortalVein. During each tick, the following sequence of actions take place:

1. The PortalVein imports glucose from the Blood. The glucose levels in the PortalVein must match the glucose levels in the Blood before the import process. The PortalVein's volume is a configurable parameter with default value 5 dl. It is used to calculate the glucose concentration.

2. The transfer of glucose takes place from the Intestine to the PortalVein (as described

previously) and then from the PortalVein to the Liver (described later).

3. After this, any glucose remaining in the PortalVein is transferred back to the Blood. Also, *CarbMetSim* moves all the amino acids received from the Intestine to the Liver during that tick itself.

4.6 Liver

When the glucose level in the portal vein is high, the cells in the liver absorb glucose from the portal vein through GLUT2s transporters. The absorbed glucose is phosphorylated to glucose 6-phosphate, which will be used for glycogen synthesis or glycolysis. In the liver, the Insulin hormone and glucose activate glycogen synthesis enzymes and block the glycogen breakdown enzymes. Moreover, the insulin hormone activates the glycolysis of glucose 6-phosphate in liver cells to produce pyruvate, some of which is oxidized, and the remaining is converted to lactate and released to the bloodstream. However, insulin insufficiency activates the process of glycogen breakdown and the gluconeogenesis process (as described in chapter 4). The gluconeogenesis flux increases with the availability of the lactate, alanine, glycerol, and other substrates in the bloodstream even if the level of insulin is high. If the glucose levels and insulin levels are high, the liver uses the excess glucose for synthesizing glycogen. However, if the insulin level is low, the excess glucose may leave the liver cells via GLUT2s and probably other means. Also, a high insulin levels make some of the excess glucose to be converted into lipid. The main roles of the liver in the fed and post-absorptive states can be summarized as follows. During the fed stage, the liver absorbs glucose and uses this for glycogen synthesis and glycolysis. However, during post-absorptive and exercise states, the liver releases glucose to the bloodstream though the glycogen breakdown and gluconeogenesis processes. Another essential operation of the liver is its oxidation of unbranched amino acids,

which supplies nearly half the energy requirements of the liver.

The Liver class in *CarbMetSim* implements the aforementioned operations of the liver. It maintains the initial and the allowable maximum amount of stored glycogen as configurable variables (parameters). The initial value of this variable guarantees that the Liver is able to produce 100 grams of glucose at the beginning of a simulation. However, the upper default amount of allowable stored glycogen in the Liver is equivalent to 120 grams of glucose.

The *Liver* object does the following at every tick:

1. Glucose Absorption\Release: When the glucose level in the PortalVein is greater than in the Liver, some glucose will be absorbed into the Liver by GLUT2 transporters. Likewise, if the concentration of glucose in the Liver is higher than into the Blood, GLUT2 transporters transfer some glucose to the Blood. The amount of glucose absorbed\released is calculated using Michaelis Menten kinetics (V_{max} = 50mg/kg/min by default and K_m = 20 mmol/l by default) [57]).

2. Glycogen Synthesis\Breakdown: The Liver synthesizes or breaks down glycogen in the particular way described in Section 4.6.

3. Lipogenesis: If the Liver glycogen production meets its configurable maximum value, the excess glycogen is converted into fat that is stored in AdiposeTissue.

4. Glycolysis and Gluconeogenesis: The Liver absorbs some glucose for glycolysis and produces glucose through *gluconeogenesis*, as stated in in Section 4.4 and Section 4.5, respectively.

5. Amino Acid Consumption: The Liver absorbs 93% of the unbranched amino acids obtained from the PortalVein and transfers the remainder togather with all the branched amino acids to the Blood.

4.7 Kidneys

One of the significant tasks for the kidneys is filtering the blood from waste and extra fluid. This task requires considerable energy. In general, the kidneys obtain the needed energy from oxidation and glycolysis processes. Their outer layer (the cortex) is well supplied with oxygen and therefore meets its energy needs through the oxidation of the absorbed glucose and fatty acids from the bloodstream. The inner center (the medulla) gets its energy from anaerobic glycolysis. Moreover, the kidneys produce glucose through gluconeogenesis. *CarbMetSim* simulates the main operations of the kidney through the Kidneys class. The *Kidneys* object do the following at every tick:

1. Glycolysis: The kidney fulfills its energy requirements through glycolysis, as mentioned in Section 4.4. The glucose consumed for glycolysis is removed from the *Blood* object and the resulting lactate is released into the *Blood* object.

2. Gluconeogenesis: The Kidneys produce glucose via gluconeogenesis in the way described in Section 4.5, and they release it to the *Blood* object.

3. Glucose Excretion in Urine: As the the BGL rises from one Glucose threshold (11 mmol/l) to another (22 mmol/l by default)[43], [77], the glucose excretion in urine increases linearly from zero to a certain peak level (100 mg/min by default). The simulator uses a configurable variable *excretionKidneysImpact_* (with default value 1) to multiplicatively modify the amount of glucose excreted per tick in urine.

4.8 Muscles

There are two types of cells or fibers in the skeletal muscles: the red fibers and the white fibers. To meet the body's energy needs, the red fibers oxidize fatty acids and glucose

absorbed from the bloodstream. Muscles mainly use insulin-sensitive GLUT4 transporters to absorb glucose from the bloodstream. Also, it uses GLUT1 transporters for some basal-level absorption. The white fibers, however, rely on *glycolysis* of glucose 6-phosphate obtained from the glycogen stored within the white fibers. Moreover, the skeletal muscles get their energy from the absorbed branched chain amino acids.

As stated previously, each individual can consume oxygen up to a certain maximal rate. This rate is called $\%VO_2max$ and the rate depends on the gender, age and fitness level of the individual [58]. Therefore, the intensity of a physical activity can be expressed by this oxygen consumption rate ($\%VO_2max$). The exercise intensity can be also expressed in Metabolic Equivalent of Task or METs, where 1 MET is 1 kcal of energy expenditure per kg of body weight per hour. Normally, 1 MET is considered equivalent to 3.5ml of oxygen consumption per kg of body weight per minute. In other words, the intensity of a particular exercise in METs can be converted to different intensities in terms of $\%VO_2max$ for different individuals.

Muscles during aerobic exercises meet their energy via oxidation of glucose and fatty acids [57], [50], [97]. The exercise intensity and the rate at which the person consumes oxygen during the exercise determines the relative fraction of the substrates used to meet the energy. About, 10% of the energy needs during aerobic exercise are met by oxidizing glucose absorbed from the bloodstream via GLUT4/GLUT1 transporters [97]. The aerobic exercise activates GLUT4 transporters to absorb glucose from the bloodstream, despite the insulin levels during the aerobic exercise [89], [46], [112]. Low intensity (e.g. $25\%VO_2max$) exercises meet most of the remaining energy needs via oxidizing fatty acids [97]. In a moderate and high intensity exercise, a significant fraction of energy needs is met by oxidation of glucose derived from the glycogen stored locally in the exercising muscles. [97] reported that when the intensity of the aerobic exercise is about $65\%VO_2max$, 30% of the energy comes from

the oxidation of glucose obtained from locally stored glycogen. Also, it is reported in [50] that the oxidation of glucose that is absorbed from the bloodstream and obtained from local stored glycogen provides for about 50% and almost 100% of the energy needs when the exercise intensities were $50\%VO_2max$ and $100\%VO_2max$ respectively. Most of the remaining energy needs are met by the oxidation of fatty acids [31]. A small quantity of the energy needs is met by the glycolysis of glucose 6-phosphate derived from locally stored glycogen. The glycolysis level increases linearly with exercise intensity. Finally, a very small fraction of energy needs is acquired by consuming branched amino acids absorbed from the bloodstream [31]. When the glycogen stored in the liver and the muscles is depleted, the individual will not be able to perform high intensity exercises (almost impossible). On the other hand, in the resting state the muscles meet 85–90% of their energy needs via the oxidation of fatty acids. The remaining energy comes from the oxidation of glucose (about 10%) and amino acids (1–2%).[57] [50] [110]. In addition, [59] reported that the absorbed glucose is used for oxidation, glycogen synthesis, and glycolysis. The glucose oxidation and glycolysis processes (in muscles) increase with the insulin level in the bloodstream during the resting conditions.

CarbMetSim uses Muscles class (object) to model skeletal muscles. The skeletal muscle (in the simulator) responds to the resting condition and the aerobic exercise only. The current version cannot simulate anaerobic exercises,and neither can it distinguish among different muscle groups. At the start of the simulation, a method in HumanBody class calculates the $\%VO_2max$ associated with the individual being simulated using the tables in [58]. The simulator uses the following parameter for the $\%VO_2max$ estimation: individual's gender, age, and self-assessed fitness level within his/her age group. These individual's parameters are all entered to the simulator as configuration parameters. In *CarbMetSim*, the intensity of exercise is translated from the units of METs into $\%VO_2max$. As stated before, the energy needs (to do the exercise) is met via the oxidation of glucose derived from locally

stored glycogen. The initial amount of glycogen stored in the Muscles and the maximum amount the simulator can hold are set via configurable parameters. By default, both these parameters have values equivalent to 500 grams of glucose.

The *Muscles* object performs the following actions when the simulator (particulary HumanBody class) is in the Fed_Exercising or PostAbsorptive_Exercising state during a tick:

1. Oxidation of glucose absorbed from the Blood: The Muscles absorb a random amount of glucose from the Blood so that the absorbed glucose can be oxidized to meet on average 10% of the energy needs during the tick as stated previously. The Muscles absorb up to a configurable variable that is equal to 30µmol/kg/min (by default). The absorption does not depend on the current *insulinLevel* in the Blood.

2. Oxidation of glucose derived from local glycogen: The Muscles absorb glucose derived from local glycogen to meet a fraction of energy needs. The exercise intensity (in $\%VO_2max$) is used (by oxidation) to determine this fraction value. As the exercise intensity increases from 0 $\%VO_2max$ to 100 $\%VO_2max$, a value between 0 and 0.9 is chosen using a sigmoid function (currently, the compressed CDF of a normal distribution), such that values close to 0.4 and 0.9 will be assigned for exercise intensities 50 $\%VO_2max$x and 100 $\%VO_2max$, respectively. This value is then used as the mean to generate a random value that gives the fraction of energy needs during the tick, as long as a sufficient amount of local glycogen is available.

3. Glycolysis: Increases of exercise intensity yield to increases in the glycolysis flux. When the exercise intensity increases from 0 $\%VO_2max$ to 100 $\%VO_2max$ during the tick, the glycolysis flux increases linearly from a (poisson distributed) random value (with glycolysisMin_ as the mean) to glycolysisMax_. The glycolysis process uses the glucose 6-phosphate from the locally stored glycogen and adds the resulting lactate to the

Blood object.

4. Fatty Acid Consumption: If the glycolysis and glucose oxidation processes do not provide the current energy needs, Muscles will consume the fat from the AdiposeTissue to meet the remaining energy needs.

The Muscles object performs the following actions when the simulator (HumanBody class) is in Fed_Resting or PostAbsorptive_Resting state during a tick:

1. Glucose Absorption: GLUT4 is responsible of the basal glucose absorption [45] as described previously. Moreover, basal absorption via GLUT1s happens at a configured rate (by default zero).

2. Glycolysis: A fraction of the absorbed glucose is consumed via glycolysis and the generated lactate is added to the Blood object as described in Section 3.4.

3. Glycogen Synthesis: Glycogen will be synthesized if the glycogen store of the Muscles is less than the maximum amount that Muscles could hold [45]. The simulator will generate a poisson distributed random amount of the absorbed glucose (with a configurable mean, 7.0mg/kg/min by default), and it will be converted to glycogen.

4. Oxidation: The rest of the absorbed glucose is consumed via oxidation.

5. Fatty Acid Consumption: If glycolysis and glucose oxidation processes do not provide the energy needs during the resting state, Muscles will consume fat from the AdiposeTissue to meet the remaining energy needs.

4.9 Adipose Tissue

In *CarbMetSim* the *AdiposeTissue* object serves as the storage for fat. The Liver class adds the exceeded glycogen in the form of fat (converted to fat) to the AdiposeTissue object. Also, the *Intestine* object adds the fat contents in chyme to the *AdiposeTissue* object. Fat in AdiposeTissue is consumed or removed by the Muscles to meet its energy needs. These are the only operations are supported by *CarbMetSim* currently. Otherwise, *CarbMetSim* does not yet have a detailed implementation of lipid metabolism.

4.10 Brain

The brain uses GLUT3 transporters to absorb glucose from the bloodstream, so the brain cells can meet their energy needs by oxidizing glucose. The brain oxidizes about 120 g of glucose per day. In other words, the brain absorbs about 83.33 mg of glucose per minute [37],[59]. In *CarbMetSim*, the brain operation is represented in the Brain class, which consumes a poisson distributed random amount of glucose every minute from the *Blood* object (with a mean 83.33 mg).

4.11 Heart

The heart uses both GLUT1 and GLUT4 transporters to absorb glucose from the bloodstream. Consuming glucose and lactate provides up to 30% of the heart's energy needs [1]. However, the heart meets most of its energy needs by oxidizing fatty acids. In *CarbMetSim* the *Heart* object absorbs a poisson distributed random amount of

glucose from Blood and oxidizes it to meet its energy needs (with a default mean 14 mg/minute [59]).

Chapter 5

Validation of CarbMetSim for a meal event

This chapter demonstrates the ability of *CarbMetSim* to model carbohydrate metabolism in normal people and type II diabetic patients in the post-absorptive and post-prandial phases. The default values of various configurable parameters had to be determined for normal subjects before the start of the simulation processes. Therefore, *CarbMetSim* is configured to provide a close match with measurements reported in Woerle et al. [114]. In their literature, Woerle et al. did in-depth study on determining the flux along different pathways for glucose arrival and consumption after a standard meal. The particpants in the study were type II diabetic patients and normal subjects. It included 26 subjects with type II diabetes, and 15 age/weight/sex-matched normal subjects (without diabetes). Diabetic subjects included 16 men and ten women with the following characteristics: age 53 ± 2 years, body weight 93 ± 4 kg, BMI 30 ± 1 kg/m^2, body fat 34 $\pm 3\%$, and average HbA1c $8.6 \pm 0.3\%$. The normal subjects included seven men and eight women with the following characteristics: age 49 ± 3 years, body weight 89 ± 4 kg, body fat 36 ± 3 %, and BMI 30 ± 1 kg/m^2. All the participants (diabetic and normal) consumed a standard breakfast consisting of 84 g of glucose, 10 g of fat and 26 g of protein, at 10am on the day of the measurements after a fast of more than 14 hours. Measurements were carried out for the post-absorptive phase before the breakfast. The post-prandial phase was assumed to be six hours in duration after the breakfast.

We performed two sets of simulations using *CarbMetSim*: one for a normal subject and one for a type II diabetic subject. In each set, 30 simulations with different seeds for a

random number generation were performed. Most of the configurable simulation parameters were set to their default values. Indeed, they were set so that the normal subject simulations produced a close match with measurements reported in [114]. The insulin level in the reported measurements did not appear to influence the gluconeogenesis flux; therefore, the impact of the insulin level on the gluconeogenesis flux was disabled in *CarbMetSim* for the reported results in this chapter. Table 5.1 shows the configurable parameters for which the default values *were not* used. In the reported experiments the parameters did not change in value with the body state. However, the simulator is able to use different values for the parameteres based on the body state. Also, *CarbMetSim* sets the value of *bodyWeight* and *age_* to the average values reported for subjects in each category in [114]. As reported earlier, the *age_*, *gender_* and *fitnessLevel_* parameters are used to estimate $\%VO_2max$ for the person being simulated. However, they are not pertinent in the reported simulations in this chapter.

The following parameters (see Tables 5.2 and 5.3) were set as per the data reported in [114]:

1. The baseGlucoseLevel_ and highGlucoseLevel_ values were set according to the reported values for the fasting and the peak BGL [114].

2. The peakInsulinLevel_ values were set to the reported peak plasma insulin levels [114].

3. The average glycogen breakdown flux in the Liver (glycogenToGlucoseInLiver_) values was set to obtain a good match with the reported values for the post-absorptive glycogen breakdown flux and the total glycogen breakdown in the liver during the post-prandial phase.

The length of each simulation run was 18 hours of simulated time. It started at 12 am and ended at 6 pm the next evening, with one breakfast meal intake that occurred at 10 am. The

meal consisted of 84 g of glucose, 10 g of fat, and 26 g of protein. During the simulated time, there were no other events. Also, at the beginning of the simulation (when the simulation started at 12 am) the simulated subject was in the post-absorptive phase.

	Normal	Type II Diabetic
age_ (years)	49	53
gender_	0 (male)	0 (male)
fitnessLevel_ (%ile)	50	50
bodyWeight (kg)	89	93
minGlucoseLevel_ (mg/dl)	50	50
baseGlucoseLevel_ (mg/dl)	90	210
highGlucoseLevel_ (mg/dl)	145	360
baseInsulinLevel_	0.001	0.001
peakInsulinLevel_	1.0	0.6
glut4Impact_	1.0	0.25
glycolysisMinImpact_	1.0	4.0
glycolysisMaxImpact_	1.0	1.5
excretionKidneysImpact_	1.0	1.3
glucoseToGlycogenInLiver_ (mg/kg/min)	4.5	6.75
glycogenToGlucoseInLiver_ (mg/kg/min)	0.9	1.25
gngLiver_ (mg/kg/min)	0.16	0.38
gngKidneys_ (mg/kg/min)	0.16	0.38

Table 5.1: Configuration parameters for simulations for a single meal event.

Following Figures shows the related results in simulating a normal subject and a diabetic subject. The Figures displays the minute-by-minute values of interest in the two simulations with a particular seed value. In the details, Figure 5.1 shows that the gastric emptying has been completed within 45 minutes of meal intake. Some of the delay in gastric emptying (shown in Figure 5.1) was caused by the fat contents of the meal. Figure 5.2 displays the quick digestion of glucose when it arrives in the Intestine. Also, Figure 5.3 shows the appearance of consumed glucose in the PortalVein as described previously. Figure 5.4 shows the changes in BGL during the post-prandial phase which starts from the post-absorptive

	Woerle et al. [114]	Simulations
	Before Breakfast	
BGL	4.7 ± 0.1 mM (84.6 ± 1.8 mg/dl)	91.937 ± 0.010 mg/dl
Glycogen Breakdown	$5.5 \pm 0.6\mu$mol/kg/min (88.1 ± 9.6 mg/min)	80.064 ± 0.171 mg/min
Gluconeogenesis	$2.6 \pm 0.2\mu$mol/kg/min (41.6 ± 3.2 mg/min)	41.720 ± 0.053 mg/min
	90 Minutes After Breakfast	
Plasma Insulin	290 ± 29 pM	0.993 ± 0.001
Glycogen Breakdown	$1.3 \pm 0.6\mu$mol/kg/min (20.8 ± 9.6 mg/min)	0 mg/min
Gluconeogenesis	$2.6 \pm 0.2\mu$mol/kg/min (41.6 ± 3.2 mg/min)	41.824 ± 0.051 mg/min
Peak Post-prandial BGL	8 mM (144 mg/dl)	144.826 ± 0.046 mg/dl
	Total Glucose Consumed/Produced During 6 Hours After The Breakfast	
Gluconeogenesis	15.3 ± 1.2 g	15.041 ± 0.001 g
Glycogen Breakdown	4.3 ± 1.7 g	16.241 ± 0.002 g
Glucose Excretion in Urine	0.7 ± 0.4 g	0 g
Oxidation	45.6 ± 2.6 g	47.055 ± 0.008 g
Glycolysis	21.5 ± 2.2 g	22.614 ± 0.002 g
Glycogen Storage	40.6 ± 3.6 g	45.616 ± 0.008 g

Table 5.2: Normal Subjects: Key Measurements From Woerle Et Al. [114] and Corresponding Results From 30 Simulations with Different Seeds. "Before Breakfast" Simulation Results Were Observed at 9.59AM. All Values Expressed as *Mean* ± *Std Error*.

levels before 10 am.

Post-Absorptive Phase: Figure 5.5 shows that *insulinLevel* during the post-absorptive phase is low enough to ensure that the glycogen breakdown in the Liver occurs at the peak level as shown in Figure 5.7. Figure 5.6 shows that there is no glycogen synthesis in the Liver during this phase. Figure 5.10 and Figure 5.9 show that glucose consumption via oxidation and glycolysis in various organs are at their minimum levels. Also, during this phase, Gluconeogenesis happens in the Liver and the Kidneys (as shown in Figure 5.8) which is unaffected by the *insulinLevel* as reported in [114]. Also, Gluconeogenesis happens at the configured rates specified in [114] and provides the second source of glucose during the phase. Since the minimum glucose oxidation flux is mostly specified by the needs of the Brain and Heart, the configured values for the minimum glycolysis flux are selected to ensure that the total glucose consumption matches the total glucose production during this phase. Hence, the glycolysisMinImpact_ parameter was set to 4.0 in simulations for the type II

	Woerle et al. [114]	Simulations
	Before Breakfast	
BGL	11.7 ± 0.6 mM (210.6 ± 10.8 mg/dl)	219.820 ± 0.063 mg/dl
Glycogen Breakdown	$7.0 \pm 0.4\mu$mol/kg/min (117.2 ± 6.7 mg/min)	116.089 ± 0.183 mg/min
Gluconeogenesis	$3.8 \pm 0.3\mu$mol/kg/min (63.6 ± 5 mg/min)	64.092 ± 0.078 mg/min
	90 Minutes After Breakfast	
Plasma Insulin	179 ± 19 pM	0.6 ± 0.000
Glycogen Breakdown	$3.8 \pm 0.7\mu$mol/kg/min (63.6 ± 11.7 mg/min)	0 mg/min
Gluconeogenesis	$3.8 \pm 0.3\mu$mol/kg/min (63.6 ± 5 mg/min)	64.127 ± 0.084 mg/min
Peak Post-prandial BGL	20 mM (360 mg/dl)	363.064 ± 0.076 mg/dl
	Total Glucose Consumed/Produced During 6 Hours After The Breakfast	
Gluconeogenesis	26.9 ± 2.2 g	23.069 ± 0.001 g
Glycogen Breakdown	10.1 ± 1.2 g	22.648 ± 0.006 g
Glucose Excretion in Urine	17.4 ± 2.7 g	16.750 ± 0.007 g
Oxidation	32.8 ± 2.8 g	35.039 ± 0.001 g
Glycolysis	28.7 ± 2.2 g	31.386 ± 0.010 g
Glycogen Storage	46.3 ± 3.3 g	46.514 ± 0.007 g

Table 5.3: Subjects with Type II Diabetes: Key Measurements From Woerle Et Al. [114] and Corresponding Results From 30 Simulations with Different Seeds. "Before Breakfast" Simulation Results Were Observed at 9.59AM. All Values Expressed as *Mean* $\pm$ *Std Error*.

diabetic subject to ensure that glycolysis flux for the type II diabetic subject during the post-absorptive phase is much higher than that for the normal subject, as shown in Figure 5.9. In other words, the total glucose production from the glycogen breakdown and gluconeogenesis processes is matched by the total glucose consumption from the oxidation, glycolysis, and excretion in urine in the post-absorptive phase. This makes the BGL stabilize at a value near the baseGlucoseLevel_. Any temporary mismatch between glucose production and consumption is quickly fixed, because the glycogen breakdown in the Liver is configured to quickly slow down with increase in the *insulinLevel*.

Post-Prandial Phase: The following paragraphs illustrate the simulation results during the post-prandial phase that begins with food intake at 10:00 am. Figure 5.4 shows that BGL begin to rise when the consumed glucose just arrives in the PortalVein. Also, Figure 5.5 shows that *insulinLevel* increases due to an increase in the BGL. The increase of the *insulinLevel* halts the glycogen breakdown in the Liver as shown in Figure 5.7 The influx of consumed glucose is more than enough to compensate for the halt in glycogen breakdown. Indeed,

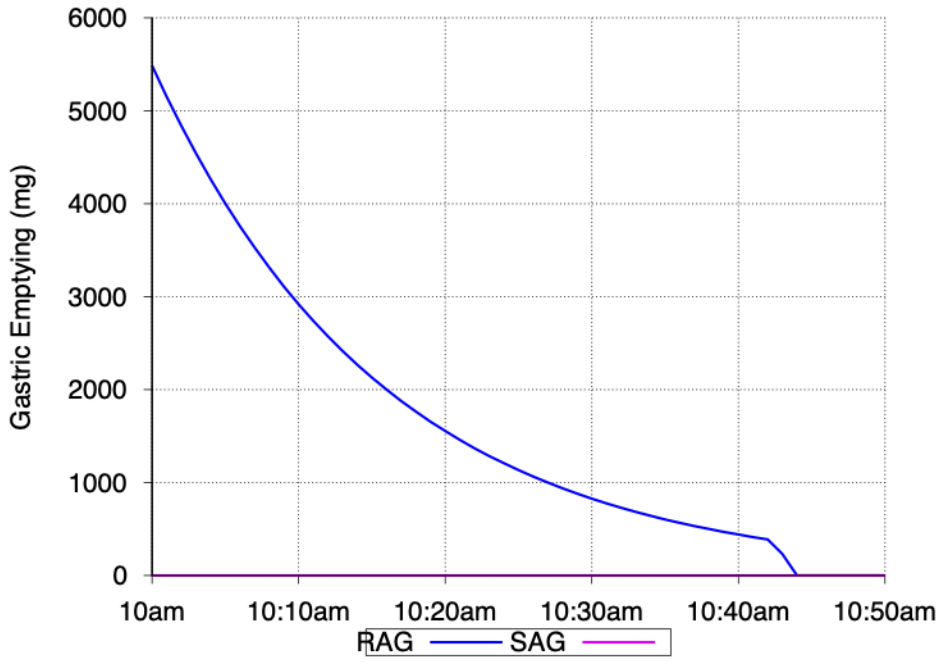

Figure 5.1: Simulating a meal event for a normal and a subject with type II Diabetes: Minute-by-minute values of **Gastric Emptying (mg/minute)** in simulations with a particular seed for random number generation.

the process of digesting glucose provides approximately 700 mg/minute at peak, while the glycogen breakdown provides approximately 120 and 80 mg/minute for type II diabetic and normal subjects respectively. Figure 5.8 shows that glucose production via gluconeogenesis continues as before, unaffected by the increase in the *insulinLevel* as reported in [114]. Figure 5.12 shows that GLUT4 activation for the normal subject increases proportionally in response to the increase in the *insulinLevel*, and therefore an increase in the glucose absorption by Muscles. The glycogen storage in the Muscles are full, and therefore, the absorbed glucose cannot be added as glycogen in the Muscle cells. Figure 5.10 shows that the increased oxidation flux in the normal subject between 10 am and 1 pm is a result of the increase in the glucose oxidation in the Muscles. On the other hand, the Muscles in the diabetic subject are not able to absorb glucose at the normal rate as in the normal subject case (Figure 12). This caused by setting the glut4Impact_ parameter to 0.25, which

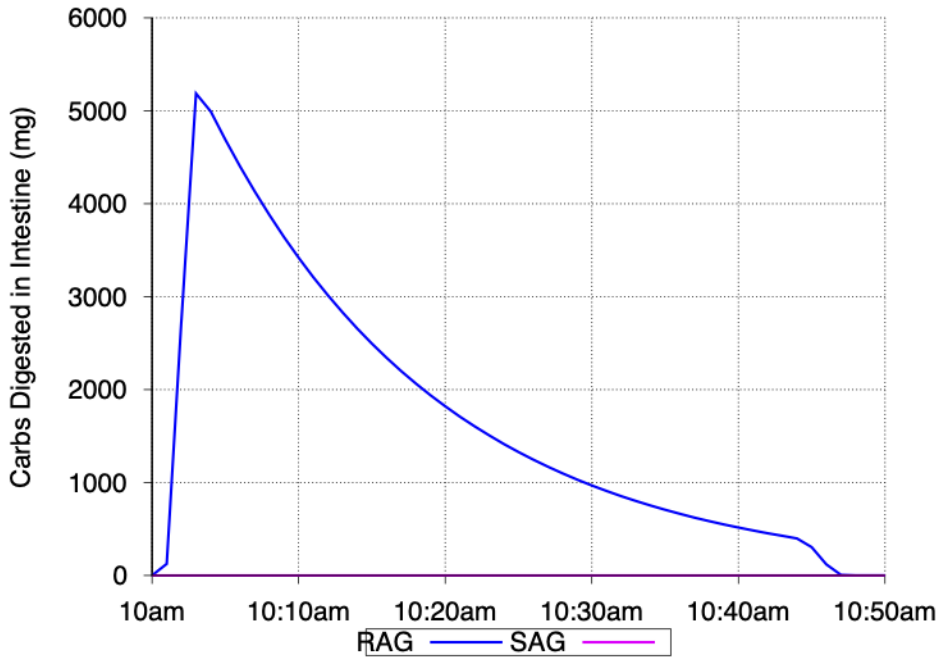

Figure 5.2: Simulating a meal event for a normal and a subject with type II Diabetes: Minute-by-minute values of **Carbohydrate Digestion in Intestine (mg/min)** in simulations with a particular seed for random number generation.

indicates an impaired in GLUT4 activation for a type II diabetic patient. Also, most of the glucose absorbed in the diabetic subject case is consumed via glycolysis because the glycolysisMinImpact_ parameter was set to 4.0, comparing to 1.0 for the normal subject. This explains why the oxidation flux shown in Figure 10 does not show any rise in the post-prandial phase for the type II diabetic subject. *CarbMetSim* sets glycolysisMaxImpact_ to 1.25 for the type II diabetic subject, so the peak glycolysis flux for the type II diabetic subject will be higher than that for the normal subject to achieve a close match with reported results in [114] for the total glycolysis flux during the post-prandial phase between 10 am and 4 pm (see Table 5.3). Also, note that the glycolysis flux has been increased in other organs due to an increase in the *insulinLevel* as it is shown in Figure 5.9. Figure 5.6 shows that when the BGL approaches the highGlucoseLevel_, the glycogen synthesis process in the Liver starts and rapidly ramps up to its peak level, and thereby significantly slows down

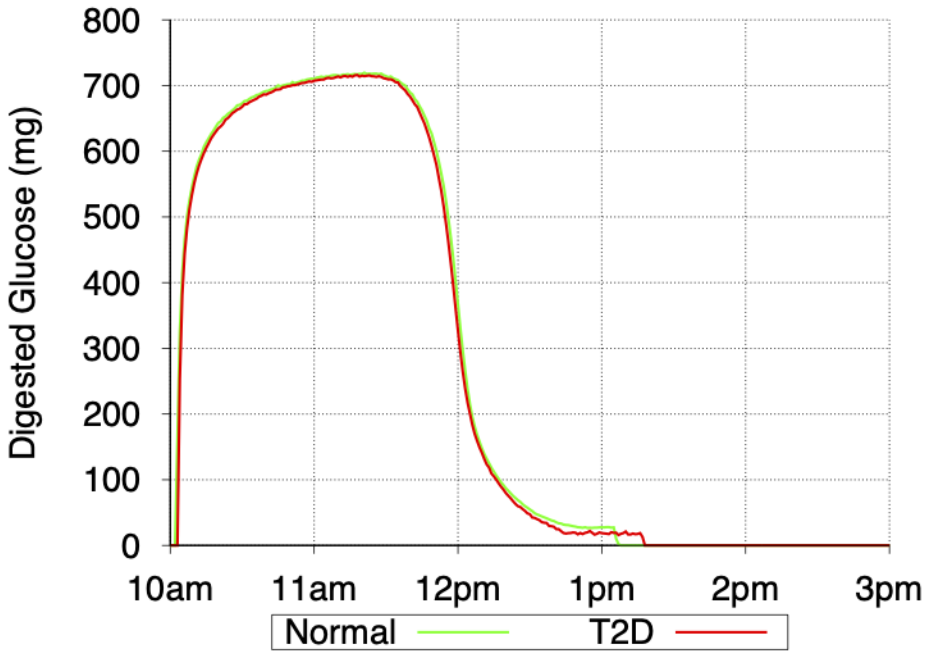

Figure 5.3: Simulating a meal event for a normal and a subject with type II Diabetes: Minute-by-minute values of **Appearance of Digested Glucose in PortalVein (mg/min)** in simulations with a particular seed for random number generation.

any further increase in BGL. As reported in [114], and shown in Table 5.2 and 5.3, the glycogen storage during the post-prandial phase is higher for the type II diabetic subject than for the normal subjects, even though the peak insulin levels for the type II diabetic subject is smaller than for a normal subject. The *insulinLevel* has a significant impact on glycogen synthesis in the Liver, as discussed previously. In order to compensate for lower insulin levels in the type II diabetic subjects, the glucoseToGlycogenInLiver_ parameter in the simulations is assigned a value equal 6.75 mg/kg/min, which is higher than the value assigned for glucoseToGlycogenInLiver_ parameter for normal subjects (4.5 mg/kg/min). The type II diabetic patient lose a significant amount of glucose via excretion in urine (see Figure 5.11). This makes BGL remain around the highGlucoseLevel_ as long as the digested glucose is appearing in the PortalVein at the peak rate. When the digested glucose occurrence in the PortalVein slows down, the BGL begins to drop and the glycogen synthesis

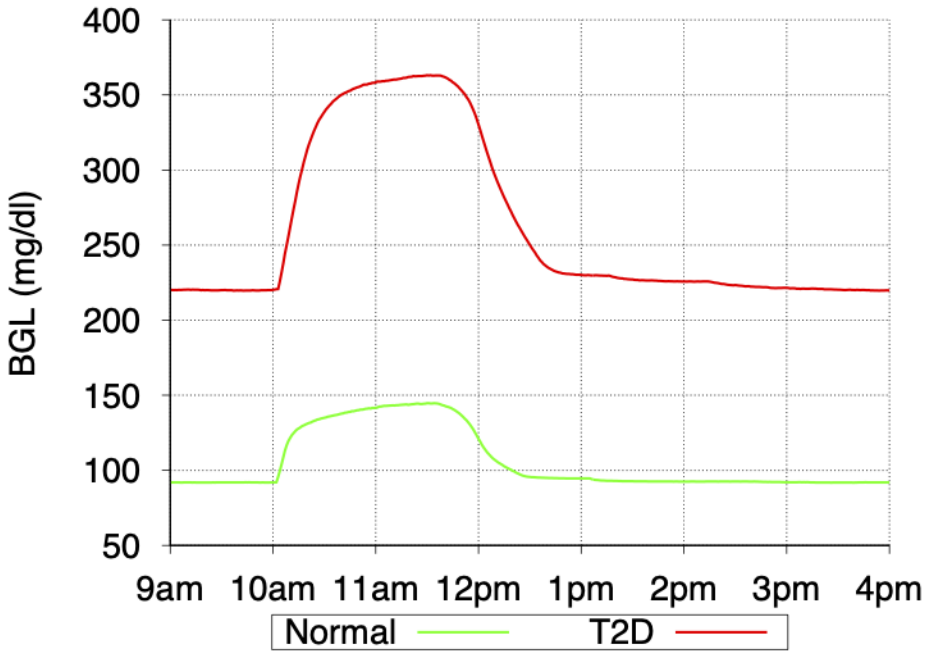

Figure 5.4: Simulating a meal event for a normal and a subject with type II Diabetes: Minute-by-minute values of **Blood Glucose Level (mg/dl)** in simulations with a particular seed for random number generation.

in the Liver rapidly comes to a halt. Therefore, this process slows down the rate at which the BGL falls. When the BGL decreases, the glycolysis flux, the glucose absorption by the Muscles, and the glucose excretion in the urine decrease consequently. This slows down the rate of the BGL decreases. When BGL approaches the baseGlucoseLevel_, the glycogen breakdown in the Liver quickly increases to prevent any more decreases in the BGL, and another post-absorptive phase begins.

Comparison with Measurements from Woerle et al.[114]: A comparison between the reported measurements in [114] and the results obtained from the simulations are discussed in the following paragraphs. Tables 5.2 and 5.3 show the significant measurements from [114] for normal and type II diabetes subjects, respectively, along with the corresponding results from the simulations. In the simulations, *CabrmetSim* were configured to use the peak glycogen breakdown and gluconeogenesis flux values during the post-absorptive phase

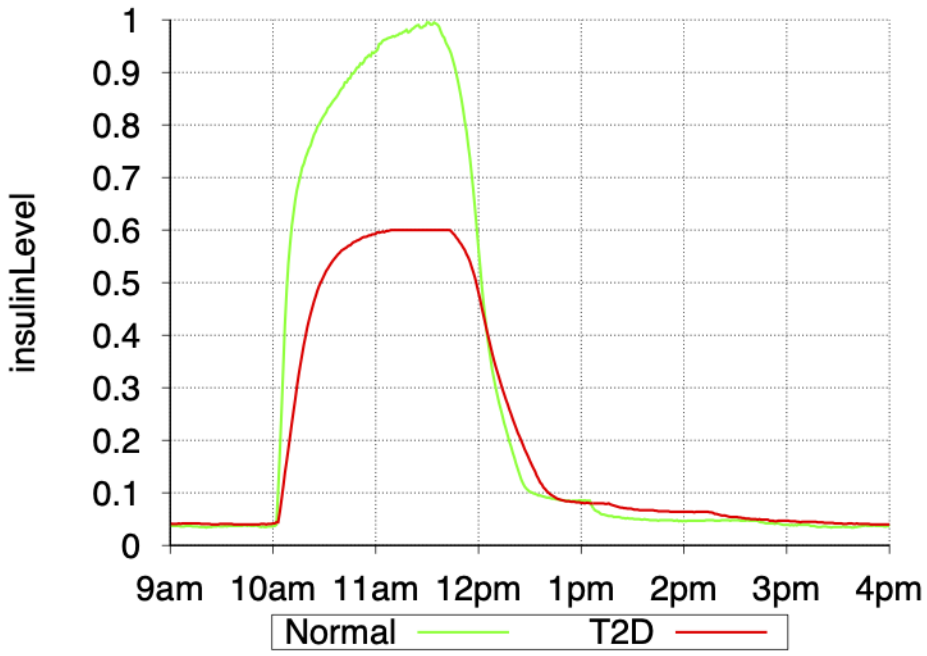

Figure 5.5: Simulating a meal event for a normal and a subject with type II Diabetes: Minute-by-minute values of **Insulin Level** in simulations with a particular seed for random number generation.

that are reported in [114]. By using the appropriate values for other configurable parameters (shown in Table 5.1), the post-absorptive BGL values in the simulations were near the values reported in [114] for both normal and type II diabetic subjects. To ensure that the *insulinLevel* does not have any impact on gluconeogenesis flux, as stated previously, the simulations were configured appropriately. In consequence, the gluconeogenesis flux in simulations 90 minutes after breakfast was the same as the ones before the breakfast, which matches the results reported in [114]. The glycogen breakdown 90 minutes after the breakfast was considerable in [114] but had completely halted in the simulations. Generally, the peak BGL during the post-prandial in simulations matched the reported results in [114]. The glucose produced and consumed through various pathways in the simulations for the normal subject during 6 hours after the breakfast matched the values reported in [114]. However, the glycogen breakdown case was an exception in the simulation results. It is clear from the Figures

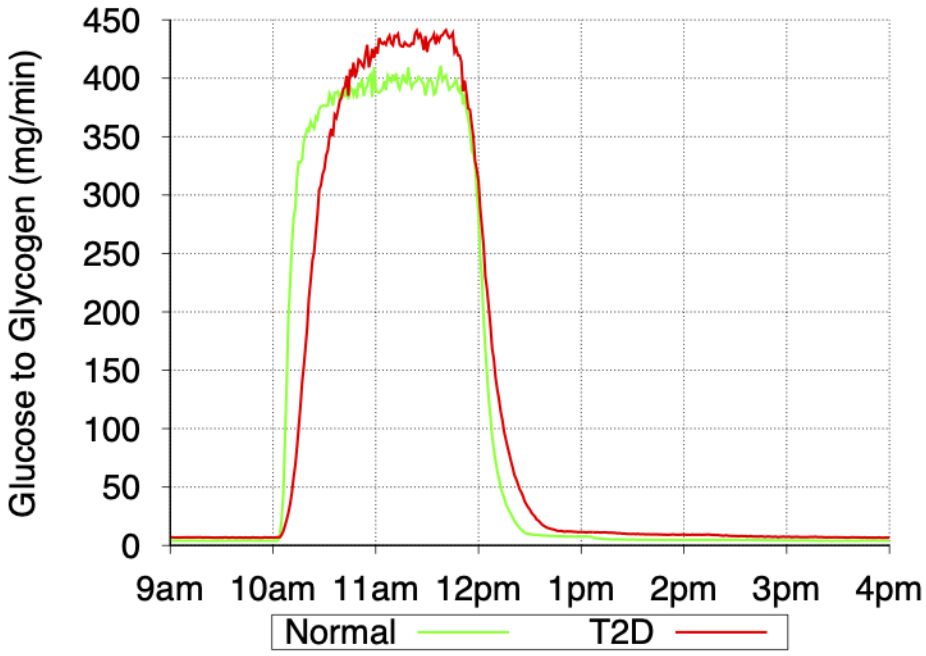

Figure 5.6: Simulating a meal event for a normal and a subject with type II Diabetes: Minute-by-minute values of **Liver Glycogen Synthesis** in simulations with a particular seed for random number generation.

that the post-prandial phase in simulations was over by 1 pm, which make the glycogen breakdown occurred at the peak level between 1 pm and 4 pm (See Figure 5.7). In [114], the case was different and the average glycogen breakdown flux for 6 hours after the breakfast was low. Also, the glycogen breakdown was still considerable 90 minutes after the breakfast when the insulin levels were at their peak. It can be reasoned that the glycogen breakdown is relatively slow in responding to the insulin levels impact. A similar mismatch in the total glycogen breakdown during 6 hours after the breakfast was observed between the simulation results and the reported values in [114] for the type II diabetic subject. Moreover, Woerle et al. reported higher total gluconeogenesis flux for the 6 hours after the breakfast (26.9 ± 2.2 g) for the type II diabetic patient than what was observed in the simulations (23.069 ± 0.001 g). The increased gluconeogenesis flux in [114] during the post-prandial phase may be attributed to the higher availability of gluconeogenesis substrates. However, the gluconeogenesis flux

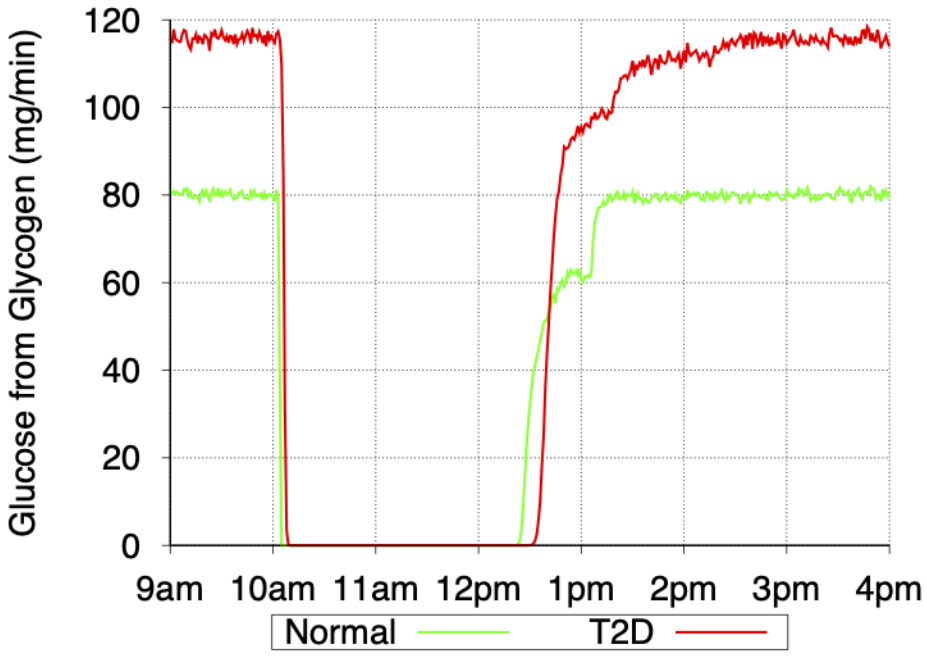

Figure 5.7: Simulating a meal event for a normal and a subject with type II Diabetes: Minute-by-minute values of **Liver Glycogen Breakdown** in simulations with a particular seed for random number generation.

in the simulation had the same values during both the post-prandial and post-absorptive phases. *CarbmetSim* does not support increase in gluconeogenesis flux due to the increased availability of substrates. The other results for type II diabetic subjects were close to the results reported in [114]. Generally, it can be said that the simulation results closely matched the results reported in [114] for both normal and type II diabetic subjects.

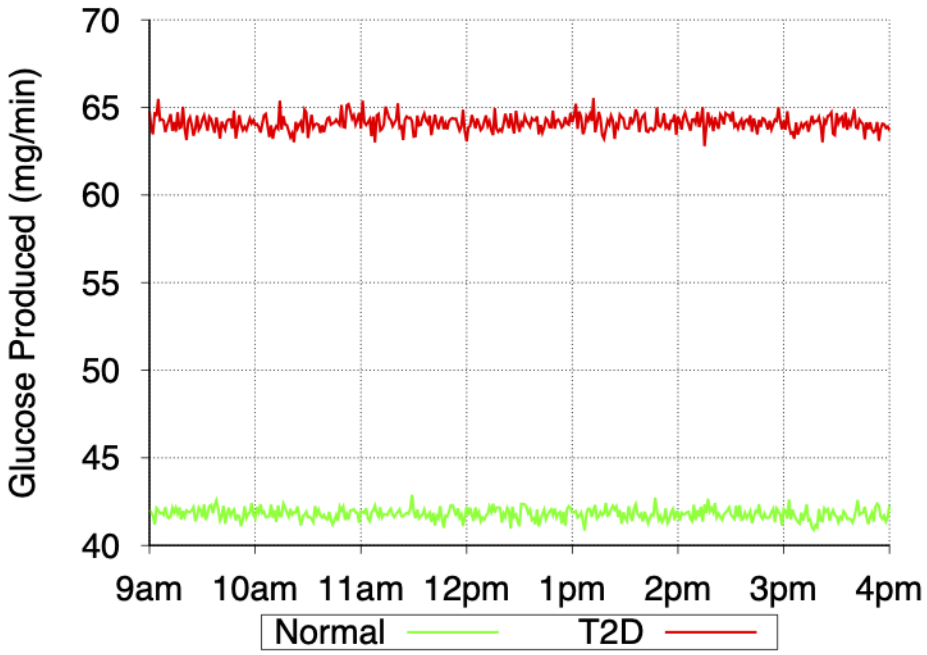

Figure 5.8: Simulating a meal event for a normal and a subject with type II Diabetes: Minute-by-minute values of **Total Gluconeogenesis in Liver and Kidneys** in simulations with a particular seed for random number generation.

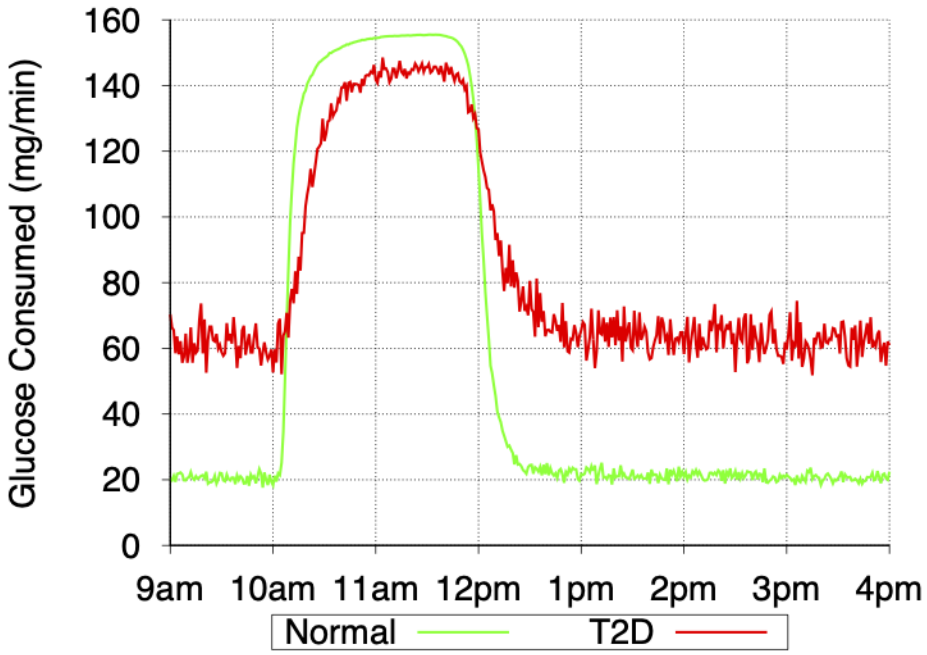

Figure 5.9: Simulating a meal event for a normal and a subject with type II Diabetes: Minute-by-minute values of **Total Glycolysis in All Organs** in simulations with a particular seed for random number generation.

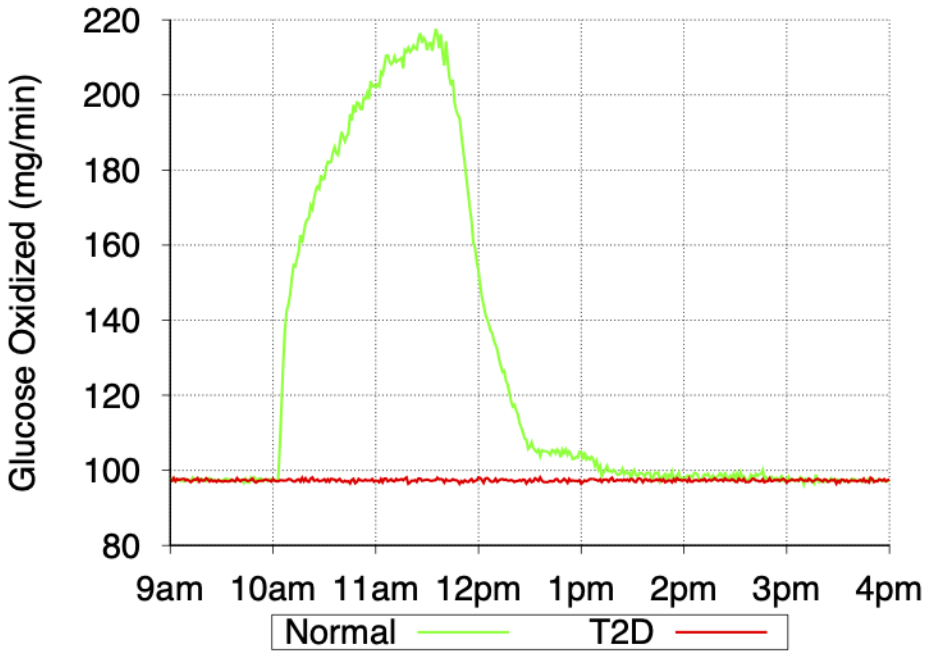

Figure 5.10: Simulating a meal event for a normal and a subject with type II Diabetes: Minute-by-minute values of **Total Glucose Oxidation in All Organs** in Liver and Kidneys in simulations with a particular seed for random number generation.

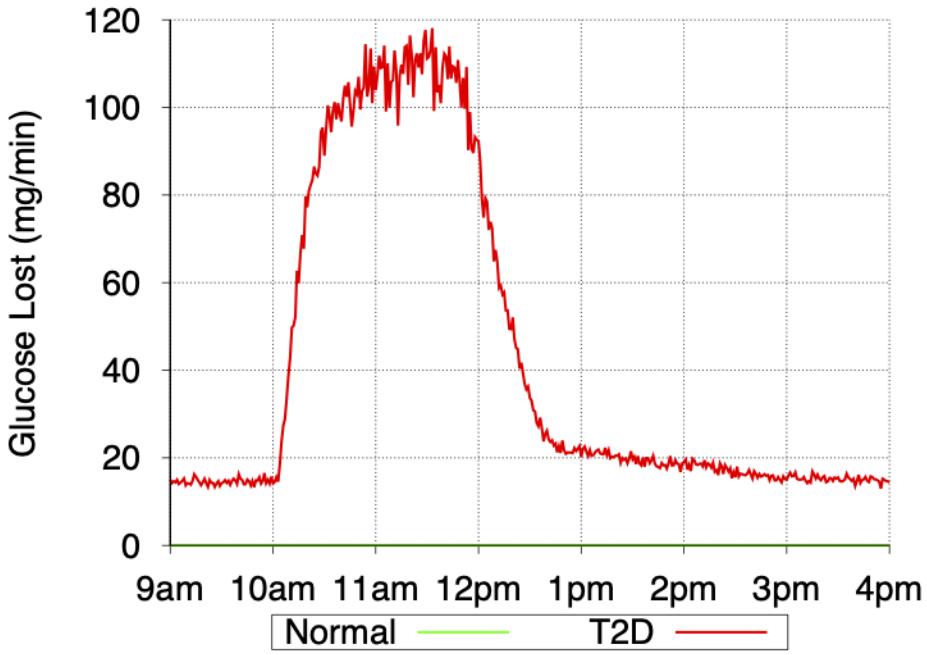

Figure 5.11: Simulating a meal event for a normal and a subject with type II Diabetes: Minute-by-minute values of **Glucose Excretion in Urine** in All Organs in Liver and Kidneys in simulations with a particular seed for random number generation.

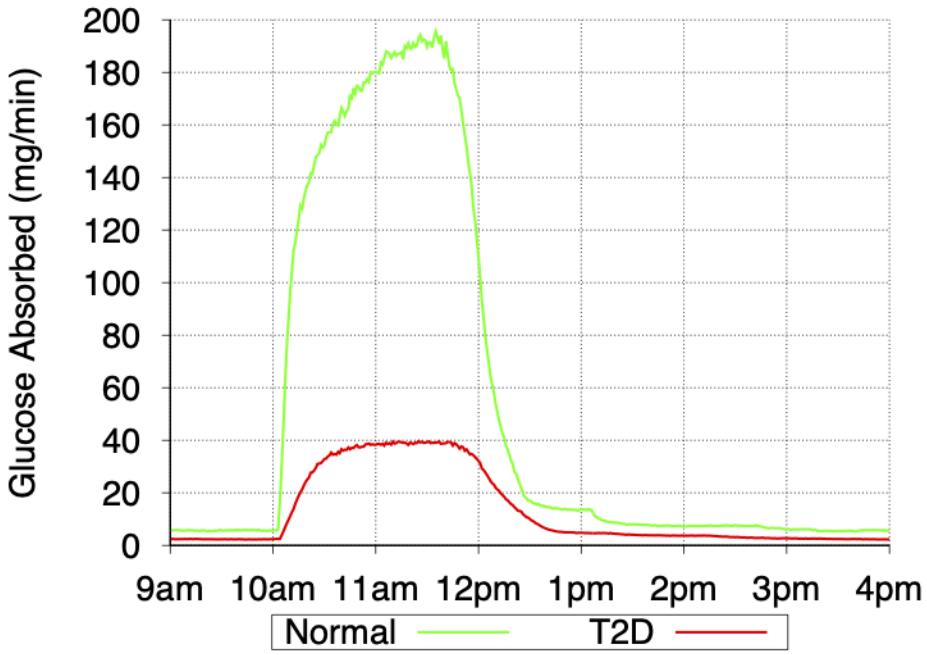

Figure 5.12: Simulating a meal event for a normal and a subject with Type II Diabetes: Minute-by-minute values of **Glucose Absorption in Muscles** in simulations with a particular seed for random number generation.

Chapter 6

Validation of CarbMetSim for an exercise event

Glucose is the main energy source utilized by muscles during moderate to high-intensity exercise. The exercise muscles absorb glucose from the bloodstream and break down the local stored glycogen to provide the energy needs during an exercise. Indeed, the muscles do not depend on the insulin level to get the absorbed glucose, because the exercise is sufficient to activate GLUT4 transporters [89][46][112]. As reported previously, glucose oxidation plays a signiifcant role in meeting energy needs during physical exercise. The metabolism of Carbohydrates during and after a physical exercise has been analyzed widely for normal and diabetic subjects in [112][50][81][16][66][67].

The physical exercise in a normal subject case induces the secretion of glucogon [4] [39] [115] [60] and inhibits the secretion of insulin [110][102][111][39][115]. As consequence, the liver will produce more glucose to meet the needs of the energy requirements by breaking down glycogen into glucose. The glycogenolysis (the process that breaks glycogen into glucose in the liver and the exercising muscles) and the gluconeogenesis (described previously) are the two processes that produce glucose as long as the glycogen is available in the liver and in the exercising muscles. The glucose production from these two processes generally matches the total glucose consumption by exercising muscles ,which makes the BGL remain at the normal level [112][50]. When the glycogen stores are used up, the BGL will drop, because the produced glucose from the gluconeogenesis process alone is not adequate to match the glucose consumption by the exercising muscles. On the other hand, the insulin level in the diabetic patients (type I and type II) is not affected (and therefore not reduced) by the

physical exercises. In consequence, the glycogen breakdown in the liver will not be sufficient to produce the additional glucose needs [118], and the BGL will drop remarkably during exercises. However, BGL in the type I diabetic case may increase during an exercise (which was high before the exercise). This happens due to an increase in glucose production via the glycogen breakdown in the liver (due to secretion of glucagon and other hormones). This increase of BGL is much higher than the impaired rate at which the exercising muscles absorb glucose in some type I Diabetic patients [112] [9] [61][50].

In *CarbMetSim*, we are able to simulate the impact of aerobic physical exercise. This chapter reports the results of simulations where normal male subjects perform a long aerobic exercise following an overnight fast. These simulations replicate the experiments reported in [3] and [5]. In [3], twenty normal male subjects were observed when they performed a leg exercise at intensity $58\%VO_2max$ for 3 to 3.5 hours after a 12 to 14 hour overnight fast. Also, in [5] study, twelve normal male subjects participated. The subjects performed a leg/arm exercise at intensity $30\%VO_2max$ for 2 hours after a 12 to 14 hour overnight fast. Table 6.1 shows the characteristics of these subjects. For each subject, the concentrations of glucose and other hormones in the blood were recorded. Table 6.2 and Figure 6.1 show the relevant BGL data reported in [3] and [5]. In this chapter, we explain each set of BGL data and show that *CarbMetSim* with proper configuration can replicate each pattern.

6.1 Exercise at intensity 58% VO2max

This section discusses the experiments that replicate the physical exercise at intensity $58\%VO_2max$ that is reported in [3]. As seen in Table 6.2 and Figure 6.1, the BGL drops continuously as the exercise progresses, and it reaches the hypoglycemic levels towards the end of the exercise. However, a modest recovery from this hypoglycemic level happens when the exercise concludes. The results indicate that the liver glycogen was drained some time

after the start of the exercise and the only sources of glucose for the exercising muscles were the local glycogen and the gluconeogenesis. This can be explained due to the fact that the exercise began after a long fast and the drops in BGL. Also, the Figure and the table show that the BGL dropped continuously because the gluconeogenesis process alone was not able to compensate for the glucose absorption by the exercising muscles from the bloodstream. Even after the exercise finished, the gluconeogenesis was the only source of glucose, and it was not adequate to bring the BGL back to pre-exercise level.

	Average	Standard Error	Range
	20 Subjects Doing Leg Exercise at 58%VO_2max [3]		
Age (years)	26	0.7	20-31
Weight(Kg)	71	1.6	57-82
Height(cm)	182	1.4	169-187
VO_2max(liters/min)	3.8	.13	2.6-4.8
	6 Subjects Doing Arm Exercise at 30%VO_2max [5]		
Age (years)	27	1	24-29
Weight(Kg)	80	6	61-100
Height(cm)	186	4	171-198
VO_2max(liters/min)	4.1	.3	3.3-4.8
	6 Subjects Doing Leg Exercise at 30%VO_2max [5]		
Age (years)	27	2	19-31
Weight(Kg)	74	4	62-93
Height(cm)	181	3	170-194
VO_2max(liters/min)	3.9	.2	3.3-4.8

Table 6.1: Characteristics of Subjects Reported in [3] and [5].

	Blood Glucose Level (mmol/l): Average ± Standard Error		
	Leg Exercise at 58%VO_2max [3]	**Arm Exercise at 30%VO_2max [5]**	**Leg Exercise at 30%VO_2max [5]**
Rest	4.39±0.08	4.00±0.11	4.33±0.09
Exercise:40min	4.09±0.10	4.01±0.31	4.28±0.10
Exercise:90min	3.86±0.28	4.06±0.20	4.07±0.16
Exercise:120min	3.55±0.11	3.98±0.23	3.81±0.15
Exercise:180min	2.78±0.13		
Exercise:210min	2.56±0.13		
Recovery:10min	3.12±0.13	3.96±0.31	4.06±0.25
Recovery:20min	3.19±0.13	3.76±0.29	4.11±0.25
Recovery:40min	3.18±0.10	3.83±0.25	4.13±0.21

Table 6.2: BGL Measurements Reported in [3] and [5].

To simulate the described experiment, we created twenty pairs of age and weight values

for normal subjects using the average and standard error values specified in [3] (also reported in Table 6.1). Each simulation was begun at the simulated time of 12 am. and we simulated a subject to do a 210-minutes long exercise at intensity $58\%VO_2max$ starting at 12 pm. Each simulation finished at the simulated time of 5 pm and used the same seed value for the random number generation. To match the reported BGL in [3], the simulation parameters were configured to make the liver glycogen exhaustion early on in the exercise. Therefore, it matches the reported BGL. Table 6.3 shows the simulation parameters for the simulated subjects. For each simulation, the initial glycogen store in the Liver was configured to 60 g; this means that a little glycogen was left in the Liver by the time the exercise event started (at 12 pm). Also, to limit the glucose production via gluconeogenesis during the exercise, the gngImpact_ parameter was set to values between 13.2 and 15.5.

The results of simulating the exercise event at intensity $58\%VO_2max$ using *CarbMetSim* is shown in Figure 6.2, Figure 6.3, Figure 6.4, and Figure 6.5. In the details, Figure 6.2 shows the BGL values for each simulated subject along with the average BGL values reported in [3]. As is clear from the figure, the BGL values in the simulations are close to the measurements reported in [3]. Also, the BGL at the beginning of the exercise were hovaring around its pre-exercise levels, and then it dropped continuously as the exercise progresses. It reached the hypoglycemic levels at the end of the exercise. However, a modest recovery from the hypoglycemic level happened after the exercise finished(did not reach the pre-exercise level though). Figure 6.3 shows the amount of glycogen left in the Liver for a simulated subject. The initial amount of glycogen in the Liver was configured in a manner that ensures that the glycogen amount will deplete in the early stages of the physical exercise. Therefore, all the glycogen in the Liver was depleted by 1 pm, after which the gluconeogenesis was the only source of glucose for this subject. The glycogen breakdown flux in the Liver and the combined gluconeogenesis flux in the Liver and Kidneys are shown in Figure 6.4 and 6.5

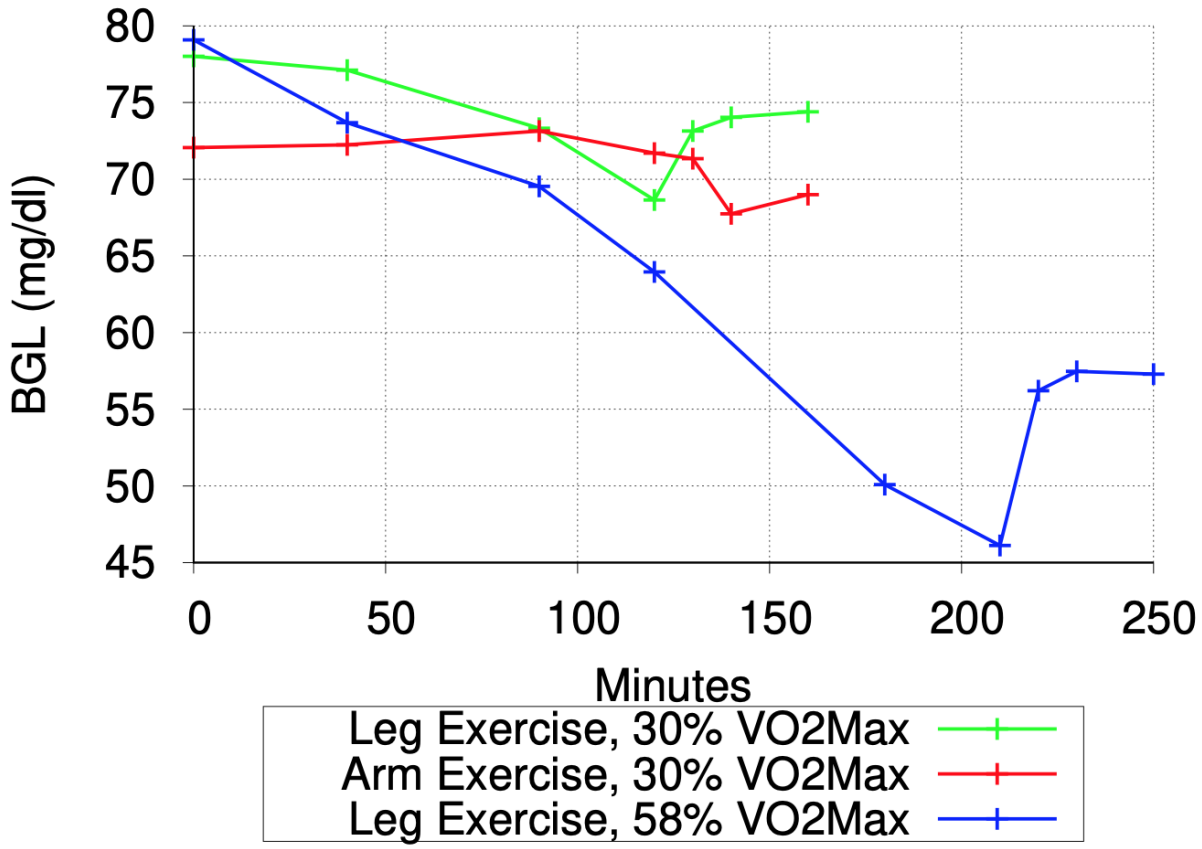

Figure 6.1: Average BGL Measurements (After Conversion to mg/dl) Reported in [3] and [5].

for the same subject. Both Figures show that the glycogen breakdown flux and the gluconeogenesis flux fluctuated between high and low values when the exercise began and before the Liver glycogen was depleted. This behavior is in agreement with our previously discussed findings on how the *insulinLevel* varies, as well as how the glycogen breakdown in the Liver and gluconeogenesis in the Liver and Kidneys react to the *insulinLevel*. Previously, we have stated that when the BGL drops below the baseGlucoseLevel_, the *insulinLevel* will be set to 0 when the simulated subject is engaged in an exercise at an intensity that is higher than the intensityPeakGlucoseProd_ (default value 20% VO2max). In the current simulation experiment, the exercise intensity was $58\% VO_2max$ and it is higher than the intensityPeakGlucoseProd_ parameter. Therefore, the *insulinLevel* dropped to zero when the

BGL dropped below the baseGlucoseLevel_. This pushes the glycogen breakdown process in the Liver and gluconeogenesis process in the Liver and Kidneys to produce glucose at the highest rates. However, when the BGL exceeded the baseGlucoseLevel_, the *insulinLevel* exceeded the baseInsulinLevel_ and, therefore the glycogen breakdown and gluconeogenesis fluxes fell down to the normal levels. After the liver glycogen was totally consumed, the gluconeogenesis process was not able to raise BGL above the baseGlucoseLevel_, even though it occurs at the highest rate. This explains why the *insulinLevel* stayed at the zero level for the rest of the exercise duration, and the gluconeogenesis process was the only source of glucose for the blood. When the exercise finished, the *insulinLevel* increased to a positive value below baseInsulinLevel_, and in response the gluconeogenesis flux assigned a value between the regular and the highest levels. In other words, the gluconeogenesis process at this time allowed the BGL to rise from the hypoglycemic level to a level below the baseGlucoseLevel_.

Subject #	1	2	3	4	5	6	7	8	9	10	11	12	13	14	15	16	17	18	19	20
age_ (years)	23	26	26	30	22	25	26	24	24	22	20	23	31	26	26	30	21	29	25	26
gender_ (0=Male)	0																			
fitnessLevel_ (%ile)	50																			
bodyWeight (kg)	57	63	59	78	60	71	75	76	72	64	74	82	71	62	64	70	78	65	65	74
minGlucoseLevel_ (mg/dl)	40																			
baseGlucoseLevel_ (mg/dl)	79																			
highGlucoseLevel_ (mg/dl)	145																			
baseInsulinLevel_	0.001																			
peakInsulinLevel_	1.0																			
gngImpact_	15.5	15.1	15.35	13.2	15.35	14.75	14.5	14.5	14.7	15.1	14.55	14.3	13.5	15.25	15.1	13.5	14.35	15	15	14.6
Initial Liver Glycogen (g)	60.0																			

Table 6.3: Configuration parameters for simulations for a single exercise event at intensity 58 $\%VO_2max$.

6.2 Arm exercise at intensity 30$\%VO_2max$

This section discusses the experiments that replicate the arm exercise at intensity 30 $\%VO_2max$ that is reported in [5]. In these simulations, the BGL maintain its pre-exercise level through the duration of the exercise, as shown in Figure 6.1 and Table 6.2. Also, it is shown that there is a small drop that occurred during the recovery phase. Analyzing the results in the table and the figure indicate that the liver glycogen did not exhaust during

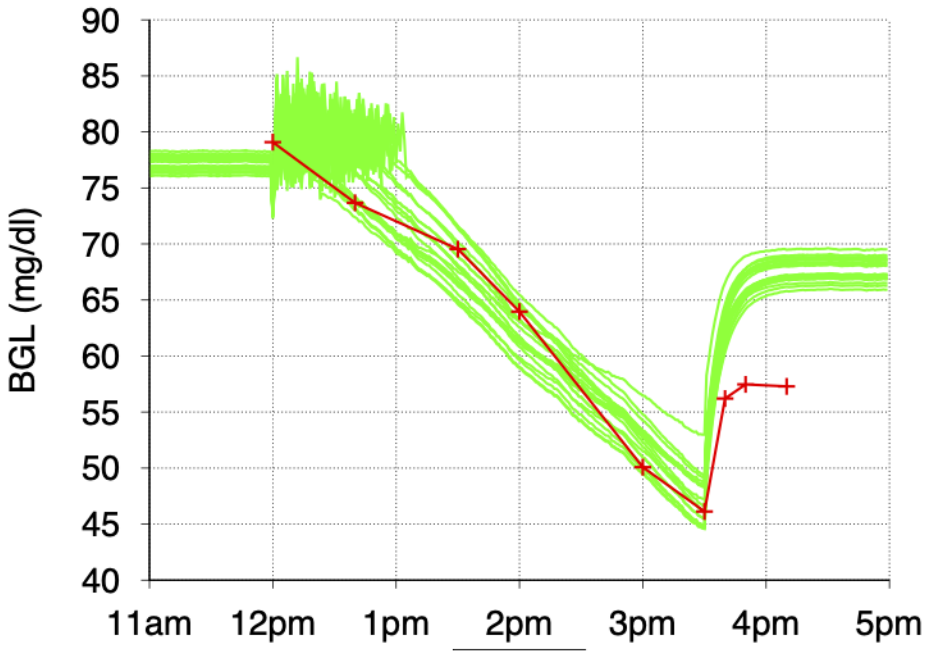

Figure 6.2: BGL results of simulations replicating a physical exercise event at intensity 58 $\%VO_2max$ as reported in [3]. Green: BGL for 20 simulated subjects; Red: average BGL reported in [3]

the exercise period and that both processes (liver glycogen breakdown and gluconeogenesis) were able to meet the glucose needs of the exercising muscles. Moreover, both processes returned to their pre-exercise levels after the exercise finished, and in consequence the BGL got back to its pre-exercise level.

CarbMetSim does not differentiate between various types of muscles. Indeed, the arm exercise was considered in the reported simulations as a regular exercise. To simulate the arm exercise experiments, we generated 6 age and weight value pairs for normal male subjects using the average and standard error values specified in [5] (reported in Table 6.1 as well). Each simulation begun at the simulated time 12 am and simulated a subject to do a 120-minutes long exercise at intensity $30\%VO_2max$ starting at 12 pm. Each simulation finished at the simulated time 5 pm and used the same seed value for the random number generation. Table 6.4 shows the simulation parameters for the simulated subjects, which is different from

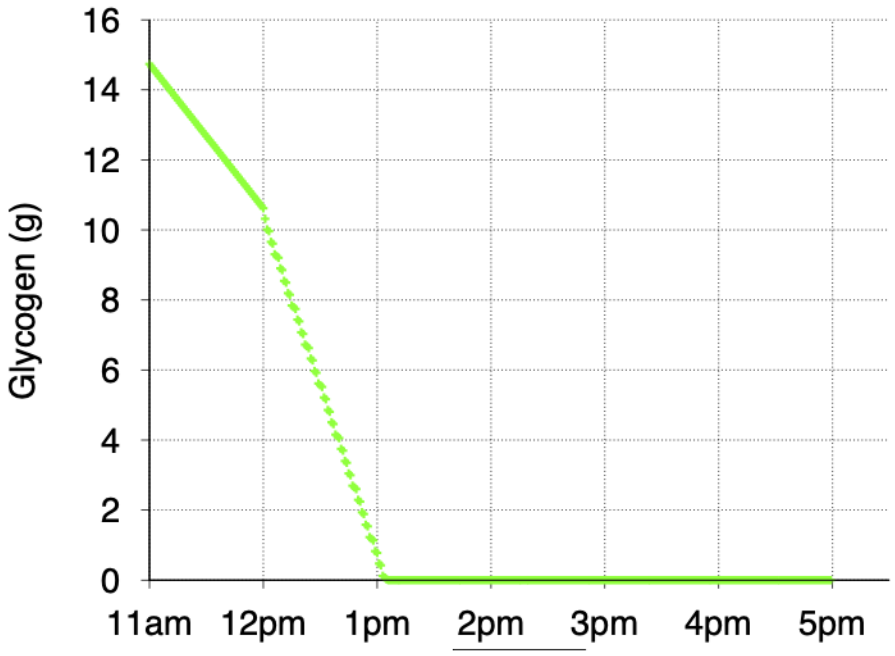

Figure 6.3: Liver glycogen for the subject # 1: results of simulations replicating a physical exercise event at intensity 58 $\%VO_2max$ as reported in [3]

the default values. For each simulation, the initial glycogen store in the Liver was configured to 100 grams to ensure that the liver glycogen does not get exhausted during the exercise. Also, to guarantee that the glucose produced from the gluconeogenesis process will rise to a high enough level when required during the exercise, the gngImpact_ parameter was set to value 15.0.

The results of simulating the arm exercise event at intensity $30\%VO_2max$ using *Carb-MetSim* is shown in Figure 6.6, Figure 6.7, Figure 6.8, and Figure 6.9. Specifically, Figure 6.6 shows BGL values for each simulated subject along with the average BGL values reported in [3]. The values in the figure indicate that the simulator was able to generate BGL values for the simulated subjects that are very close to the measurements reported in [3]. Indeed, the BGL values for all the simulated subjects were hovering around its pre-exercise level during the exercise time and then returned to the pre-exercise level. The results show that

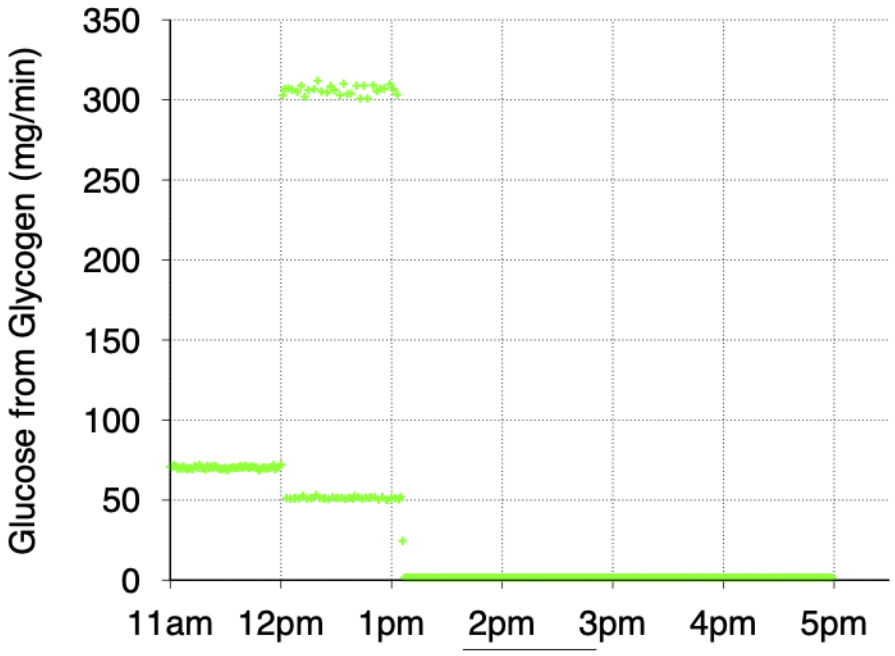

Figure 6.4: Liver glycogen breakdown for the subject # 1: results of simulations replicating a physical exercise event at intensity 58 $\%VO_2max$ as reported in [3]

the liver glycogen did not deplete during the exercise and in the recovery phase as it is clear in Figure 6.7, which shows the amount of glycogen left in the Liver for a simulated subject. The glycogen breakdown flux in the Liver and the combined gluconeogenesis flux in the Liver and Kidneys for the particular subject are shown in Figure 6.8 and Figure 6.9 respectively. The figures show that the glycogen breakdown flux and the gluconeogenesis flux oscillated between high and low values when the exercise started, exactly similar to the corresponding simulations result for the $58\%VO_2max$ exercise (Section 6.1). The fluctuations happened for the same reasons mentioned in section 6.1, and they explain the reasons of BGL oscillating during the exercise duration. When the exercise concluded, the *insulinLevel* increased to the baseInsulinLevel_ (as explained in Section 3.2) and in response the liver glycogen breakdown and gluconeogenesis fluxes (and also the BGL) reached their pre-exercise levels.

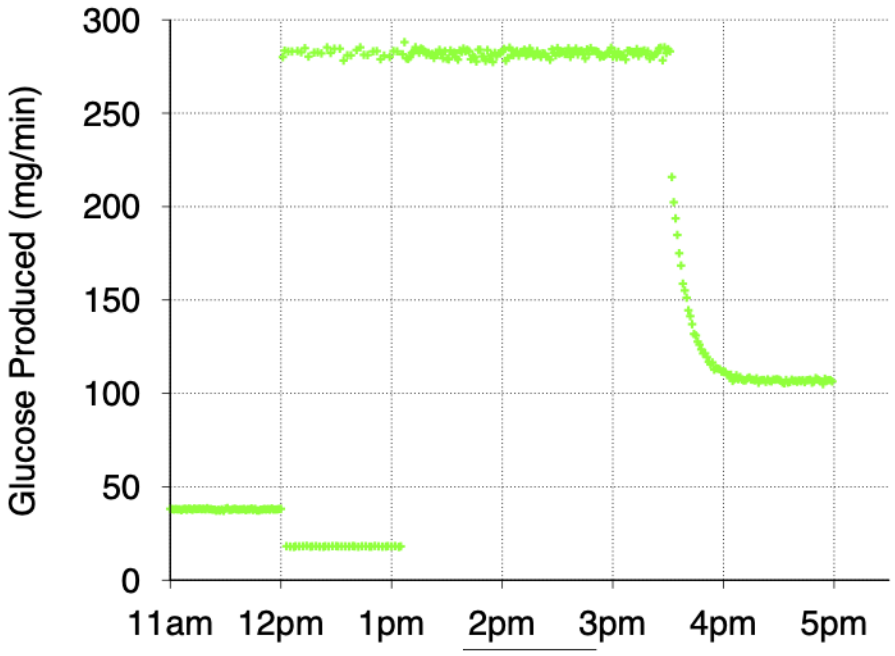

Figure 6.5: Total gluconeogenesis in Liver and Kidneys for the subject # 1: results of simulations replicating a physical exercise event at intensity 58 $\%VO_2max$ as reported in [3]

6.3 Leg exercise at intensity 30 $\%VO_2max$

The leg exercise at intensity $30\%VO_2max$ experiments are discussed in this section. Using Table 6.2 and Figure 6.1, the reader will realize that the BGL dropped modestly during the exercise and then seemed to returned back to the pre-exercise level. Moreover, the liver glycogen was not depleted during the exercise or in the recovery phase as the post-exercise BGL approached the pre-exercise level. The modest drop of BGL throughout the exercise indicates that the leg exercise was not able to stimulate both the liver glycogen breakdown and gluconeogenesis processes to produce enough glucose to match the demands of the exercising muscles. In other words, the total glucose production during exercise was a little less than the amount absorbed from the blood by the exercising muscles.

As mentioned before, *CarbMetSim* does not differentiate between various types of muscles, and hence the leg exercise was considered in the reported simulations as a regular

Subject #	1	2	3	4	5	6
age_ (years)	24	29	28	27	27	28
gender_ (0=Male)	0					
fitnessLevel_ (%ile)	50					
bodyWeight (kg)	61	100	97	62	88	87
minGlucoseLevel_ (mg/dl)	40					
baseGlucoseLevel_ (mg/dl)	72					
highGlucoseLevel_ (mg/dl)	145					
baseInsulinLevel_	0.001					
peakInsulinLevel_	1.0					
gngImpact_	15.0					
Initial Liver Glycogen (g)	100.0					

Table 6.4: Configuration parameters for simulations for a single "arm" exercise event at intensity $30\%VO_2max$.

exercise. To simulate the leg exercise experiments, we generated 6 age and weight value pairs for normal male subjects using the average and standard error values specified in [5] (reported in Table 6.1 as well). Each simulation begun at the simulated time of 12 am and simulated a subject to do a 120-minutes long exercise at intensity $30\%VO_2max$ starting at 12 pm. Each simulation finished at simulated time 5 pm and used the same seed value for the random number generation. In this experiment, the goal was to control the glucose production precisely via liver glycogen breakdown and gluconeogenesis during the exercise to ensure that the total glucose production during the exercise was just a little less than what the exercising muscles would absorb from the blood. Therefore, the liverGlycogenBreakdownImpact_ that controls the liver glycogen breakdown during exercise was reduced to value 1.0, to limit extra glycogen breakdown in the Liver during the exercise. Also, the glycogenToGlucoseInLiver_ parameter was increased appropriately (this variable controls

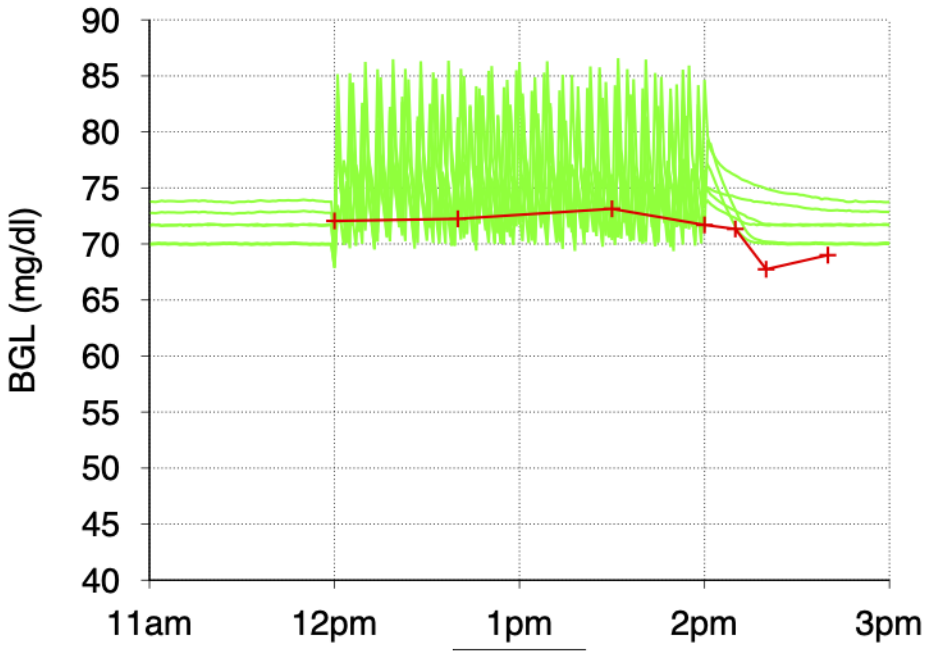

Figure 6.6: BGL results of simulations replicating a physical exercise event involving arms at intensity $30\%VO_2max$ as reported in [5].Green: BGL for 6 simulated subjects; Red: average BGL reported in [5]

the regular glycogen breakdown in the Liver).

Similarly, the parameter that controls the gluconeogenesis flux during the exercise gngImpact_ was set properly to restrict glucose production via gluconeogenesis during the exercise. Table 6.5 shows all simulation parameters for the simulated subjects, which is different than the default values. For each simulation, the initial glycogen store in the Liver was configured to 100 grams to ensure that the liver glycogen would not be depleted during the exercise or the recovery phase. The results of simulating the leg exercise event at intensity $30\%VO_2max$ using *CarbMetSim* is shown in Figure 6.10, Figure 6.11, Figure 6.12, and Figure 6.13. In detail, Figure 6.10 shows BGL values for each simulated subject along with the average BGL values reported in [3]. The values in the figure indicate that the simulator was able to generate BGL values for the simulated subjects that reasonably match the measurements reported

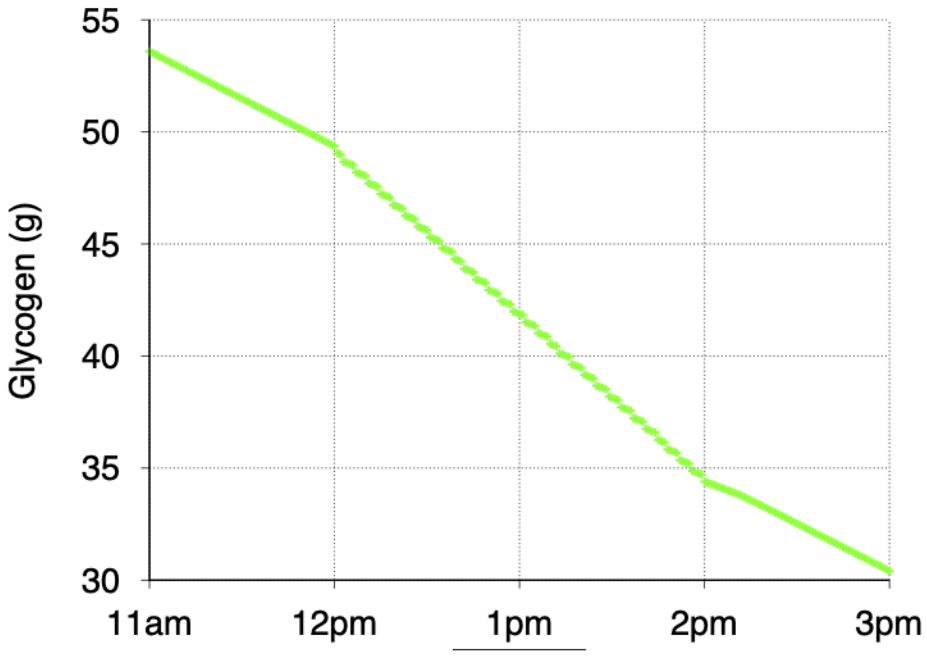

Figure 6.7: Liver glycogen for the subject # 1: results of simulations replicating a physical exercise event involving arms at intensity 30 $\%VO_2max$ as reported in [5]

in [5]. The BGL for all the simulated subjects dropped modestly during the exercise duration and then returned to the pre-exercise level. Figure 6.11 shows the amount of glycogen left in the Liver for a simulated subject. The glycogen breakdown flux in the Liver and the combined gluconeogenesis flux in the Liver and Kidneys for the particular subject are shown in Figure 6.12 and Figure 6.13 respectively. In Figure 6.12 it is clear that the liver glycogen flux did not increase during the exercise . Also, in Figure 6.13 the reader will notice that the gluconeogenesis happened at its highest level during the exercise time. This happened because the BGL was below the baseGlucoseLevel_ during the exercise time and the exercise intensity was greater than intensityPeakGlucoseProd_. Accordingly, the *insulinLevel* was set to 0 throughout the exercise time, and this made the gluconeogenesis take place at its highest level. Also, the *insulinLevel* was not able to stimulate liver glycogen breakdown because liverGlycogenBreakdownImpact_ was set to value 1. The BGL dropped modestly

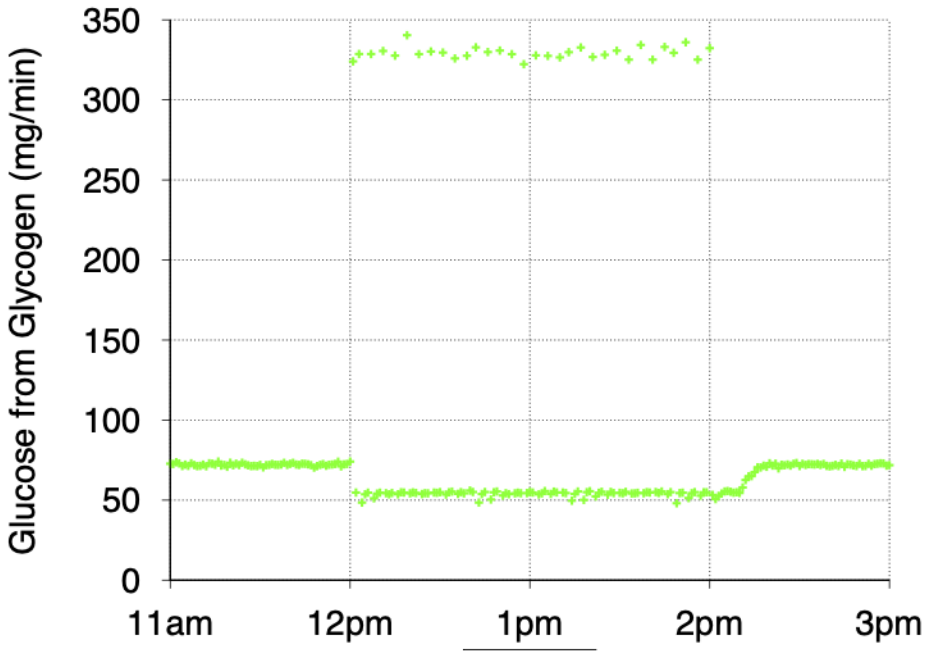

Figure 6.8: Liver glycogen breakdown for the subject # 1: results of simulations replicating a physical exercise event involving arms at intensity 30 $\%VO_2max$ as reported in [5]

during the exercise time (as desired) because the combined glucose production from the gluconeogenesis and liver glycogen breakdown processes was below the glucose absorbed from the blood by the exercising muscles. When the exercise finished, the *insulinLevel* increased to the baseInsulinLevel_ and consequently the gluconeogenesis flux and the BGL achieved their pre-exercise level.

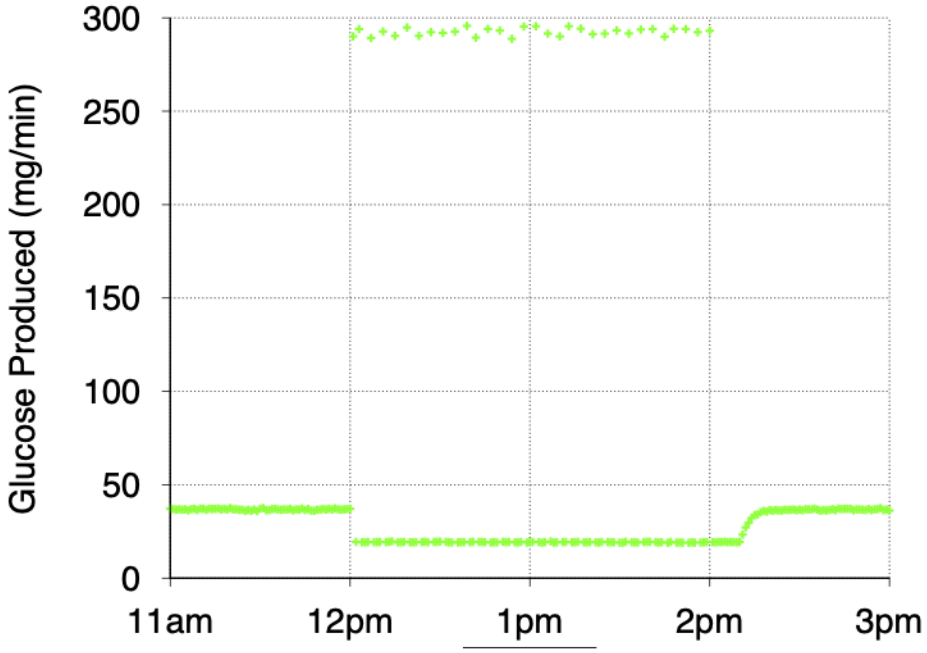

Figure 6.9: Total gluconeogenesis in Liver and Kidneys for the subject # 1: results of simulations replicating a physical exercise event involving arms at intensity 30 $\%VO_2max$ as reported in [5]

Subject #	1	2	3	4	5	6
age_ (years)	20	31	22	29	30	25
gender_ (0=Male)	0					
fitnessLevel_ (%ile)	50					
bodyWeight (kg)	62	93	68	70	82	71
minGlucoseLevel_ (mg/dl)	40					
baseGlucoseLevel_ (mg/dl)	78					
highGlucoseLevel_ (mg/dl)	145					
baseInsulinLevel_	0.001					
peakInsulinLevel_	1.0					
gngImpact_	6.2	5.6	6.2	6.2	5.6	6.1
Initial Liver Glycogen (g)	100.0					
glycogenToGlucoseInLiver_(mg/kg/min)	1.4	0.9	1.3	1.25	1.05	1.25
liverGlycogenBreakdownImpact_	1.0					

Table 6.5: Configuration parameters for simulations for a single "leg" exercise event at intensity 30%VO_2max.

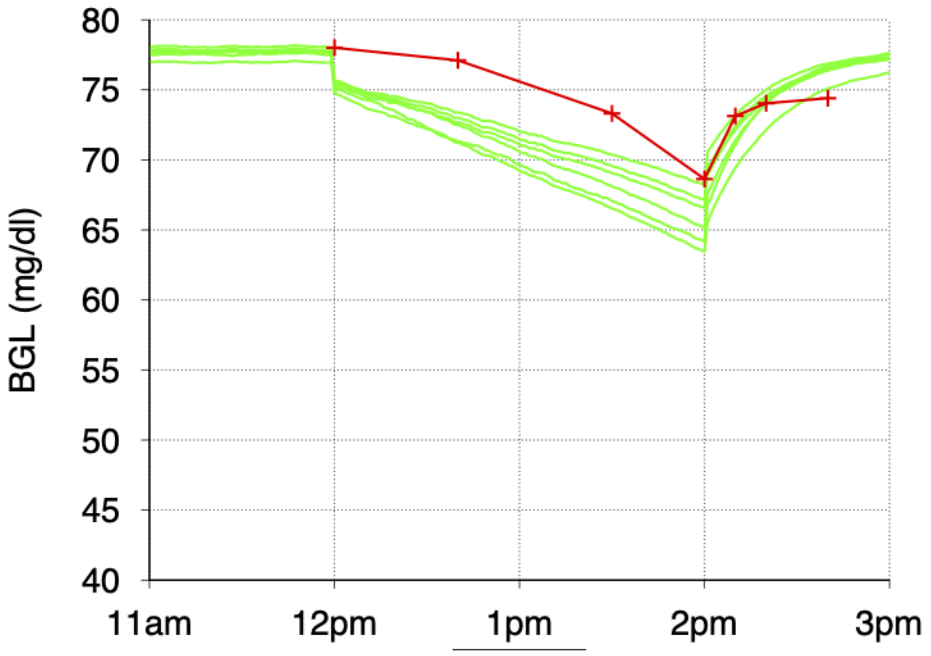

Figure 6.10: BGL results of simulations replicating a physical exercise event involving legs at intensity 30%VO_2max as reported in [5].Green: BGL for 6 simulated subjects; Red: average BGL reported in [5]

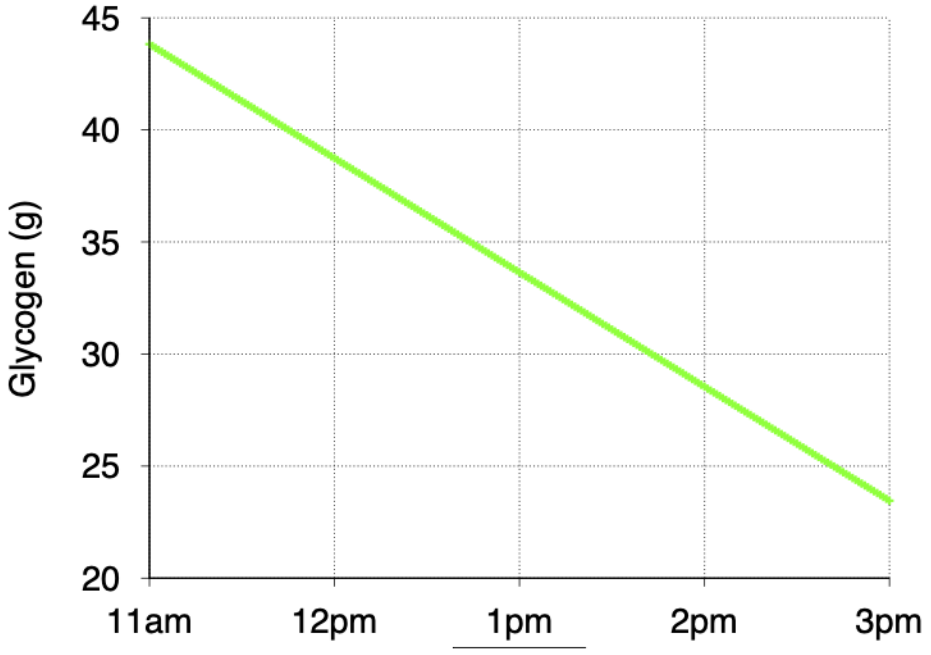

Figure 6.11: Liver glycogen for the subject # 1: results of simulations replicating a physical exercise event involving legs at intensity 30 %VO_2max as reported in [5]

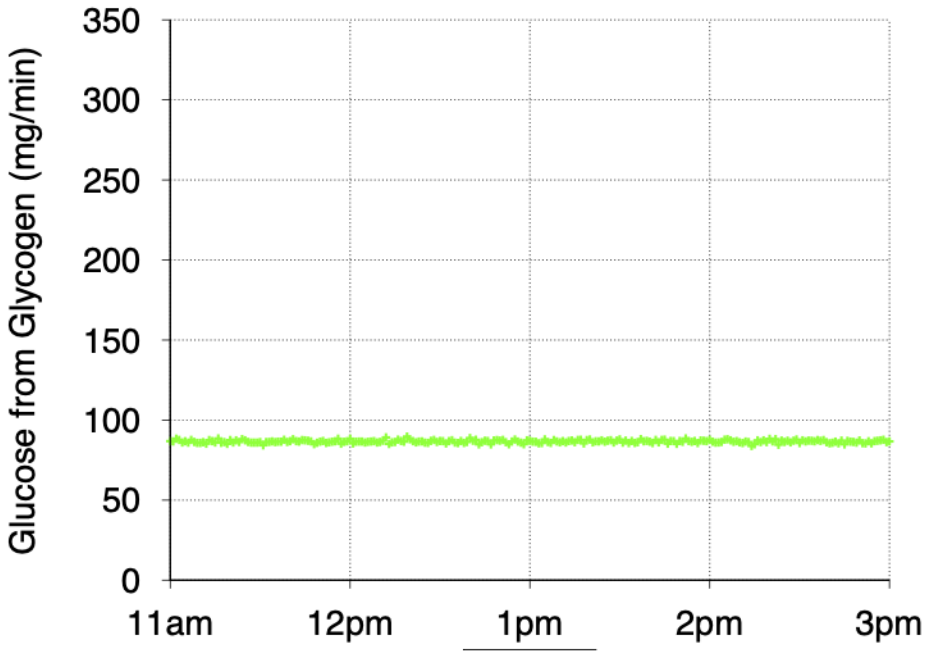

Figure 6.12: Liver glycogen breakdown for the subject # 1: results of simulations replicating a physical exercise event involving legs at intensity $30\%VO_2max$ as reported in [5]

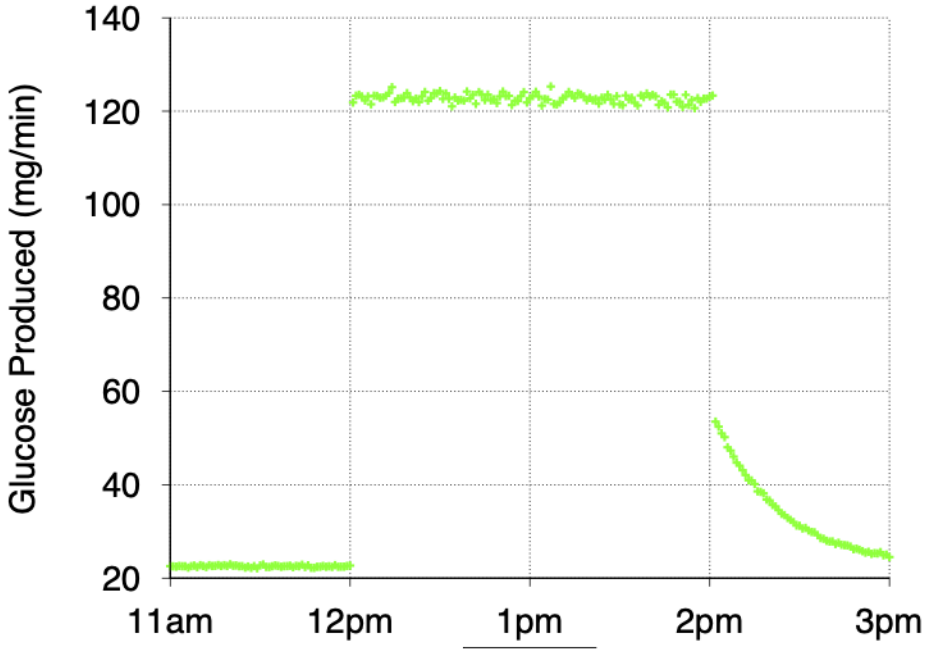

Figure 6.13: Total gluconeogenesis in Liver and Kidneys for the subject # 1: results of simulations replicating a physical exercise event involving legs at intensity $30\%VO_2max$ as reported in [5]

Chapter 7

Conclusion and Future Work

CarbMetSim is an open-source discrete event simulator that models carbohydrate metabolism in human beings. Also, it predicts minute by minute the BGL of the user in response to an arbitrary length sequence of food and exercise activities. The simulator is implemented in an object-oriented paradigm, where the key organs are represented as classes in the *CarbMetSim*. Other simulation tools exist, but they are classified as continuous time models that use differential and algebraic equations to describe the physiological details. It can be argued that it is much easier to revise and modify behavior described in software than differential equations. Moreover, the other simulators are designed to predict the impact of individual meals and are not available in a manner that can be freely used by individuals. The key aspects of *CarbMetSim's* design is covered in Chapter 3, while Chapter 4 covered the implementation and the operation of the different organs of the simulator. The simulator implements the following key organs: stomach, intestine, portal vein, liver, kidney, muscles, adipose tissue, brain and heart. The organs have been implemented to the extent necessary to simulate their impact on the production and consumption of glucose. Chapter 5 and Chapter 6 present a validation of *CarbMetSim's* behavior in response to single meal and exercise events, where the simulator's results were compared against the group-level averages reported in the published research. However, important additional validation is required before the simulator is considered ready to be used in diabetes self-management applications and\or for research. For instance, it is required to have a validation against the continuous blood glucose data of individuals representing various races, ages, and genders.

Also, a validation against continuous blood glucose data of individuals representing different forms and levels of diabetes and different lifestyles is needed.

Our future work on *CarbMetSim* will include more validation for the *CarbMetSim's* behavior and provide functionalities that enhance the current limitations specified in chapter 1. Also, *CarbMetSim* can be used in predicting HbA1c. This marker is considered the golden indicator of average glycemic control. It measures the BGL periodically and evaluates the impact of treatments on the individual's BGL in the past three to four months. *CarbMetSim* can be used to build a tool that can suggest user-specific real-time recommendations on diet and exercise routines. These recommendations, if followed over the remainder of the day, will allow the patient to achieve the target glycemic control regardless of the user's current BGL. Another future area of work is to model the fat metabolism to be utilized in predicting changes in body weight in response to a diet and exercise activities.

Finally, we are aiming forward to reaching a stage where the *CarbMetSim* simulator can be very a useful underlying platform for a number of diabetes self-management tools and a good simulation platform for diabetes research due to its nature and ease of modification and extension.

Bibliography

[1] E Dale Abel. Glucose transport in the heart. *Front Biosci*, 9(201-215):608, 2004.

[2] Eugene Ackerman, Laël C Gatewood, John W Rosevear, and George D Molnar. Model studies of blood-glucose regulation. *The bulletin of mathematical biophysics*, 27(1):21–37, 1965.

[3] Gunvor Ahlborg and Philip Felig. Lactate and glucose exchange across the forearm, legs, and splanchnic bed during and after prolonged leg exercise. *The Journal of clinical investigation*, 69(1):45–54, 1982.

[4] Gunvor Ahlborg, Philip Felig, Lars Hagenfeldt, Rosa Hendler, John Wahren, et al. Substrate turnover during prolonged exercise in man: splanchnic and leg metabolism of glucose, free fatty acids, and amino acids. *The Journal of clinical investigation*, 53(4):1080–1090, 1974.

[5] Gunvor Ahlborg, John Wahren, and Philip Felig. Splanchnic and peripheral glucose and lactate metabolism during and after prolonged arm exercise. *The Journal of clinical investigation*, 77(3):690–699, 1986.

[6] American Diabetes Association. The path to understanding diabetes starts here. August 2019. URL: `https://www.diabetes.org`.

[7] Buket Aydas. *A Discrete-Event Simulation Approach for Modeling Human Body Glucose Metabolism*. PhD thesis, University of Wisconsin Milwaukee, 2018.

[8] Golnaz Baghdadi and Ali Motie Nasrabadi. Controlling blood glucose levels in diabetics by neural network predictor. In *Engineering in Medicine and Biology Society, 2007. EMBS 2007. 29th Annual International Conference of the IEEE*, pages 3216–3219. IEEE, 2007.

[9] M Berger, P Berchtold, HJ Cüppers, H Drost, HK Kley, WA Müller, W Wiegelmann, H Zimmermann-Telschow, FA Gries, HL Krüskemper, et al. Metabolic and hormonal effects of muscular exercise in juvenile type diabetics. *Diabetologia*, 13(4):355–365, 1977.

[10] Richard N Bergman, Y Ziya Ider, Charles R Bowden, and Claudio Cobelli. Quantitative estimation of insulin sensitivity. *American Journal of Physiology-Endocrinology And Metabolism*, 236(6):E667, 1979.

[11] Richard N Bergman, Lawrence S Phillips, Claudio Cobelli, et al. Physiologic evaluation of factors controlling glucose tolerance in man: measurement of insulin sensitivity and beta-cell glucose sensitivity from the response to intravenous glucose. *The Journal of clinical investigation*, 68(6):1456–1467, 1981.

[12] Christopher M Bishop. *Pattern recognition and machine learning*. springer, 1 edition, 2006.

[13] Victor W Bolie. Coefficients of normal blood glucose regulation. *Journal of applied physiology*, 16(5):783–788, 1961.

[14] Christian Bommer, Vera Sagalova, Esther Heesemann, Jennifer Manne-Goehler, Rifat Atun, Till Bärnighausen, Justine Davies, and Sebastian Vollmer. Global economic burden of diabetes in adults: projections from 2015 to 2030. *Diabetes care*, 41(5):963–970, 2018.

[15] Troy Bremer and David A Gough. Is blood glucose predictable from previous values? a solicitation for data. *Diabetes*, 48(3):445–451, 1999.

[16] D Caron, P Poussier, EB Marliss, and B Zinman. The effect of postprandial exercise on meal-related glucose intolerance in insulin-dependent diabetic individuals. *Diabetes Care*, 5(4):364–369, 1982.

[17] E Cerasi, G Fick, and M Rudemo. A mathematical model for the glucose induced insulin release in man. eur j clin invest. *European journal of clinical investigation*, 4:267–278, 1974.

[18] Wilfred Peter Charette. *Control Systems Theory Applied to Metabolic Homeostatic System, and the Derivation and Identification of Mathematical Models*. PhD thesis, California Institute of Technology, 1969.

[19] Claudio Cobelli, Chiara Dalla Man, Giovanni Sparacino, Lalo Magni, Giuseppe De Nicolao, and Boris P Kovatchev. Diabetes: models, signals, and control. *IEEE reviews in biomedical engineering*, 2:54–96, 2009.

[20] Claudio Cobelli, G Federspil, G Pacini, A Salvan, and C Scandellari. An integrated mathematical model of the dynamics of blood glucose and its hormonal control. *Mathematical Biosciences*, 58(1):27–60, 1982.

[21] Emerging Risk Factors Collaboration et al. Diabetes mellitus, fasting blood glucose concentration, and risk of vascular disease: a collaborative meta-analysis of 102 prospective studies. *The Lancet*, 375(9733):2215–2222, 2010.

[22] DG Cramp and ER Carson. The dynamics of short-term blood glucose regulation. In *Carbohydrate Metabolism: Quantitative Physiology and Mathematical Modelling*, pages 349–367. Wiley Chichester, 1981.

[23] Chiara Dalla Man, Michael Camilleri, and Claudio Cobelli. A system model of oral glucose absorption: validation on gold standard data. *IEEE Transactions on Biomedical Engineering*, 53(12):2472–2478, 2006.

[24] Chiara Dalla Man, Robert A Rizza, and Claudio Cobelli. Meal simulation model of the glucose-insulin system. *IEEE Transactions on biomedical engineering*, 54(10):1740–1749, 2007.

[25] Mohammed Derouich and Abdesslam Boutayeb. The effect of physical exercise on the dynamics of glucose and insulin. *Journal of biomechanics*, 35(7):911–917, 2002.

[26] Janet D Elashoff, Terry J Reedy, and James H Meyer. Analysis of gastric emptying data. *Gastroenterology*, 83(6):1306–1312, 1982.

[27] Hans N Englyst, SM Kingman, and JH Cummings. Classification and measurement of nutritionally important starch fractions. *European journal of clinical nutrition*, 46:S33–50, 1992.

[28] Meriyan Eren-Oruklu, Ali Cinar, and Lauretta Quinn. Hypoglycemia prediction with subject-specific recursive time-series models. *Journal of Diabetes Science and Technology*, pages 25–33, 2010.

[29] Meriyan Eren-Oruklu, Ali Cinar, Lauretta Quinn, and Donald Smith. Adaptive control strategy for regulation of blood glucose levels in patients with type 1 diabetes. *Journal of process control*, 19(8):1333–1346, 2009.

[30] Meriyan Eren-Oruklu, Ali Cinar, Lauretta Quinn, and Donald Smith. Estimation of future glucose concentrations with subject-specific recursive linear models. *Diabetes technology & therapeutics*, 11(4):243–253, 2009.

[31] Philip Felig and John Wahren. Fuel homeostasis in exercise. *New England Journal of Medicine*, 293(21):1078–1084, 1975.

[32] Michael E Fisher. A semiclosed-loop algorithm for the control of blood glucose levels in diabetics. *IEEE transactions on biomedical engineering*, 38(1):57–61, 1991.

[33] Centers for Disease Control and Prevention. National diabetes statistics report, 2017 [online]. 2017. URL: `https://www.cdc.gov/diabetes/data/statistics/statistics-report.html`.

[34] Centers for Disease Control and Prevention [online]. August 2018. URL: `https://www.cdc.gov/diabetes/basics/type2.html`.

[35] RO Foster, JS Soeldner, MH Tan, and JR Guyton. Short term glucose homeostasis in man: a systems dynamics model. *Journal of Dynamic Systems, Measurement, and Control*, 1973.

[36] Diabetes Research Institute Foundation. https://www.diabetesresearch.org/what-is-diabetes, August 2019. URL: `https://www.who.int`.

[37] KN Frayn. Important endocrine organs and hormones. *Metabolic regulation: a human perspective. 3rd ed. West Sussex, United Kingdom: Wiley-Blackwell*, pages 144–68, 2010.

[38] Stuart M Furler, Edward W Kraegen, Robert H Smallwood, Donald J Chisholm, et al. Blood glucose control by intermittent loop closure in the basal mode: computer simulation studies with a diabetic model. *Diabetes care*, 8(6):553–561, 1985.

[39] Henrik Galbo. The hormonal response to exercise. *Diabetes/metabolism reviews*, 1(4):385–408, 1986.

[40] Laël C Gatewood, Eugene Ackerman, John W Rosevear, and George D Molnar. Simulation studies of blood-glucose regulation: Effect of intestinal glucose absorption. *Computers and Biomedical research*, 2(1):15–27, 1968.

[41] Eleni I Georga, Vasilios C Protopappas, and Dimitrios I Fotiadis. Glucose prediction in type 1 and type 2 diabetic patients using data driven techniques. In *Knowledge-oriented applications in data mining*. InTech, 2011.

[42] John E Gerich. The importance of tight glycemic control. *The American journal of medicine*, 118(9):7–11, 2005.

[43] John E Gerich. Role of the kidney in normal glucose homeostasis and in the hyperglycaemia of diabetes mellitus: therapeutic implications. *Diabetic Medicine*, 27(2):136–142, 2010.

[44] N Ghevondian and H Nguyen. Modelling of blood glucose profiles non-invasively using a neural network algorithm. In *Proceedings of the First Joint BMES/EMBS Conference. 1999 IEEE Engineering in Medicine and Biology 21st Annual Conference and the 1999 Annual Fall Meeting of the Biomedical Engineering Society (Cat. N*, volume 2, pages 928–vol. IEEE, 1999.

[45] Michael Gleeson. Interrelationship between physical activity and branched-chain amino acids. *The Journal of nutrition*, 135(6):1591S–1595S, 2005.

[46] LAURIE J Goodyear, PATRICIA A King, MICHAEL F Hirshman, CHARLOTTE M Thompson, ELIZABETH D Horton, and EDWARD S Horton. Contractile activity increases plasma membrane glucose transporters in absence of insulin. *American Journal of Physiology-Endocrinology And Metabolism*, 258(4):E667–E672, 1990.

[47] Mukul Goyal, Buket Aydas, and Husam Ghazaleh. Carbmetsim: The carbohydrate metabolism simulator, 2018. https://github.com/mukulgoyalmke/carbmetsim.

[48] Mukul Goyal, Buket Aydas, Husam Ghazaleh, and Sanjay Rajasekharan. Carbmetsim: A discrete-event simulator for carbohydrate metabolism in humans. *Plos one*, 15(3):e0209725, 2020.

[49] John R Guyton, Richard O Foster, J Stuart Soeldner, Meng H Tan, Charles B Kahn, L Koncz, and Ray E Gleason. A model of glucose-insulin homeostasis in man that incorporates the heterogeneous fast pool theory of pancreatic insulin release. *Diabetes*, 27(10):1027–1042, 1978.

[50] Edward S Horton. Role and management of exercise in diabetes mellitus. *Diabetes care*, 11(2):201–211, 1988.

[51] Roman Hovorka, Valentina Canonico, Ludovic J Chassin, Ulrich Haueter, Massimo Massi-Benedetti, Marco Orsini Federici, Thomas R Pieber, Helga C Schaller, Lukas Schaupp, Thomas Vering, et al. Nonlinear model predictive control of glucose concentration in subjects with type 1 diabetes. *Physiological measurement*, 25(4):905, 2004.

[52] JN Hunt, JL Smith, and CL Jiang. Effect of meal volume and energy density on the gastric emptying of carbohydrates. *Gastroenterology*, 89(6):1326–1330, 1985.

[53] JN Hunt and WR Spurrell. The pattern of emptying of the human stomach. *The Journal of Physiology*, 113(2-3):157, 1951.

[54] JN Hunt and DF Stubbs. The volume and energy content of meals as determinants of gastric emptying. *The Journal of physiology*, 245(1):209–225, 1975.

[55] Paul A Insel, John E Liljenquist, Jordan D Tobin, Robert S Sherwin, Paul Watkins, Reubin Andres, Mones Berman, et al. Insulin control of glucose metabolism in man: a new kinetic analysis. *The Journal of clinical investigation*, 55(5):1057–1066, 1975.

[56] Frayn K. *Metabolic Regulation: A Human Perspective*. Wiley-Blackwell, 3rd edition, 2010.

[57] Frayn K. *Metabolic Regulation: A Human Perspective*, volume 3rd Edition. Wiley-Blackwell, 2010.

[58] Leonard A Kaminsky, Ross Arena, and Jonathan Myers. Reference standards for cardiorespiratory fitness measured with cardiopulmonary exercise testing: data from the fitness registry and the importance of exercise national database. In *Mayo Clinic Proceedings*, volume 90, pages 1515–1523. Elsevier, 2015.

[59] D Kelley, A Mitrakou, H Marsh, F Schwenk, J Benn, G Sonnenberg, M Arcangeli, T Aoki, J Sorensen, M Berger, et al. Skeletal muscle glycolysis, oxidation, and storage of an oral glucose load. *The Journal of clinical investigation*, 81(5):1563–1571, 1988.

[60] F Kemmer and M Vranic. The role of glucagon and its relationship to other glucoregulatory hormones in exercise. *Glucagon, Physiology, Pathophysiology and Morphology of the Pancreatic A-Cells. Elsevier*, pages 297–331, 1981.

[61] FW Kemmer, P Berchtold, M Berger, A Starke, HJ Cüppers, FA Gries, and H Zimmermann. Exercise-induced fall of blood glucose in insulin-treated diabetics unrelated to alteration of insulin mobilization. *Diabetes*, 28(12):1131–1137, 1979.

[62] David C Klonoff. Continuous glucose monitoring: roadmap for 21st century diabetes therapy. *Diabetes care*, 28(5):1231–1239, 2005.

[63] Peter Kok. Predicting blood glucose levels of diabetics using artificial neural networks. Master's thesis, Delft University of Technology, the Netherlands, 2004.

[64] Boris P Kovatchev, Marc Breton, Chiara Dalla Man, and Claudio Cobelli. In silico preclinical trials: a proof of concept in closed-loop control of type 1 diabetes, 2009.

[65] Boris P Kovatchev, Daniel J Cox, Linda A Gonder-Frederick, and William Clarke. Symmetrization of the blood glucose measurement scale and its applications. *Diabetes Care*, 20(11):1655–1658, 1997.

[66] JJS Larsen, Flemming Dela, Michael Kjær, and Henrik Galbo. The effect of moderate exercise on postprandial glucose homeostasis in niddm patients. *Diabetologia*, 40(4):447–453, 1997.

[67] JJS Larsen, Flemming Dela, Sten Madsbad, and Henrik Galbo. The effect of intense exercise on postprandial glucose homeostasis in type ii diabetic patients. *Diabetologia*, 42(11):1282–1292, 1999.

[68] ED Lehmann and T Deutsch. A physiological model of glucose-insulin interaction in type 1 diabetes mellitus. *Journal of biomedical engineering*, 14(3):235–242, 1992.

[69] Eldon D Lehmann. The freeware aida interactive educational diabetes simulatorhttp. *Med Sci Monit*, 7(3):504–515, 2001.

[70] AG Low. Nutritional regulation of gastric secretion, digestion and emptying. *Nutrition Research Reviews*, 3(1):229–252, 1990.

[71] I Magnusson, DL Rothman, LD Katz, RG Shulman, and GI Shulman. Increased rate of gluconeogenesis in type ii diabetes mellitus. a 13c nuclear magnetic resonance study. *The Journal of clinical investigation*, 90(4):1323–1327, 1992.

[72] Chiara Dalla Man, Francesco Micheletto, Dayu Lv, Marc Breton, Boris Kovatchev, and Claudio Cobelli. The uva/padova type 1 diabetes simulator: new features. *Journal of diabetes science and technology*, 8(1):26–34, 2014.

[73] Paul R McHugh and Timothy H Moran. Calories and gastric emptying: a regulatory capacity with implications for feeding. *American Journal of Physiology-Regulatory, Integrative and Comparative Physiology*, 236(5):R254–R260, 1979.

[74] Christian Meyer, Jean M Dostou, Stephen L Welle, and John E Gerich. Role of human liver, kidney, and skeletal muscle in postprandial glucose homeostasis. *American Journal of Physiology-Endocrinology And Metabolism*, 282(2):E419–E427, 2002.

[75] Christian Meyer, Michael Stumvoll, Jean Dostou, Stephen Welle, Morey Haymond, and John Gerich. Renal substrate exchange and gluconeogenesis in normal postabsorptive humans. *American Journal of Physiology-Endocrinology and Metabolism*, 282(2):E428–E434, 2002.

[76] Howard Minami and Richard W Mccallum. The physiology and pathophysiology of gastric emptying in humans. *Gastroenterology*, 86(6):1592–1610, 1984.

[77] Orson W Moe, Stephen H Wright, and Manuel Palacín. Renal handling of organic solutes. *Brenner & Rector's the kidney*, 1:214–47, 2008.

[78] SG Mougiakakou, K Prountzou, et al. A neural network based glucose-insulin metabolism models for children with type i. In *Annual International Conference of the IEEE Engineering in Medicine and Biology Society. Proceedings*, 2005.

[79] Stavroula G Mougiakakou, Aikaterini Prountzou, Dimitra Iliopoulou, Konstantina S Nikita, Andriani Vazeou, and Christos S Bartsocas. Neural network based glucose-insulin metabolism models for children with type 1 diabetes. In *2006 International Conference of the IEEE Engineering in Medicine and Biology Society*, pages 3545–3548. IEEE, 2006.

[80] David M Nathan, Judith Kuenen, Rikke Borg, Hui Zheng, David Schoenfeld, Robert J Heine, et al. Translating the a1c assay into estimated average glucose values. *Diabetes care*, 2008.

[81] Jill D Nelson, Philipee Poussier, Errol B Marliss, A Michael Albisser, and Bernard Zinman. Metabolic response of normal man and insulin-infused diabetics to post-prandial exercise. *American Journal of Physiology-Endocrinology And Metabolism*, 242(5):E309–E316, 1982.

[82] The National Institute of Diabetes, Digestive, and Kidney Diseases. Diabetes statistics, August 2019. URL: https://www.niddk.nih.gov/health-information/health-statistics/diabetes-statistics.

[83] RL Ollerton. Application of optimal control theory to diabetes mellitus. *International Journal of Control*, 50(6):2503–2522, 1989.

[84] World Health Organization. Global report on diabetes, Dec 2019. URL: https://apps.who.int/iris/bitstream/handle/10665/204871/9789241565257_eng.pdf;jsessionid=DD5362D2D82000A95B2DA6CC3C3AD023?sequence=1.

[85] Silvia Oviedo, Josep Vehi, Remei Calm, and Joaquim Armengol. A review of personalized blood glucose prediction strategies for t1dm patients. *International journal for numerical methods in biomedical engineering*, 33(6), 2017.

[86] Konstantinos Papatheodorou, Maciej Banach, Eleni Bekiari, Manfredi Rizzo, and Michael Edmonds. Complications of diabetes 2017. *Journal of diabetes research*, 2018, 2018.

[87] Robert S Parker, Francis J Doyle, and Nicholas A Peppas. A model-based algorithm for blood glucose control in type i diabetic patients. *IEEE Transactions on biomedical engineering*, 46(2):148–157, 1999.

[88] Robert S Parker, Francis J Doyle III, Jennifer H Ward, and Nicholas A Peppas. Robust h glucose control in diabetes using a physiological model. *AIChE Journal*, 46(12):2537–2549, 2000.

[89] Thorkil Ploug, Henrik Galbo, and ERIK A Richter. Increased muscle glucose uptake during contractions: no need for insulin. *American Journal of Physiology-Endocrinology And Metabolism*, 247(6):E726–E731, 1984.

[90] Ilpoo Puhakainen, Veikko A Koivisto, and H Yki-Järvinen. Lipolysis and gluconeogenesis from glycerol are increased in patients with noninsulin-dependent diabetes mellitus. *The Journal of Clinical Endocrinology & Metabolism*, 75(3):789–794, 1992.

[91] SA Quchani and Ehsan Tahami. Comparison of mlp and elman neural network for blood glucose level prediction in type 1 diabetics. In *3rd Kuala Lumpur International Conference on Biomedical Engineering 2006*, pages 54–58. Springer, 2007.

[92] C Edward Rasmussen and CKI Williams. *Gaussian Processes for Machine Learning Cambridge*. MA: MIT Press, 2006.

[93] EA Richter, T Ploug, and H Galbo. Increased muscle glucose uptake during contractions: no need for insulin. *Medicine & Science in Sports & Exercise*, 16(2):173, 1984.

[94] Derrick K Rollins and Nidhi Bhandari. Constrained mimo dynamic discrete-time modeling exploiting optimal experimental design. *Journal of Process Control*, 14(6):671–683, 2004.

[95] Derrick K Rollins, Nidhi Bhandari, Jim Kleinedler, Kaylee Kotz, Amber Strohbehn, Lindsay Boland, Megan Murphy, Dave Andre, Nisarg Vyas, Greg Welk, et al. Free-living inferential modeling of blood glucose level using only noninvasive inputs. *Journal of process control*, 20(1):95–107, 2010.

[96] Derrick K Rollins, Nidhi Bhandari, and Kaylee R Kotz. Critical modeling issues for successful feedforward control of blood glucose in insulin dependent diabetics. In *American Control Conference, 2008*, pages 832–837. IEEE, 2008.

[97] JA Romijn, EF Coyle, LS Sidossis, A Gastaldelli, JF Horowitz, E Endert, and RR Wolfe. Regulation of endogenous fat and carbohydrate metabolism in relation to exercise intensity and duration. *American Journal of Physiology-Endocrinology And Metabolism*, 265(3):E380–E391, 1993.

[98] Anirban Roy and Robert S Parker. Dynamic modeling of free fatty acid, glucose, and insulin: An extended" minimal model". *Diabetes technology & therapeutics*, 8(6):617–626, 2006.

[99] Anirban Roy and Robert S Parker. Dynamic modeling of exercise effects on plasma glucose and insulin levels. *Journal of Diabetes Science and Technology*, Volume 1(3), 2007.

[100] WA Sandham, DJ Hamilton, A Japp, and K Patterson. Neural network and neuro-fuzzy systems for improving diabetes therapy. In *Proceedings of the 20th Annual International Conference of the IEEE Engineering in Medicine and Biology Society. Vol. 20 Biomedical Engineering Towards the Year 2000 and Beyond (Cat. No. 98CH36286)*, volume 3, pages 1438–1441. IEEE, 1998.

[101] Alex J Smola and Bernhard Schölkopf. A tutorial on support vector regression. *Statistics and computing*, 14(3):199–222, 2004.

[102] Vijay R Soman, Veikko A Koivisto, David Deibert, Philip Felig, and Ralph A DeFronzo. Increased insulin sensitivity and insulin binding to monocytes after physical training. *New England Journal of Medicine*, 301(22):1200–1204, 1979.

[103] John Thomas Sorensen. *A physiologic model of glucose metabolism in man and its use to design and assess improved insulin therapies for diabetes*. PhD thesis, Massachusetts Institute of Technology, 1985.

[104] Giovanni Sparacino, Francesca Zanderigo, Stefano Corazza, Alberto Maran, Andrea Facchinetti, and Claudio Cobelli. Glucose concentration can be predicted ahead in time from continuous glucose monitoring sensor time-series. *IEEE Transactions on biomedical engineering*, 54(5):931–937, 2007.

[105] Fredrik Ståhl and Rolf Johansson. Diabetes mellitus modeling and short-term prediction based on blood glucose measurements. *Mathematical biosciences*, 217(2):101–117, 2009.

[106] Cristina Tarin, Edgar Teufel, Jesús Picó, Jorge Bondia, and H-J Pfleiderer. Comprehensive pharmacokinetic model of insulin glargine and other insulin formulations. *IEEE Transactions on Biomedical Engineering*, 52(12):1994–2005, 2005.

[107] J Tiran, LI Avruch, and AM Albisser. A circulation and organs model for insulin dynamics. *American Journal of Physiology-Endocrinology and Metabolism*, 237(4):E331, 1979.

[108] Volker Tresp, Thomas Briegel, and John Moody. Neural-network models for the blood glucose metabolism of a diabetic. *IEEE Transactions on Neural networks*, 10(5):1204–1213, 1999.

[109] John Joseph Valletta, Andrew J Chipperfield, and Christopher D Byrne. Gaussian process modelling of blood glucose response to free-living physical activity data in people with type 1 diabetes. In *2009 Annual International Conference of the IEEE Engineering in Medicine and Biology Society*, pages 4913–4916. IEEE, 2009.

[110] J Wahren, P Felig, G Ahlborg, R Hendler, and L Hagenfeldt. Substrate turnover during prolonged exercise in man. *The Journal of Clinical Investigation*, 53:1080–1090, 1974.

[111] John Wahren, Philip Felig, Gunvor Ahlborg, and Lennart Jorfeldt. Glucose metabolism during leg exercise in man. *The Journal of clinical investigation*, 50(12):2715–2725, 1971.

[112] David H Wasserman and Bernard Zinman. Exercise in individuals with iddm. *Diabetes Care*, 17(8):924–937, 1994.

[113] Hans J Woerle, Christian Meyer, Jean M Dostou, Niyaz R Gosmanov, Nazmul Islam, Emilia Popa, Steven D Wittlin, Stephen L Welle, and John E Gerich. Pathways for glucose disposal after meal ingestion in humans. *American Journal of Physiology-Endocrinology and Metabolism*, 284(4):E716–E725, 2003.

[114] Hans J Woerle, Ervin Szoke, Christian Meyer, Jean M Dostou, Steven D Wittlin, Niyaz R Gosmanov, Stephen L Welle, and John E Gerich. Mechanisms for abnormal postprandial glucose metabolism in type 2 diabetes. *American Journal of Physiology-Endocrinology and Metabolism*, 290(1):E67–E77, 2006.

[115] Robert R Wolfe, Ethan R Nadel, JH Shaw, Lou A Stephenson, and Marta H Wolfe. Role of changes in insulin and glucagon in glucose homeostasis in exercise. *The Journal of clinical investigation*, 77(3):900–907, 1986.

[116] Zarita Zainuddin, Ong Pauline, and Cemal Ardil. A neural network approach in predicting the blood glucose level for diabetic patients. *Int J Comput Intell*, 5(1):72–79, 2009.

[117] Bin Zhou, Yuan Lu, Kaveh Hajifathalian, James Bentham, Mariachiara Di Cesare, Goodarz Danaei, Honor Bixby, Melanie J Cowan, Mohammed K Ali, Cristina Taddei, et al. Worldwide trends in diabetes since 1980: a pooled analysis of 751 population-based studies with 4· 4 million participants. *The Lancet*, 387(10027):1513–1530, 2016.

[118] Bernard Zinman, Frederick T Murray, Mladen Vranic, A Michael Albisser, Bernard S Leibel, Patricia A Mcclean, and Errol B Marliss. Glucoregulation during moderate exercise in insulin treated diabetics. *The Journal of Clinical Endocrinology & Metabolism*, 45(4):641–652, 1977.

[119] R Abu Zitar. Towards neural network model for insulin/glucose in diabetics. *International Journal of Computing & Information Sciences*, 1(1):25, 2003.

[120] Raed Abu Zitar and Abdulkareem Al-Jabali. Towards neural network model for insulin/glucose in diabetics-ii. *Informatica*, 29(2), 2005.

Husam Ghazaleh

husamcse@gmail.com

SUMMARY

-Research experience in bio-informatics ,machine learning, stochastic modeling in computer science, and wireless networks.
-Experienced programmer in multiple programming languages including C\C++, Core Java, Android Java and SQLite, and Python.
-Communicates effectively with a wide range of people by showing interest and carefully listening to their needs.
-Organized, proactive, confident ,and self-motivated.

EDUCATION

***Ph.D**, Computer Science* **GPA:3.63**
University of Wisconsin-Milwaukee, Milwaukee, USA, Expected Fall 2020.

***Masters of Science**, Computer Science* **GPA:3.88**
Al-Balqa Applied University, Salt City, Jordan, Dec 2007
Thesis: Design a Protocol for Wireless 4G Systems.

***Bachelor of Science**, Computer Science*
Mutah University, Al-Karak City, Jordan, May 2004
Senior Project: Shopping Online, an Automated System.

TEACHING EXPERIENCE

Visiting Instructor of Computer Science Aug 2018 - to Date
Division of Science and Technology Department, Quincy University, Illinois.

- Taught several computer science courses such as CSC115 Introduction to Computer Science, CSC150 Computer Programming I, CSC160 Computer Programming II, CSC200 Computer Science Experience, CSC250 Software Systems, CSC361 Aartificial intelligence, CSC330 Operating Systems, CSC340 Computer Architecture, CSC495 Capstone Computing Project I, and CSC496 Capstone Computing Project ll.
- Developed and revised courses syllabi and other materials as required.
- Developed courses outlines, courses lectures, programming assignments, quizzes, projects and exams.
- Served as academic adviser for computer science students.
- Served actively on the university and division committees and work cooperatively with colleagues in assigned projects.

Full-Time Instructor Summer 2016, Summer 2017, Summer 2018
Department of Electrical Engineering and Computer Science, University of Wisconsin, Milwaukee.

- Taught Android Programming course (CS790 Advanced Topics in Computer Science) including UI/UX principles and techniques for 25 undergraduate and graduate students.
- Developed Diabetes Care App (DCA).
- Developed the course syllabus, course outlines, course lectures, programming assignments, quizzes, project and exams.

– Graded homework, programming assignments, and exams.

Teaching Assistant Aug 2011 - May 2018

Department of Electrical Engineering and Computer Science, University of Wisconsin, Milwaukee.

– Taught labs for: CS201 Introductory Computer Programming (Java), CS337 System Programming (C,C++), and CS537 Operating Systems.

– Responsible for up to three sections, sixteen students per section.

– Held weekly TA sessions, deliver weekly lectures, grade homework, programming assignments, and exams, maintain course website, hold weekly office hours, help create homework assignments, and create homework solution sets.

Full-Time Lecturer Feb 2009 - Feb 2010

Math and Computer Science Department, Tafila Technical University, Jordan.

– Taught Visual Programming (Java Language) and AI courses for more than 300 undergraduate students.

– Participated as a member in the team who designed computer science courses by creating syllabi and choosing text books.

MCSE Course Instructor Jan 2005 - Mar 2005

Nevada Center for Computer and Language Training, Amman, Jordan.

– Taught Microsoft Windows XP, Microsoft Windows Server 2000, Microsoft Active Directory 2000 and Microsoft Internet Security and Acceleration Server.

– Mentored the trainees to pass the exams of the Microsoft Certified Systems Engineering certificate.

PROFESSIONAL EXPERIENCE

Software Engineer (Internship) Jun 2015 - Aug 2015

Yellow Cab Cooperative, Milwaukee, USA.

– Analyzed, designed, implemented, and tested of an Android mobile app to provide online reservation services for customers.

– Troubleshot system and network problems in order to meet the PCI data security standards.

– Secured computer systems and networks from unauthorized accesses.

Senior IT Officer Jun 2005 - Jan 2009

IT Department, Jordan Press Foundation (JPF), Amman, Jordan.

– Provided technical support and handled queries for JPF employees (1000+ employees).

– Configured and maintained of the following operating systems: Apple Macintosh 9, Apple OS X Tiger, Microsoft Windows XP, Sun Solaris 9 and Microsoft Active Directory 2003

– Administrated and troubleshot the News Agency applications.

– Installed and configured computer hardware, operating systems, and applications such as Quark and Adobe.

– Monitored and maintained computer systems and networks.

– Troubleshot system and network problems and solved hardware or software faults.

– Tested and evaluated new technologies.

Senior IT Officer Nov 2004 - Jun 2005

IT Department, AL-Numow Company for Trade Services and Marketing, Amman, Jordan.

– Trained AL-Numow Company's employees on Intuit QuickBooks system.

– Configured and maintained the workgroup network and the company distributed database.

PUBLICATIONS

– Goyal, M., Aydas, B., **Ghazaleh, H.**, and Rajasekharan, S. (2020). CarbMetSim: A discrete-event simulator for carbohydrate metabolism in humans. Plos one, 15(3), e0209725.

– Muhanna, M. and **Ghazaleh, H**., Interactive Environment for Command and Control Simulation Scenarios Inside CAVE. 2012 International Conference on Systems and Informatics (ICSAI), China, IEEE Computer Society Press, May 2012, pp.2113 - 2118.

– Gibbs, I. and **Ghazaleh, H**., Message Adaptor Code Generation. Proceedings of 9th IEEE International Conference on Industrial Informatics, Portugal, IEEE Computer Society Press, July 2011, pp.676 -681.

– BAAREH,A. **Ghazaleh, H**. SHETA,A. and KHNAIFES,K. Forecasting the Daily Flow of the Black Water River Using Soft-Computing Techniques. 2010 Annual International Conference on Advanced Topics in Artificial Intelligence (ATAI 2010), Thailand. **(accepted not published)**

– **Ghazaleh, H**. and Muhanna, M., Enhancement of Throughput Time Using MS-TCP Transport Layer Protocol for 4G Mobiles, Proceedings of the 5th IEEE International Multi-conference on Systems, Signals, and Devices, Amman, Jordan, IEEE Computer Society Press, July 2008, pp.105-111.

– **Ghazaleh, H**. Design a Protocol for Wireless 4G Systems, Thesis, Master of Science, Al-Balqa Applied University, Salt City, Jordan, December 2007.

POSTERS

– **Ghazaleh, H.** and Goyal, M., A diabetes self-management tool, 2016 Annual Student Research Poster Competition, University of Wisconsin-Milwaukee, 2016.

– **Ghazaleh, H**. and Omari, A., Sniffing Voice over IP (VoIP) with Wireshark, University of Wisconsin-Milwaukee,2013.

AWARDS

– **Chancellors Graduate Student Award**, College of Engineering and Applied Science, University of Wisconsin, Milwaukee, 2016.

– **Chancellors Graduate Student Award**, College of Engineering and Applied Science, University of Wisconsin, Milwaukee, 2015.

– **Student Success Award**, Student Success Center, University of Wisconsin, Milwaukee, 2014.

– **CEAS Dean's Scholarship**, College of Engineering and Applied Science, University of Wisconsin, Milwaukee, 2013

– **Chancellors Graduate Student Award**, College of Engineering and Applied Science, University of Wisconsin, Milwaukee, 2012.

– **Chancellors Graduate Student Award**, College of Engineering and Applied Science, University of Wisconsin, Milwaukee, 2011.

COMPUTER SKILLS

– Programming Languages: C++, C, Android Java, Java, MATLAB.
– Environments: UNIX, Mac OS X, Windows.

INDIVIDUAL CREATIVITY

- Participating in Quincy University Presidential Scholarship Committee, 2019,2020.
- Representing the computer science program on Quincy University Discovery Day 2018,2019.
- Volunteering in Quincy University Day of Service (2018,2019).
- Volunteering in the Girl Scout Coding Event, Quincy University, 2018.
- Volunteer tutor in the CEAS Tutoring Center. Assisting students in preparation for successful completion of computer science and programming courses through one-on-one tutoring relationship. Feb-May 2012.
- Frequent reviewer for various conferences including IEEE transactions on wireless communication and networking conference, IEEE transactions on Software Engineering and Data Engineering conference, and IEEE transaction on Information Technology conference.
- Nominated by the faculty committee to participate in the IT Department Show at Mutah University, Jordan. Presented the graduation project "Shopping Online" that we designed and implemented using JSP, Servlet and Oracle 9i, May 2004.